NASA CR-135194
PT-4964

ELECTRONIC AND MECHANICAL IMPROVEMENT OF THE RECEIVING TERMINAL OF A FREE-SPACE MICROWAVE POWER TRANSMISSION SYSTEM

by

William C. Brown

RAYTHEON COMPANY

Prepared for

NATIONAL AERONAUTICS AND SPACE ADMINISTRATION
NASA Lewis Research Center

Contract NAS 3-19722

1. Report No.	2. Government Accession No.	3. Recipient's Catalog No.
NASA CR-135194		

4. Title and Subtitle	5. Report Date
Electronic and Mechanical Improvement of the Receiving Terminal of a Free-Space Microwave Power Transmission System	August 1, 1977
	6. Performing Organization Code
7. Author(s)	8. Performing Organization Report No.
William C. Brown	PT-4964
	10. Work Unit No.
9. Performing Organization Name and Address	11. Contract or Grant No.
Raytheon Company, Equipment Division and Microwave and Power Tube Division 430 Boston Post Road, Wayland, Mass. 01778	NAS3-19722
	13. Type of Report and Period Covered
12. Sponsoring Agency Name and Address	Contractor Report
National Aeronautics and Space Administration Washington, D.C. 20546	14. Sponsoring Agency Code

15. Supplementary Notes

Program Managers: Ira T. Myers and Stanley Domitz, Power Devices Section, NASA Lewis Research Center, Cleveland, Ohio 44135

16. Abstract

Significant advancements were made in a number of areas: improved efficiency of basic receiving element at low power density levels ; improved resolution and confidence in efficiency measurements; mathematical modelling and computer simulation of the receiving element; and the design, construction, and testing of an environmentally protected two-plane construction suitable for low-cost, highly automated construction of large receiving arrays.

17. Key Words (Suggested by Author(s))	18. Distribution Statement
Rectenna Solar Power Satellite Microwave Power Microwave Transmission	Unclassified - unlimited

19. Security Classif. (of this report)	20. Security Classif. (of this page)	21. No. of Pages	22. Price*
Unclassified	Unclassified	158	

*For sale by the National Technical Information Service, Springfield, Virginia 22151

TABLE OF CONTENTS

TABLE OF CONTENTS (Cont'd)

LIST OF ILLUSTRATIONS

LIST OF ILLUSTRATIONS (Cont'd)

LIST OF ILLUSTRATIONS (Cont'd)

LIST OF ILLUSTRATIONS (Cont'd)

LIST OF ILLUSTRATIONS (Cont'd)

LIST OF ILLUSTRATIONS (Cont'd)

LIST OF ILLUSTRATIONS (Cont'd)

SUMMARY

This technology development was concerned with improvements in the reception and rectification of microwave power at the receiving terminal of a free-space power transmission system and, more specifically, with its application to the rectenna receiving array in the solar power satellite concept. In this system, large areas of the array operate at relatively low power density levels. A 20 percent improvement in the efficiency of elements operating at these levels was obtained by a combination of circuit and diode redesign. GaAs-W Schottky barrier diodes were designed and constructed to provide a lower voltage drop across the diodes to improve efficiency.

A major accomplishment was the adaptation of previous rectenna technology to the more economically desirable two-plane construction format in which the foreplane provides the functions of collection, rectification, filtering, and DC power bussing and collection. A metal shield in the foreplane was designed to provide environmental protection and to act as a structural element in the rectenna array.

Improvements in measurement and analytical techniques that were achieved were: mathematical modeling and computer simulation of the basic receiving element that checked out well with experimental data; quantitative measurement techniques for experimentally measuring diode and circuit losses; and an accounting method for balancing the microwave power input against the sum of DC power output and diode and circuit losses to achieve better confidence in efficiency measurements.

1.0 INTRODUCTION

The RF to DC Collector/Converter technology development with which this report is concerned is in support of the larger technological development of free space power transmission by means of a microwave beam. The efficient free-space transportation of energy by electromagnetic beam brings a new three-dimensional aspect to the transfer of electrical power and permits the coupling of terrestrial power transmission systems to power sources and sinks located in the earth's atmosphere and space.

This report relates to the application of free space power transmission in which the sun's energy is captured in equatorial geosynchronous orbit, converted to electrical power, and then sent to Earth by means of a microwave beam. At the earth's surface the microwave power is efficiently collected and converted back into DC electrical power. Improvements in the performance of this receiving system and its reduction to a practical design are the specific subject matter of this report.

To place the work to be reported upon in proper perspective, it is desirable to define and review the technology of free-space power transmission with particular emphasis upon prior RF to DC collector/converter technology.

1.1 Description of free-space power transmission by microwave beam and its early development.

Free-space power transmission by microwave beam is defined as the efficient point-to-point transfer of energy through free space by a highly collimated microwave beam. As a technology [1] it includes the interchanging of dc and microwave power at the transmitting and receiving ends of the system. Free-space is defined to exclude the use of any physically injected material such as waveguides or reflectors between the transmitting and receiving points of the system but not to exclude the presence of gaseous, liquid, or congealed material that exists naturally in the earth's atmosphere.

Free-space power transmission as a technology is differentiated from the use of microwaves in free space for point to point communication purposes by its very high efficiency and by the magnitude of the power which is handled at the receiving point - being in many cases over 90 percent of the microwave power launched at the transmitting point. The efficient collection and conversion of this incoming microwave power to conventional electrical power comprises a unique technology which bears little relationship to the traditional methods of receiving and processing microwave energy in communication and radar applications.

The concept of power transfer by radio waves was first pioneered by Tesla [2], [3] at the turn of the century. An acknowledged genius in low-frequency electric power generation and distribution, Tesla became interested in the general concept of resonance and sought to apply this to the transmission of electrical power from one point to another without wires. He built a large "Tesla coil" with which he hoped to produce oscillations of electrical energy around the surface of the earth and set up standing waves into which he could immerse his receiving antennas at the optimum point.

With the advantage of historical perspective, we realize that these experiments were decades ahead of the unfolding of a technology that could accomplish his objective. This new technology was based upon the early microwave experiments of Hertz [4], but had to await the development of efficient generators of microwave power. This capability began to emerge with the microwave generators developed for the radar of World War II and later for microwave communications.

The event which directly precipitated interest in the use of microwaves for power transmission was the support of the development of super-power microwave tubes by the Department of Defense in the early 1960's, [5]. This program resulted in high-efficiency tubes with such high power handling capability (several hundreds of kilowatts) that the use of microwaves for the efficient transfer of large amounts of power became a distinct feasibility.

The first demonstration of the efficient transmission of meaningful amounts of power by microwaves took place at the Spencer Laboratory of Raytheon Co. in May 1963 [6]. In this first demonstration, shown in Figure 1-1, the means used for collecting the power at the receiving end of the system utilized conventional antenna technology in the form of a pyramidal horn. The means used for rectifying the microwave power to DC power was a close-spaced thermionic diode. Neither of these technologies was completely satisfactory. The receiving horn was highly directive and because of the difficulty of matching its antenna pattern to that of the incoming beam its collecting efficiency was only 87%. The rectifier efficiency was only 50%.

Nevertheless, as a result of this demonstration the Rome Air Development Center of the Air Force became interested in the concept of a microwave powered platform for communication purposes. The Raytheon proposal of a microwave powered helicopter to accomplish this objective and the resulting contract became crucial in determining the evolutionary path of the collection and rectification of microwave power from a free-space microwave beam.[7] It was recognized that the pyramidal horn would not be satisfactory because of a combination of its high directivity with the natural roll and pitch of the vehicle. It was also recognized that the limitations of the close-spaced thermionic rectifier would place severe limitations on the practicality of the platform. The "rectenna" device was proposed to the Air Force as a solution to this problem. The rectenna device made it possible to simultaneously solve the directivity and antenna pattern matching problems of microwave power collection and at the same time make practical use of the semiconductor device whose power handling capability had prevented it from being seriously considered for a system in which significant amounts of power were being handled.

The Raytheon Company actually demonstrated a microwave powered helicopter using a rectenna prior to active work on the Air Force contract. But the Air Force contract was the basis for an extension of the effort and several notable demonstrations, including a ten hour continuous flight of the vehicle[7]. Figure 1-2 shows the helicopter in flight. It was necessary, of course, to use laterally constraining tethers to keep the helicopter on the microwave beam but this limitation was later removed by a study and experimental confirmation

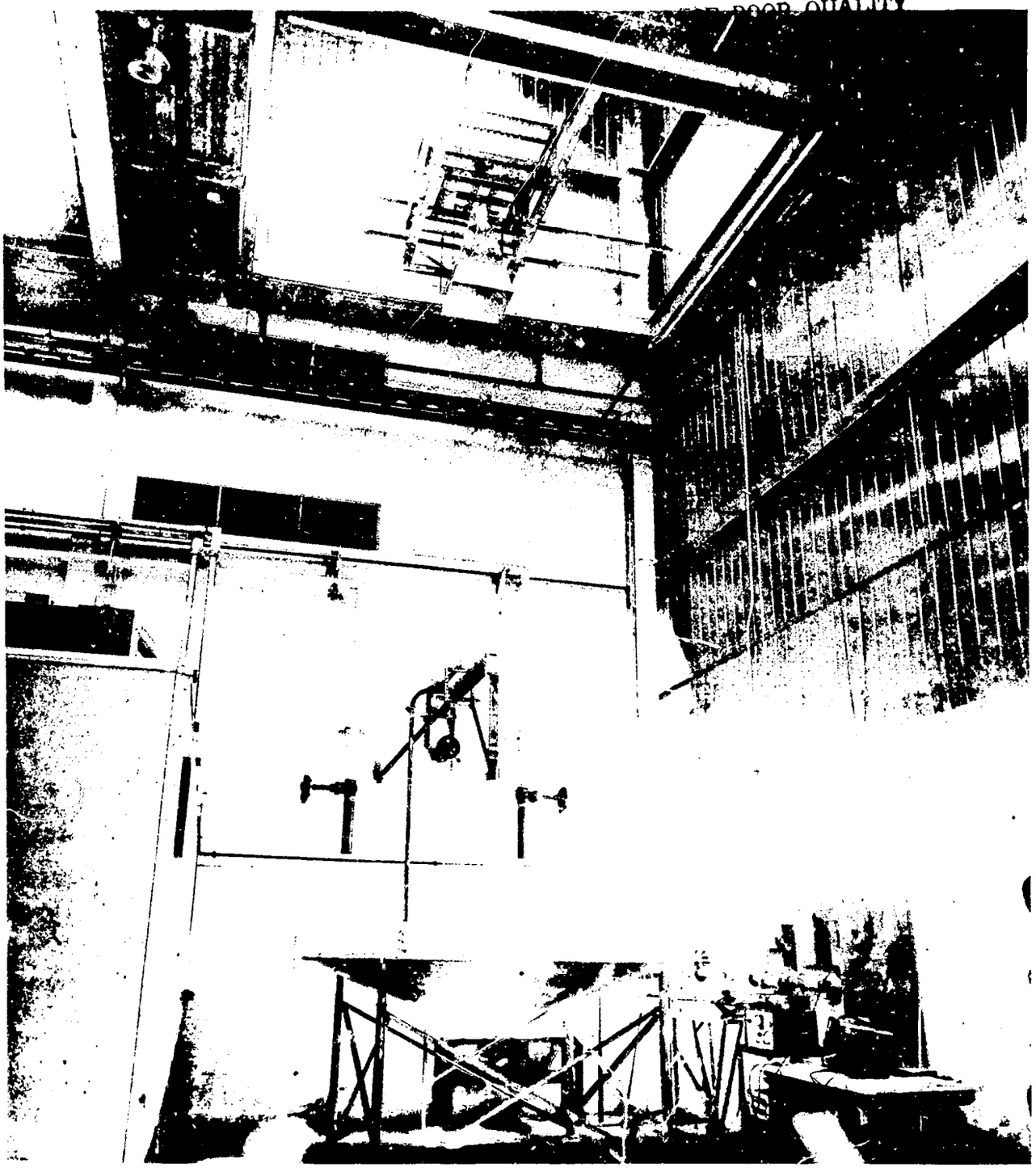

Figure 1-1. First experiment in the efficient transfer of power by means of microwaves at the Spencer Laboratory of Raytheon Co. in May 1963. In this experiment microwave power generated from a magnetron was transferred 5.48 meters and then converted with DC power with an overall efficiency of 16%. A conventional pyramidal horn was used to collect the energy at the receiving end and a close-spaced thermionic diode was used to convert the microwaves into DC power. The DC power output was 100 watts.

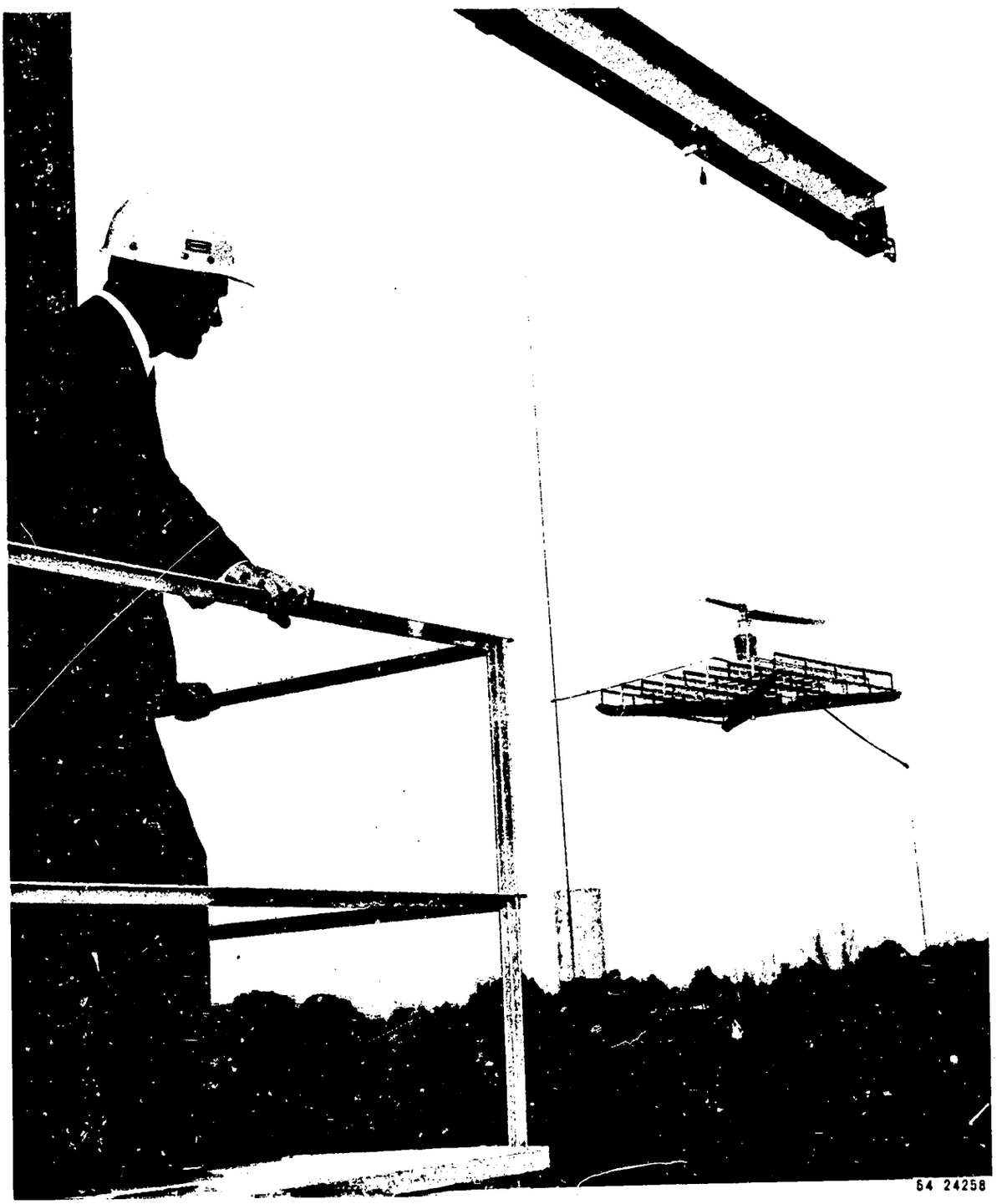

Figure 1-2. Microwave powered helicopter in flight 18.28 meters above a transmitting antenna. The receiving array for collecting the microwave power and converting it to DC power was made up of several thousand point contact silicon diodes. DC power level was approximately 200 watts.

that the microwave beam could be used successfully as a position reference in a control system in an automated helicopter which would keep it self positioned over the center of the beam[7].

This progression of efforts established the rectenna device as a probable solution to the collection and rectification problem in a broad class of microwave power transmission applications, but much work remained to be done to make it a practical device in the context of the SSPS type of application. The opportunity to further evolve the rectenna device was largely the result of the interest of the Marshall Space Flight Center in applying microwave power transmission to the transfer of energy and power between satellites, [8] and the contractual effort supported at Raytheon Company. [9]

In a more recent time frame very substantial advances in overall system performance have been made. These advances include a certified overall transmission efficiency of 54% starting with the DC power applied to the microwave generator and ending with the DC power out of the rectenna at the receiving point. [10] A particularly impressive demonstration was made at the Goldstone facility of the Jet Propulsion Laboratory. In this demonstration power was transmitted over a distance of 1.6 kilometers and a DC power output of over 30 kilowatts was obtained at the receiving point. [11, 12]

Table 1-1 presents a summary of the early chronology of the collection and rectification of microwave power. It will be noted that there was interest in microwave power transmission prior to any capability of efficiently converting microwave power directly into DC power. [13]

TABLE 1-1

CHRONOLOGY OF COLLECTION & RECTIFICATION OF MICROWAVE POWER

1958	First interest in microwave power transmission
1958	No rectifiers available - turbine proposed and studied
1959-1962	Some government support of rectifier technology (1) Semiconductors at Purdue University (2) Magnetron analogue at Raytheon
1962	Semiconductor and close-spaced thermionic diode rectifiers made available.
1963	First power transmission using pyramidal horn and close-spaced thermionic diode rectifiers - 39% capture and rectification efficiency not practical for aerospace application.
1964	RADC microwave powered helicopter application demanded non-directive reception, light weight, high reliability.
1964	Rectenna concept developed to utilize many semiconductor rectifiers of small power handling capability to terminate many small apertures to provide non-directive reception and high reliability.
1968-Present	Continued development of rectenna concept to format with high power handling capability, much higher capture and rectification efficiency, and potentially low production cost.

1.2 Major Microwave Collector-Converter Technology Developments

As a result of the early experience with the severe demands placed upon the receiving portion of a free-space microwave power transmission system and the discovery of the ability of the rectenna concept to cope with all of these demands, the history of microwave collector/converter technology is almost exclusively that of the development of the rectenna.

The following general requirements are placed upon the collector/converter:

- large aperture
- high power handling capability
- non-directive
- high efficiency
- ability to operate efficiently over a substantial frequency range
- light weight
- easy mechanical tolerances
- ability to passively radiate any heat resulting from inefficient
- operation
- high reliability
- very long life
- minimal radio frequency interference
- low cost.

The rectenna has been found to successfully meet all of these requirements, with the possible exception of radio frequency interference. RFI, however in the form of harmonic power, is a special problem that confronts both the transmitter and the receiver. Since the harmonic level must be down to such low levels to meet non-interference requirements and meeting it by wave filters would result in such higher cost and reduced efficiency, the proper solution may be to have an allocation of frequencies for the harmonics that are generated in the system.

The rectenna has gone through a number of development stages whose nature was largely determined by the motivational influences of the period and the state of development of diodes. These stages are outlined with the aid of Table 1-2.

The microwave powered helicopter application was the dominant early influence and was responsible for the initial development of two separate embodiments of the rectenna concept. The very first rectenna, Figure 1-3, which established its general properties made use of a rectenna element characterized by a halfwave dipole antenna terminated in a full-wave bridge. This development was based upon an early study of the solid-state diode as an efficient rectifier of microwave power by George [14] and its adaptation as a rectifier of free-space radiation by Brown, et al. [15, 16] The rectenna elements were separated from each other by approximately one-half wavelength. Unfortunately, such a construction using the then existing point-contact diodes could not handle nearly enough power density to be used for the demonstration of a microwave-powered helicopter. A new configuration characterized by a dense compaction of diodes

TABLE 1-2

MAJOR RECTENNA DEVELOPMENT PROGRAMS

RECTENNA SEQUENCE NO.	DATE	SPONSOR	DEVELOPERS	MOTIVATION	STYLE	MAJOR CONTRIBUTION	LIT. REF.*	FIGURE NO.
1	1964	Raytheon	George, Brown, Heenan	For Microwave Powered Helicopter	Half-Wave Antennae. Full-Wave Bridge	Established General Characteristics of Rectenna	16	3
2	1964	Raytheon Air Force	Brown	For Microwave Powered Helicopter	String Type Array	High Power Density Receiver. First Successful Application - Microwave Powered Helicopter.	7	4, 2
3	1968	Brown	Brown	Improved Rectenna Lower Specific Wt.	Half-Wave Antennae. Full-Wave Bridge Rectifier	Specific Wt. - 1 Gram per Watt	17	5
4	1970	MSFC NASA	Brown	Improved Efficiency	Half-Wave Antennae. Full-Wave Bridge Rectifier	51% Capture and Rectification Efficiency	8	6, 7
5	1971	MSFC NASA	Brown	Improved Efficiency	Half-Wave Antennae. Full-Wave Bridge Rectifier	64% Capture and Rectification Efficiency	1, 9	8
6	1974	MSFC NASA	Brown	Improved Efficiency Increase Power Output - Increase Power Density.	Half-Wave Antennae. Half-Wave Rectifier Low Pass Filters	78-80% Capture and Rectification Efficiency 140 Watt/Sq. Ft. Power Density	1, 9	9, 10
7	1975	JPL NASA	Brown	Improve Efficiency. Certify Efficiency	Half-Wave Antennae. Half-Wave Rectifier Low Pass Filter	Certified DC-DC efficiency at 54%. 82% Capture and Rectification Efficiency	10	12, 13
8	1975	JPL NASA	Dickinson Maynard Brown	Large Scale Demonstration of Power and Transmission Distance	Half-Wave Antennae. Half-Wave Rectifier Low Pass Filter	High Power Level of 30 KW and 82% efficiency.	11, 12	14, 15

* See references in bibliography at end of this report.

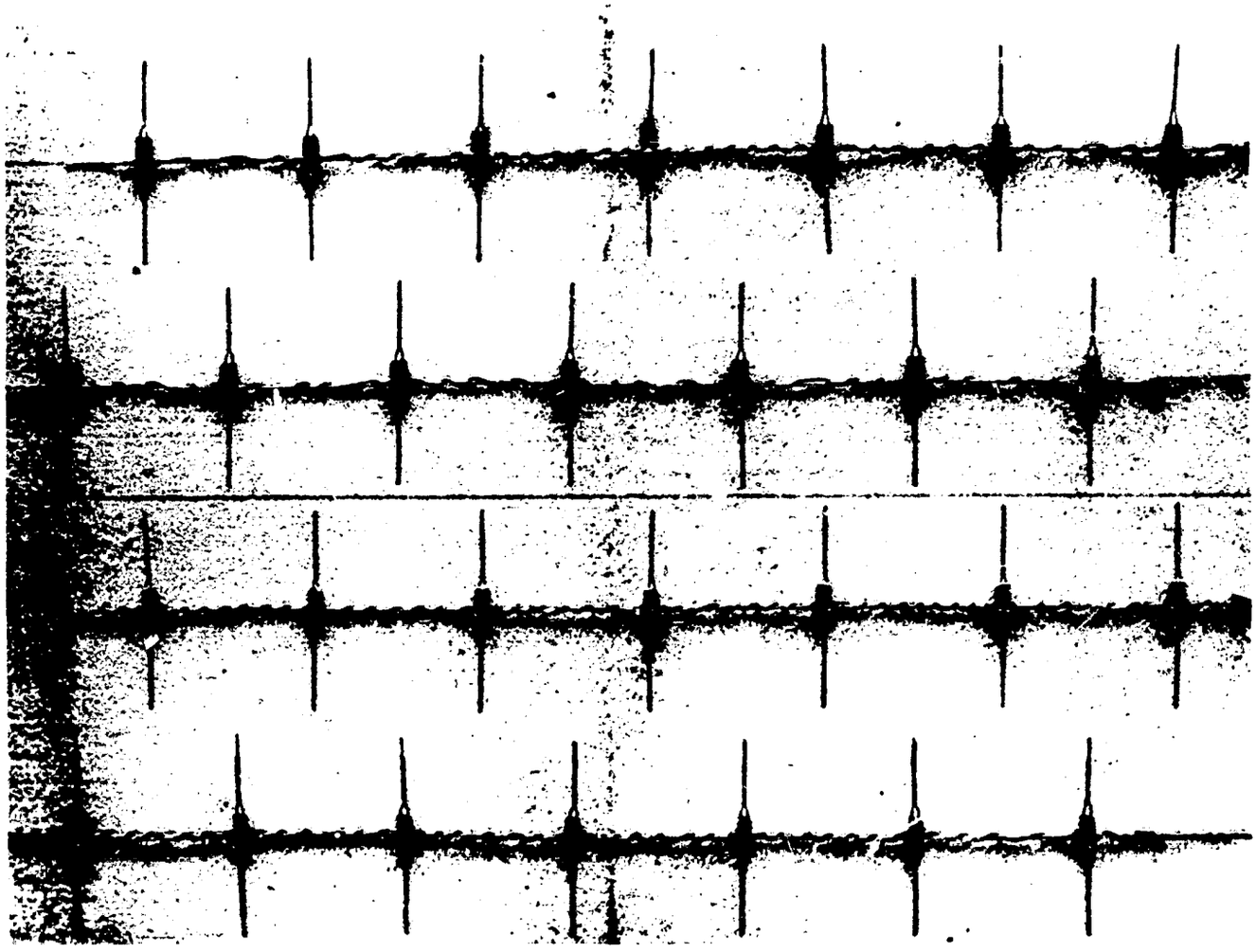

Figure 1-3. The first rectenna. Conceived at Raytheon Company, it was built and tested by R. George of Purdue University. Composed of 28 half-wave dipoles spaced one-half wave-length apart, each dipole terminated in a bridge-type rectifier made from four IN82G point-contact semi-conductor diodes. A reflecting surface consisting of a sheet of aluminum was placed one-quarter wavelength behind the array.

in a string-like construction in which the diodes themselves were part of the collection process as well as the rectification process was developed and used successfully in the early helicopter work. (Figures 1-2 and 1-4.)

In time coincidence with the demonstration of the helicopter, Hewlett Packard Associates had developed a new physical format for a silicon Schottky barrier diode with the potential for much greater reliability and power handling capability than the point contact diode as well as offering considerably greater efficiency. A number of these were forwarded by HPA for evaluation and their superiority as rectifiers was confirmed by R.H. George (18). They were not put into a rectenna element format.

In the time period from 1965 until 1970 there was no direct support of rectenna development from either government or industry. During this time period, the Air Force did support the development of a helicopter which would automatically position itself over the center of a microwave beam, a capability necessary for the practical use of a microwave powered helicopter.

However, a substantial amount of development work on the rectenna was carried out by W. C. Brown using private funds and time during the1967 to 1968 time period. (19) This work was primarily aimed at designing a very light weight rectenna structure which utilized a rectenna element format consisting of a half-wave dipole antenna terminated in a full-bridge rectifier made up of HPA 2900 diodes (17, 19) (Figure 1-5.) This work was important in that it established the physical format of the rectenna development effort that was to be undertaken later at MSFC and that was also to be supported under MSFC contract at Raytheon Company. It was also used in a demonstration of microwave power transmission to the MSFC Director, Werner von Braun, and his staff. This demonstration may have been a decisive factor in a decision to undertake the support of this work at MSFC during a time period of NASA contraction.

In Spetember 1970 a demonstration involving the measurement of the various efficiencies in complete microwave power transmission system (DC to DC) was made at Marshall Space Flight Center (8) (Figure 1-6). The rectenna used for this purpose, Figure 1-7, employed rectenna elements patterned after those just discussed but developed to the point where their individual capture and rectification efficiencies approximated 70%. The configuration is important in the context of rectenna development for satellite power stations in that the collection, rectification, and DC collection was performed in a single plane positioned approximately a quarter wave-length above the reflection plane. This is the intended approach whose development was a part of the activity under this contract.

The MSFC demonstration of 1970 (8) indicated a number of deficiencies in the system including a rectenna collection efficiency of only 74% versus the theoretical maximum of 100%. This low collection efficiency was associated with improper spacing of the rectenna elements from each other in the rectenna array.

It was therefore decided to space the elements more closely to each other and, in addition, terminate the DC output of each rectenna element in a

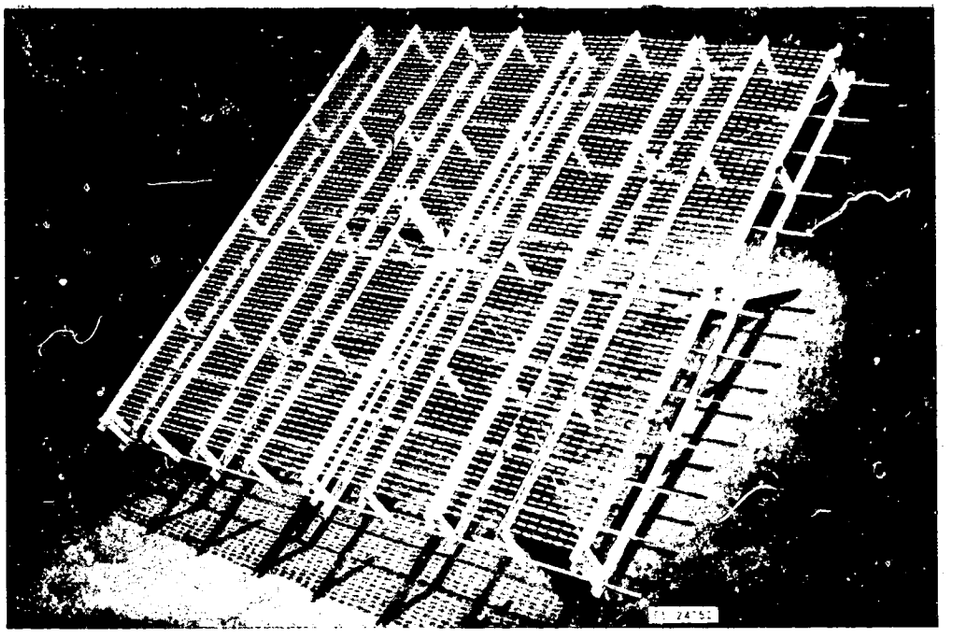

Figure 1-4. The special rectenna made for the first microwave-powered helicopter. The array is 0.6 meters square and contains 4480 IN82G point-contact rectifier diodes. Maximum DC power output was 200 watts.

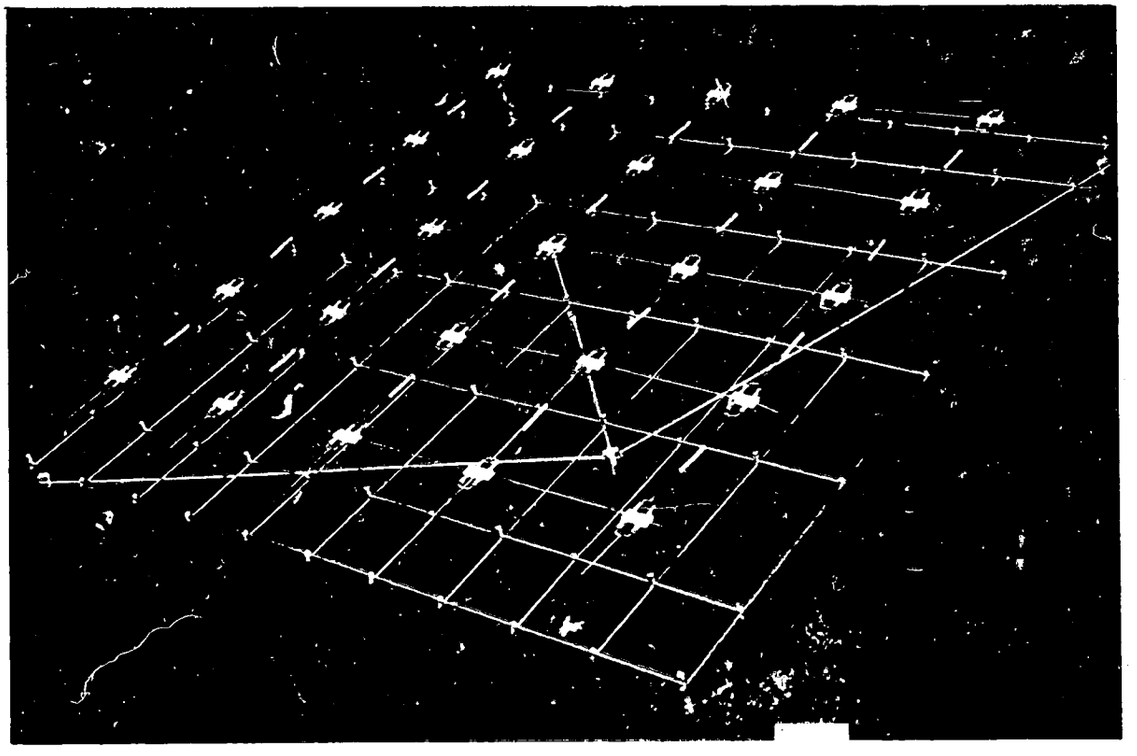

Figure 1-5. Greatly improved rectenna made from improved diodes (HP2900) which are commercially available. The 0.3 meter square structure weighs 20 grams and can deliver 20 watts of output power.

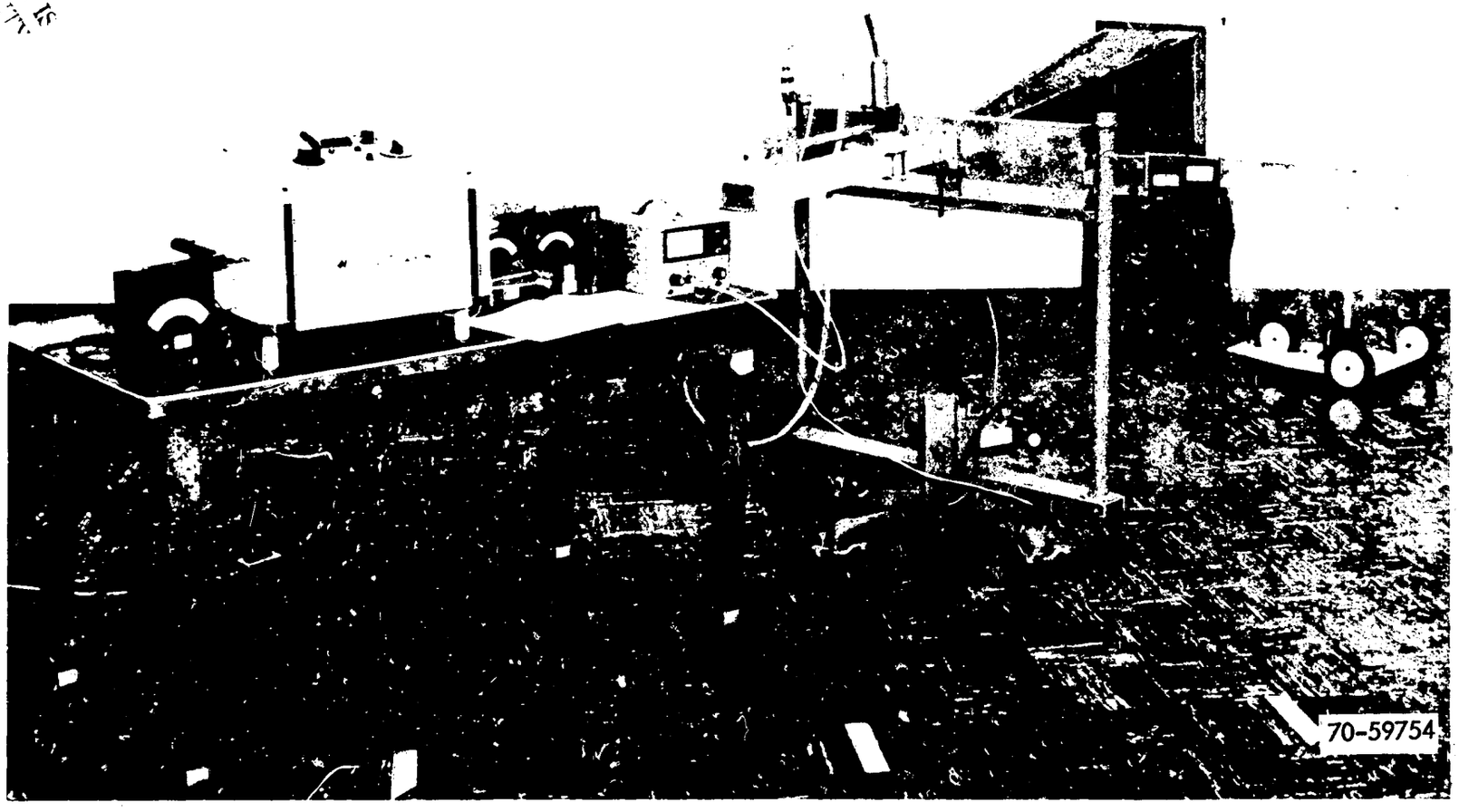

Figure 1-6. Test set-up of microwave power transmission system at Marshall Space Flight Center in 1970. The magnetron which converts dc power at 2450 MHz is mounted on the waveguide input to the pyramidal horn transmitting antenna. The rectenna in the background intercepts most of the transmitted power and converts it to dc power. Ratio of dc power out of rectenna to the rf power into the horn was 40.8%. Overall dc-to-dc efficiency was 26.5%.

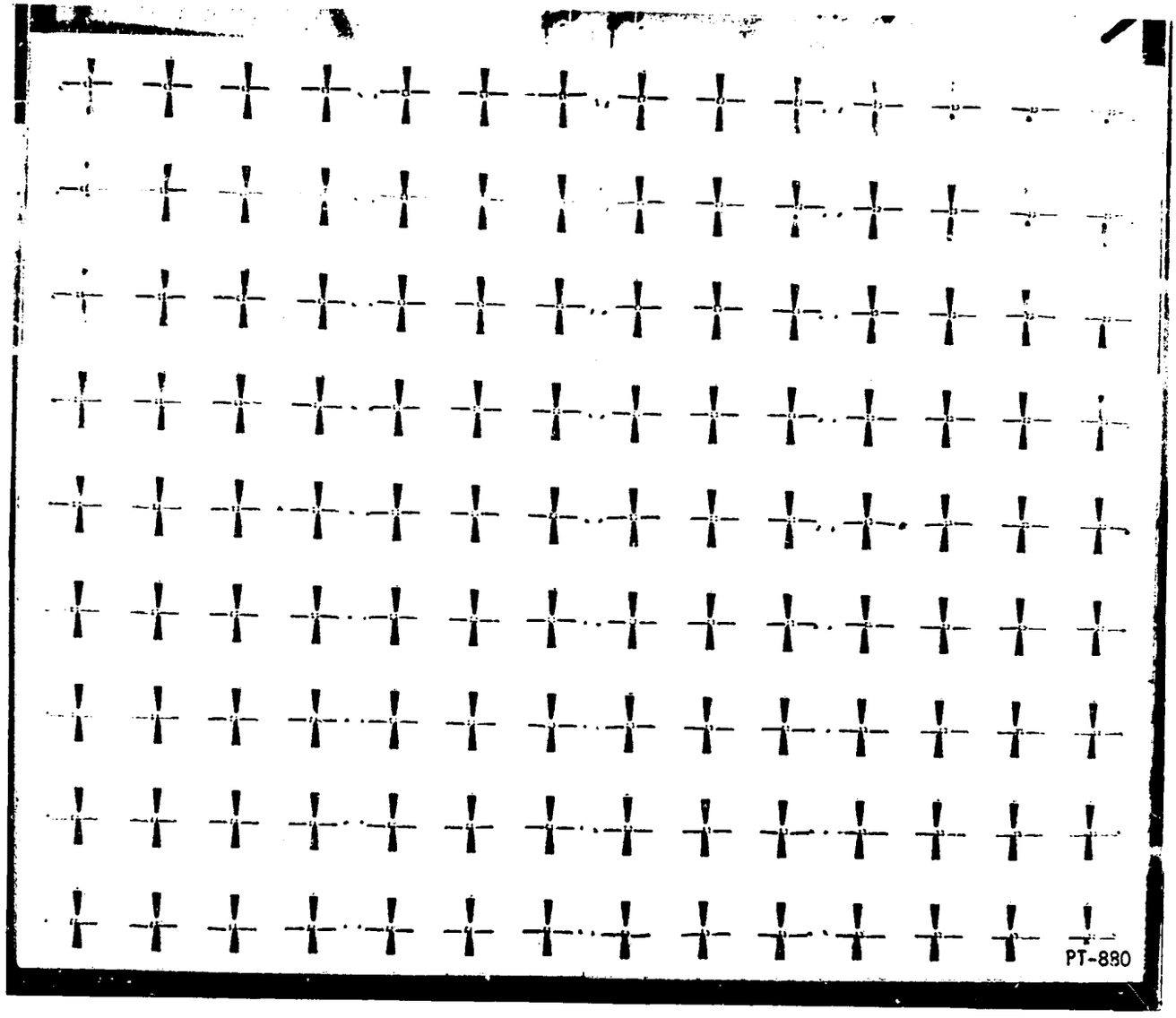

Figure 1-7. Close-up view of first rectenna developed by Raytheon under MSFC contract. Microwave collector, rectification, and DC bussing of rectified power are all carried out in one plane. Rectenna elements are connected in series.

separate resistor to obtain a much greater range of data on the behavior of the rectenna. This latter decision involved a change in the manner in which the DC power was collected and instrumented.[20] The output of each rectenna element was brought back through the reflector plane. This arrangement shown in Figure 1-8 provided such an enhanced capability to study and understand the performance of the rectenna that it was retained in the further development of the rectenna. (See Figure 1-9 for the later adaptation to a more recent MSFC rectenna.) The construction, however, is not economical and is not recommended for most applications.

The changed collection geometry as shown in Figure 1-8 improved the collection efficiency to about 93%. Other changes improved the overall transmission, collection, and rectification considerably [20].

Because the diode rectifier is such an important element in the collection and rectification process, a search for diodes which would improve the efficiency and power handling capability of the rectenna has been a continuing procedure. In 1971, Wes Mathei suggested that the Gallium Arsenide Schottky-barrier diode that had reached an advanced state of development for Impatt devices might be a very good power rectifier and provided a number of diodes for testing.[1, 9] These devices were indeed much better. Their revolutionary behavior in terms of higher efficiency and much greater power handling capability rapidly became the basis for the planning of improved rectenna performance.

The knowledge of the superior performance of this device was coincident with the advancement of the concept of the Satellite Solar Power Station by Dr. Glaser of the A. D. Little Co. [21] The earliest investigation of a rectenna design for this concept indicated that the economics of its construction would be crucial and that mechanical and electrical simplicity of the collection and rectification circuitry would be of paramount importance. This factor, combined with the fact that no harmonic filters had existed in previous rectenna element designs but would be necessary in any acceptable microwave power transmission system, motivated a completely new direction of rectenna element development. This new direction was the development of a rectenna element employing a single diode in a half-wave rectifier configuration with adequate wave filters to attenuate the radiation of harmonics and to store energy for the rectification process.

The construction of such a rectenna element and its insertion into a DC bus collection system is shown in Figure 1-9. This rectenna element was used in the last phase of the MSFC sponsored work at Raytheon to construct a rectenna 1.21 meters in diameter which was illuminated by a gaussian beam horn (Figure 1-10). The combined collection and rectification efficiency of this rectenna was measured at 80%.

A lower cost and slightly more efficient form of this rectenna element was developed for the RXCV work sponsored by NASA at JPL. This element is shown in Figures 1-11 and 1-12, together with a greatly simplified equivalent electrical circuit of the device. The same electrical circuit applies to the MSFC rectenna element of Figures 1-9 and 1-10.

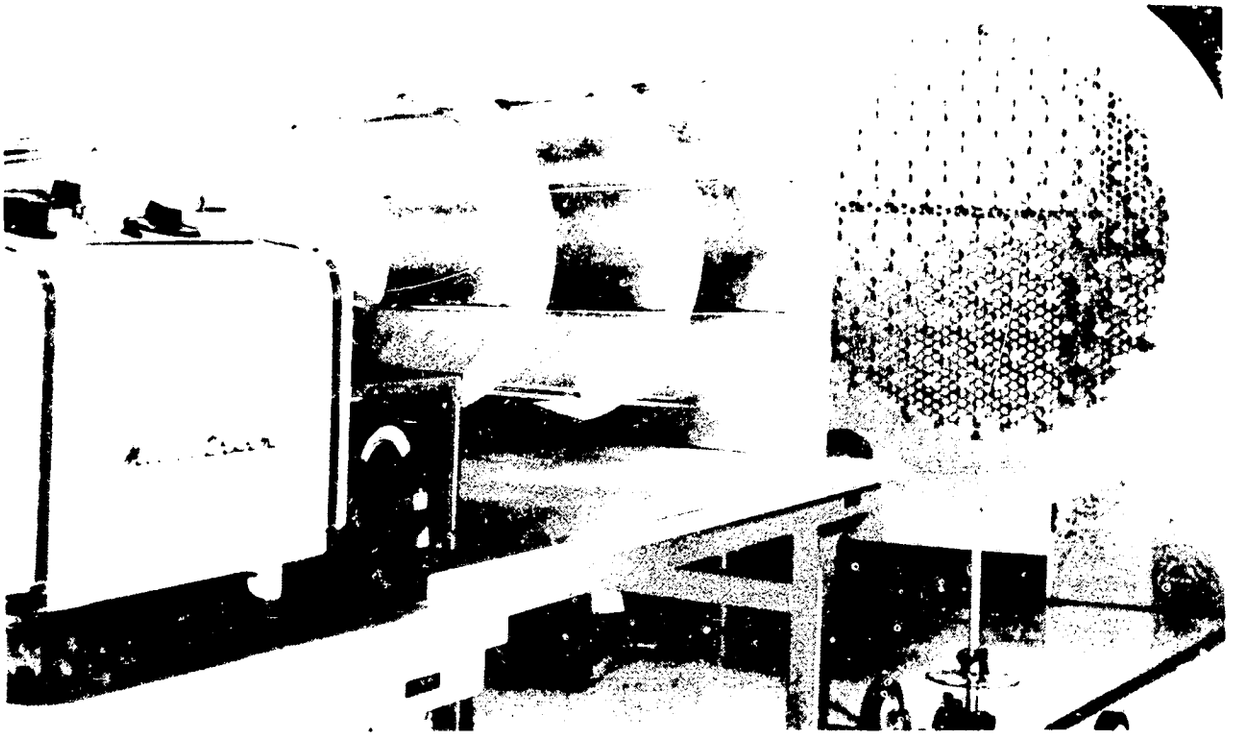

Figure 1-8. Experimental set-up comprised of dual-mode horn and improved rectenna. The efficiency ratio of the dc power from the rectenna to the microwave power at the input to the dual-mode horn was measured and found to be 60.2%.

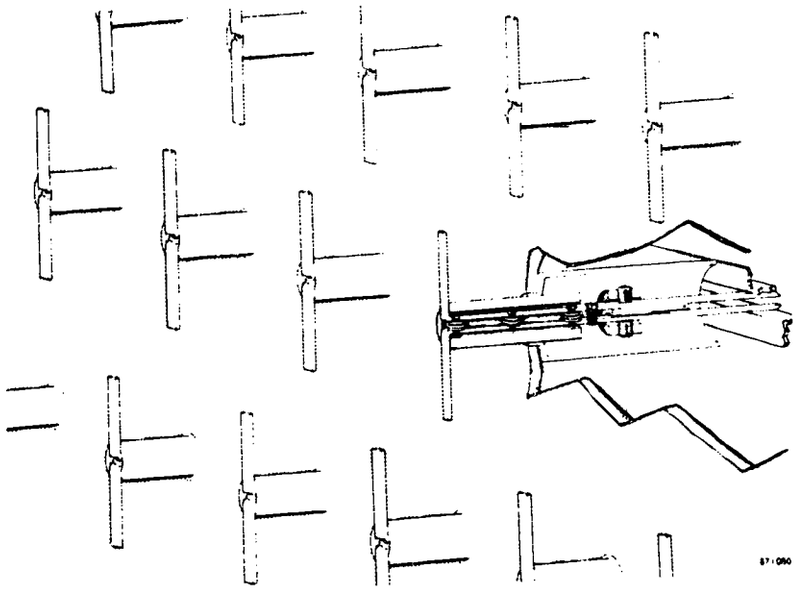

Figure 1-9. Sketch of the Marshall Space Flight Center rectenna which was constructed in spring of 1974. Cutaway section of rectenna element shows the two section input low pass filter, the diode, and a combination tuning element and by-pass capacitor.

Figure 1-10. Photograph of the MSFC rectenna constructed in 1974 under test. Horn at left of picture illuminates the rectenna (white panel) with a Gaussian distribution of power. Rectified DC power is collected from rectenna in circular ring path and dissipated in resistive loads on the test panel at the right.

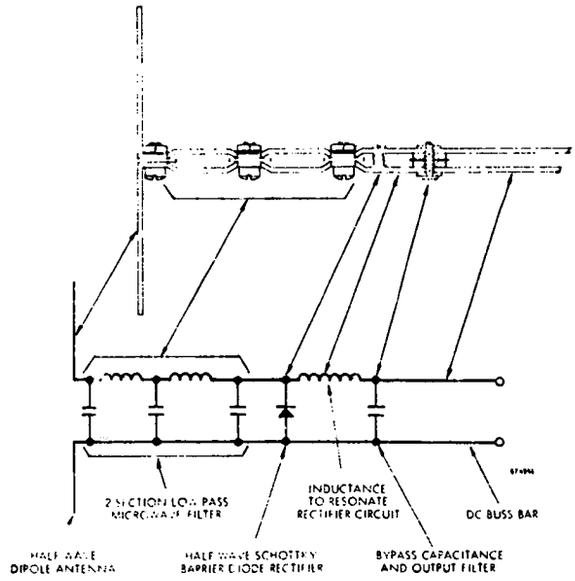

Figure 1-11. Simplified Electrical Schematic for the rectenna element used in the RXCV receiving array at the Venus site of the JPL Goldstone facility.

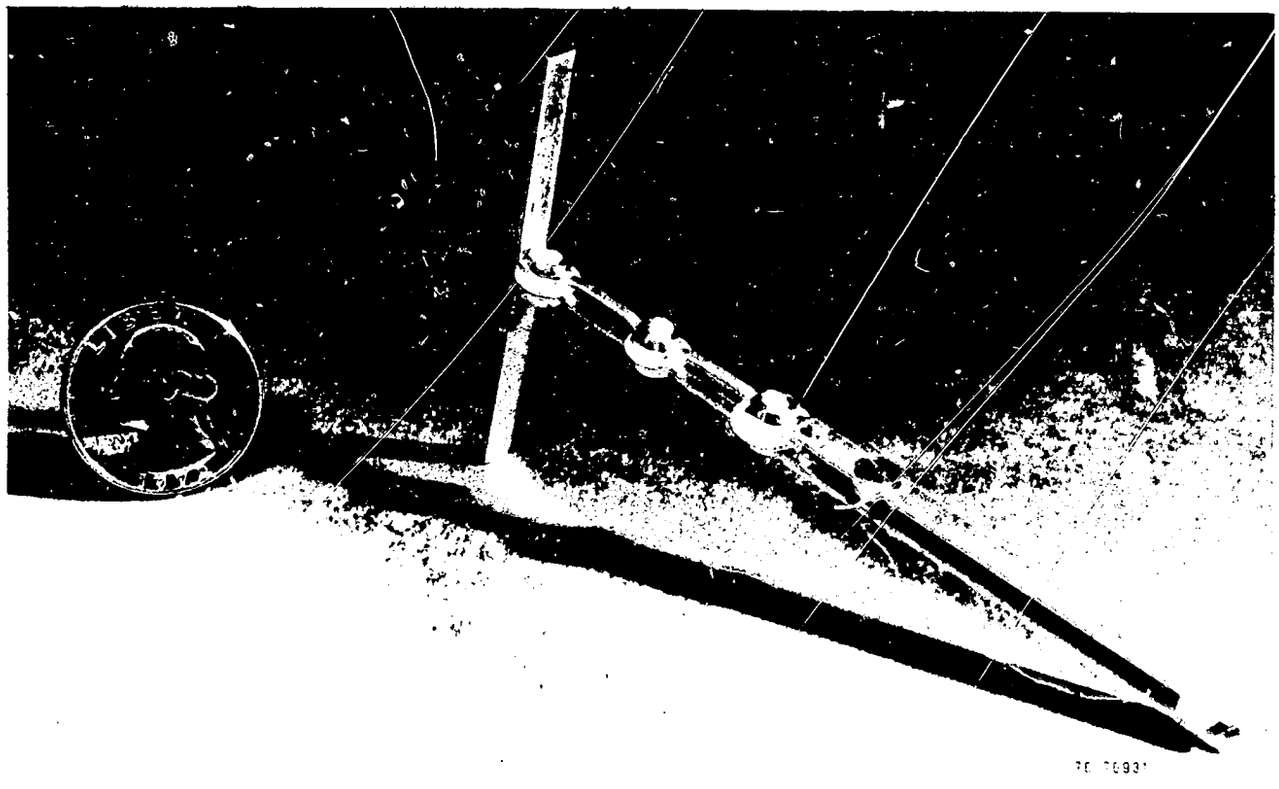

Figure 1-12. Photograph of rectenna element designed for JPL RXCV demonstration at Goldstone. This element represents the departure point for the technology development being reported upon.

The last measurements of overall system efficiency and overall rectenna efficiency were made in March of 1975 at Raytheon Company with the experimental setup shown in Figure 1-13.[10] The rectenna elements used in the rectenna array were those developed for the JPL RXCV demonstration at Goldstone but optimized for performance at 2.45 GHz. In order to establish a greater degree of credibility to the values of efficiency that might be obtained from the setup the Quality Assurance department of the Jet Propulsion Laboratory supervised the taking of the data. The overall DC to DC efficiency was measured at 54.18% with a probable error of ± 0.94%. The overall collection efficiency of the rectenna was more difficult to ascertain because of the inaccuracy in determining the fraction of the generated microwave power which is intercepted by the rectenna. The most probable efficiency, however, was 82%. A schematic of the test set up and the breakdown of efficiencies and inefficiencies is given in Figure 1-14.

The last major rectenna effort [11, 12] to be reported upon is the relatively large scale reception-conversion subsystem (RXCV) for a microwave power transmission system located at the Venus site of the JPL Goldstone facility in the Mojave desert. This effort was not undertaken as a technology development as such but nevertheless gave useful output in terms of (1) confirmation of the reliability and efficiency of advanced diode design, (2) evaluation of rectenna subarray performance with incident uniform power density, (3) protective measures to be taken to guard against rectenna failure with accidental load removal or with unusual wave-forms of the envelope of the transmitted microwave power, (4) protection of the rectenna elements from the atmospheric environment. The rectenna shown in Figure 1-15 consisted of seventeen subarrays each 1.22 meters square and containing 270 rectenna elements. The rectenna element shown in Figures 1-11 and 1-12 that was designed for this application constitutes the point of departure for the technology development program being reported upon.

The collection and conversion efficiency of this array was measured to be 82% at a total DC output of 30 kilowatts.

1.3 Progress in Rectenna Efficiency Using Progress in Rectenna Element Efficiency as an Index.

The rectenna efficiency is given by the product of the microwave power collection efficiency and the rectification or conversion efficiency. The maximum theoretical collection efficiency is 100% and it has been measured at over 99% efficiency by means of VSWR measurements of a probe in front of the array. The validity of measuring collection efficiency by this means rests upon a small amount of power being reflected from the rectenna and upon a gaussian distribution of energy in the incoming wave and in the reflected wave. These conditions are closely approximated by the set up shown in Figure 1-13 where the gaussian illumination is laid down by means of a dual-mode horn.

If it is assumed then that the collection efficiency can be made close to 100%, it follows then that the efficiency of the conversion of the collected power

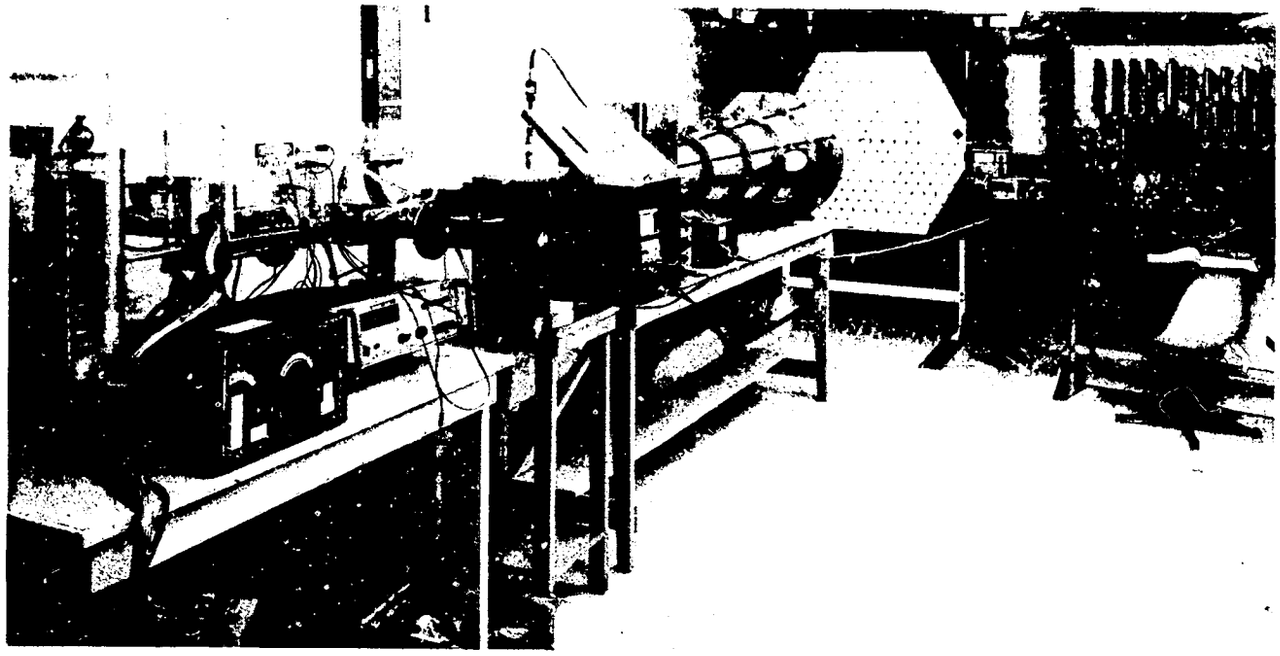

Figure 1-13. Photograph of the microwave power transmission system at the Raytheon Co. in which a certified overall DC to DC efficiency of 54% was obtained in March 1975. Magnetron at left of picture converts dc power into microwave power which is fed into the throat of the dual-mode horn. The horn illuminates the rectenna panel with a gaussian distribution of power. Rectified dc power is collected from the rectenna in circular ring paths and is dissipated in resistive loads on the test panel at the right.

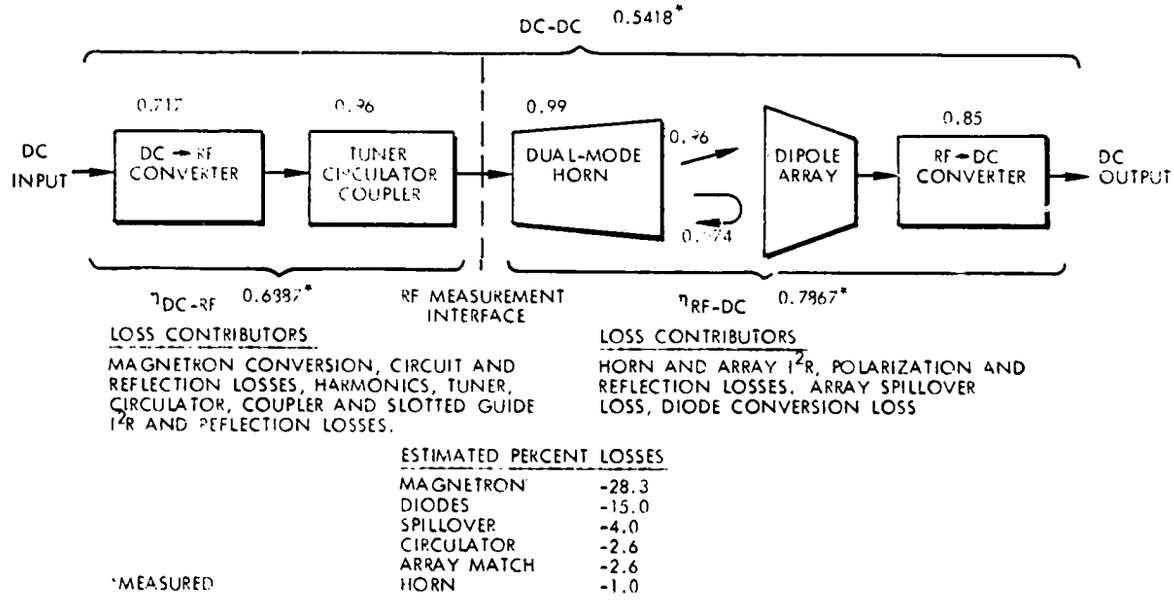

Figure 1-14. Distribution of system and subsystem efficiencies (measured and estimated) in the experiment to obtain a certified measurement of DC to DC efficiency in March 1975 at the Raytheon Company.

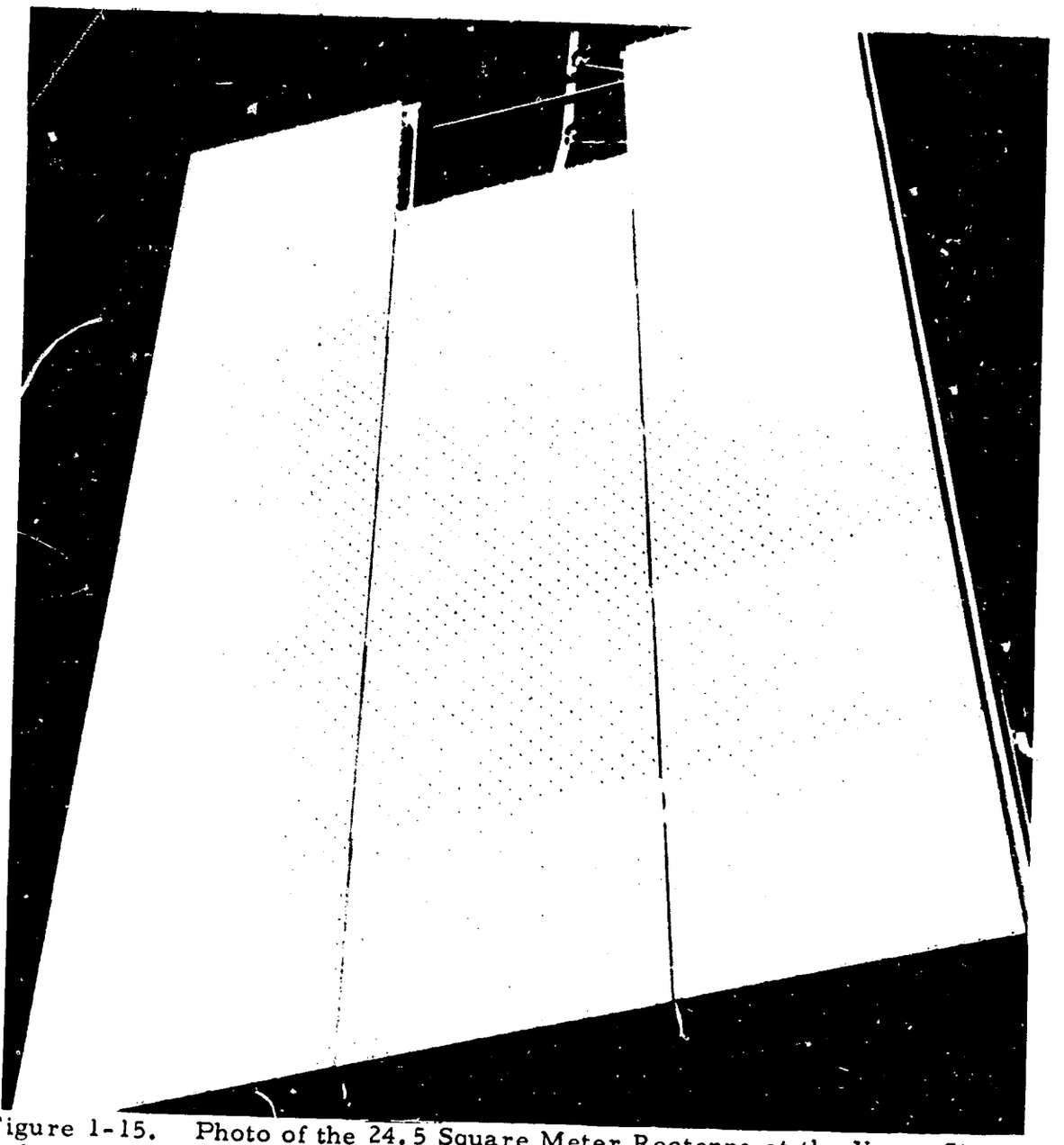

Figure 1-15. Photo of the 24.5 Square Meter Rectenna at the Venus Site of the Goldstone Facility of the Jet Propulsion Laboratory. Power was transferred by microwave beam over a distance of 1.6 km and converted into over 30 kW of cw power which was dissipated in lamp and resistive load. Of the microwave power impinging upon the rectenna, over 82% was converted into dc power. The rectenna consisted of 17 subarrays, each of which was instrumented separately for efficiency and power output measurements. Each rectenna housed 270 rectenna elements, each consisting of a half-wave dipole, an input filter section, and a Schottky-barrier diode rectifier and rectification circuit. The dc outputs of the rectenna elements were combined in a series-parallel arrangement that produced up to 200 volts across the output load. Each subarray was protected by means of a self-resetting crowbar in the event of excessive incident power or load malfunction. Each diode was self-fused to clear it from short-circuiting the array in the event of a diode failure.

into DC power is really the measure of the overall rectenna element efficiency where the rectenna element is defined as shown in Figure 1-11.

The progress that has been made in rectenna element efficiency as determined by test equipment to be described in Section 2.0 of this report is shown in Figure 1-16. According to Figure 1-16 the efficiency has now exceeded 90%. The validity of this figure is the subject of discussion in Section 2.0 of this report. The progress in efficiency is closely associated with the use of improved diodes but the choice of circuitry is also important.

1.4 The Energy Problem and the Solar Power Satellite Concept as Factors in Determining the Extent and Direction of Rectenna Development

The early stages of rectenna development were carried out in response to the need for high altitude atmospheric platforms that could stay aloft indefinitely propelled by the power beamed to them by microwaves, and for the transmission of power from one vehicle to another in space where wire transmission would be impractical. There was no generally recognized energy problem at that time and certainly no general recognition that our budding space capability could be associated with fulfilling an energy need should one exist.

Now, of course, the energy problem is well recognized, as it is also recognized that the use of electrical power is growing at a faster rate than our requirements for energy as a whole and that there is a strong indication that the electrical growth rate will be further increased as energy consumers turn to electrical power as a substitute for natural gas and oil. Unfortunately, the present methods of generating electrical power pollute the environment and consume natural resources at a prodigious rate. Under these circumstances it is only natural that we turn to the sun and investigate it as an answer to our electrical energy requirements. However, two serious problems confront us when we seek to use if for this purpose. The first problem is its diffuse nature which makes it difficult to capture in large amounts without enormously large and expensive physical structures. The second problem is its low duty cycle and only partial dependability. We can be certain of its unavailability at night, but never certain of its availability in the daytime with an intensity sufficient for electrical energy producing purposes.

Out in space in geosynchronous orbit, however, the sun is available over 99% of the time and its infrequent and short term eclipses by the earth can be precisely predicted and planned for. That desirable condition would be of no practical importance if it were not possible to place large energy collecting arrays into synchronous orbit and in some manner get that energy back to earth where it is needed. Dr. Glaser [21, 22] was the first to point out that we could combine three technologies, all developed within the past 20 years, to accomplish this task. These three technologies are (1) the new capability to transport material into space, (2) the solar photovoltaic cell which directly converts solar flux into DC electrical power, and (3) free space power transmission by means of a microwave beam. As a result of this proposal and initial feasibility study performed by a team made up of personnel from Arthur D. Little, Inc., Raytheon Company,

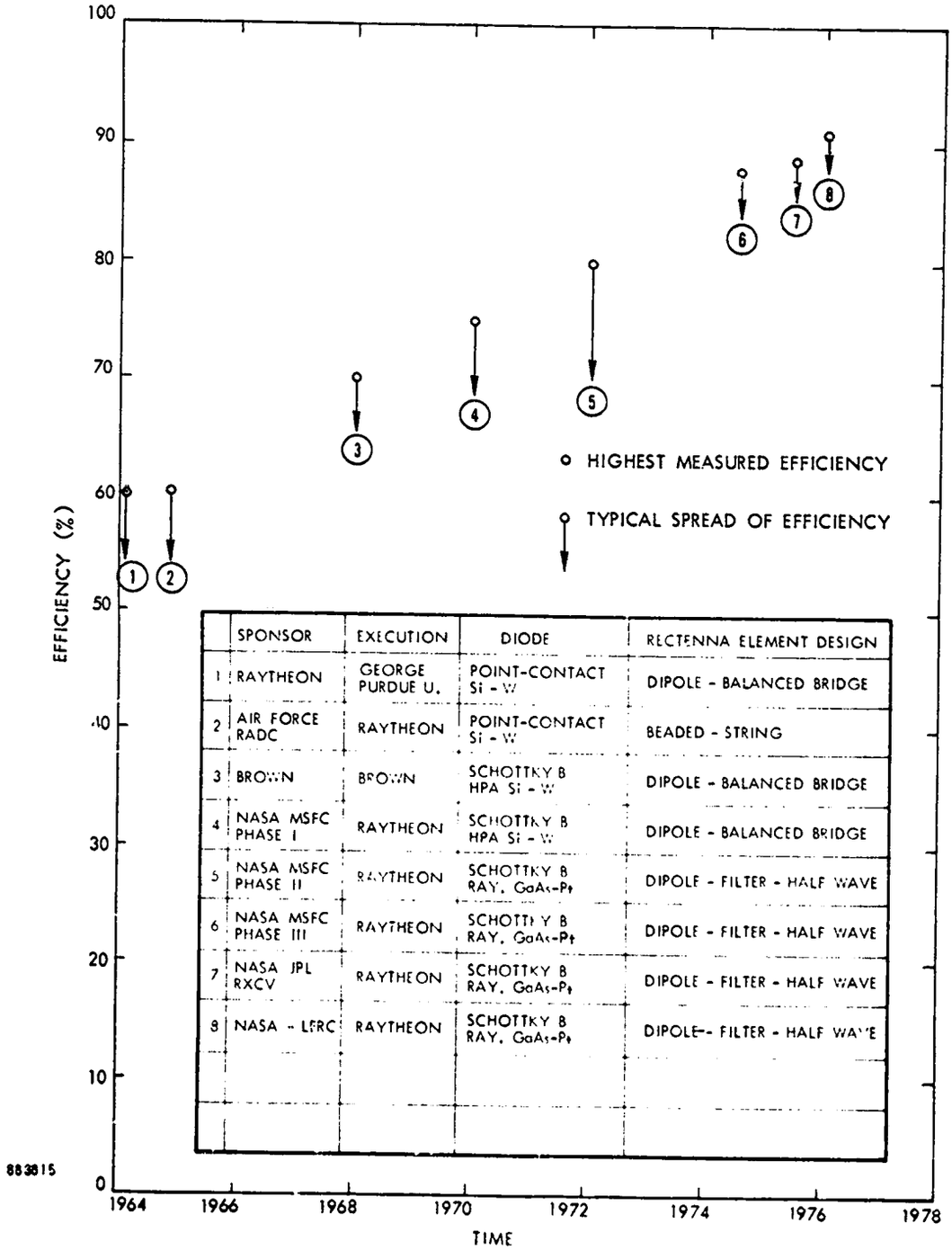

	SPONSOR	EXECUTION	DIODE	RECTENNA ELEMENT DESIGN
1	RAYTHEON	GEORGE PURDUE U.	POINT-CONTACT Si - W	DIPOLE - BALANCED BRIDGE
2	AIR FORCE RADC	RAYTHEON	POINT-CONTACT Si - W	BEADED - STRING
3	BROWN	BROWN	SCHOTTKY B HPA Si - W	DIPOLE - BALANCED BRIDGE
4	NASA MSFC PHASE I	RAYTHEON	SCHOTTKY B HPA Si - W	DIPOLE - BALANCED BRIDGE
5	NASA MSFC PHASE II	RAYTHEON	SCHOTTKY B RAY. GaAs-Pt	DIPOLE - FILTER - HALF WAVE
6	NASA MSFC PHASE III	RAYTHEON	SCHOTTKY B RAY. GaAs-Pt	DIPOLE - FILTER - HALF WAVE
7	NASA JPL RXCV	RAYTHEON	SCHOTTKY B RAY. GaAs-Pt	DIPOLE - FILTER - HALF WAVE
8	NASA - LERC	RAYTHEON	SCHOTTKY B RAY. GaAs-Pt	DIPOLE - FILTER - HALF WAVE

Figure 1-16. Progress in rectenna element efficiency as a function of time.

Grumman Aerospace Corporation, and Textron Inc., the concept was accepted for study by NASA. [23, 24] Subsequent studies supported by NASA [25, 26, 27] have not only confirmed its technical feasibility but have established the possibility of it being economically competitive in the future with conventional and other advanced approaches to electrical energy production.

One of these studies was devoted to the microwave power transmission system associated with the solar power satellite. [26] The study confirmed the previous finding that to be most economical the power rating of the systems would be large. The typical rectenna would receive over five gigawatts of microwave power, and have an area of 70 square kilometers. The maximum power per rectenna element would be 1.5 watts while the minimum would be 0.15 watts, although there is a good reason to believe that in the eventual system these power levels may be increased by a factor of two. The rectenna would have to be fully environmentally protected and have to meet cost goals by a low material cost per unit area and by a low-cost material handling operation which would convert basic materials into completed rectenna subarrays at high speed.

1.5 Objectives of the Technology Development Reported Upon in this Report

The previous sections have been included to serve as a background for understanding the appropriateness of the objectives of the technology development to be reported upon, and for understanding the approaches to achieving those objectives.

The broad objective of the effort covered in the subsequent sections of this report is to improve those features of the rectenna which are important to its function in a full scale solar power satellite system. One feature of particular importance is the efficiency associated with the rating of the individual element in the system. Surprisingly the problem is not one of power handling capability since the element has more than enough power handling capability. The problem lies rather in the reduced efficiency that is obtained at the lower power levels which are more representative of the manner in which the rectenna is used in the solar power satellite. Hence, one objective was to do those things to both circuit and diode which would improve efficiencies at lower power levels.

Another objective was to develop better instrumentation and procedures to provide better resolution in measurements and to provide a higher confidence level in the efficiency measurements being made. Finally, but of great importance, was the first iteration of an electrical and mechanical design aimed at the high speed, low-cost fabrication of a fully environmentally protected rectenna. The achievement of this latter objective is crucial to the credibility of the economic aspect of the satellite power system.

2.0 IMPROVEMENTS IN TECHNIQUES FOR MEASURING THE EFFICIENCY AND LOSSES OF RECTENNA ELEMENTS; MATHEMATICAL MODELING AND COMPUTER SIMULATION OF THE RXCV RECTENNA ELEMENT

2.1 Introduction

As indicated in Section 1.0, there have been many improvements in the rectenna over a period of time. One of the major improvements has been in the overall efficiency of the rectenna. The overall efficiency is the product of the absorption or collection efficiency and the conversion efficiency. Since it is known that the absorption efficiency is theoretically 100% and that this has been closely approached experimentally, the concern with respect to efficiency is now centered upon the conversion efficiency which is a property of the rectenna element. Improvements in conversion efficiency of the rectenna element through circuit and diode improvements have been an important part of the current technology development contract.

As incremental improvements in the efficiency of the rectenna element have become smaller, and as further techniques for improving the efficiency have become less obvious, the need has arisen for more refined measurements. The need exists for increased sensitivity of the measurements, for greater confidence in the data from which the efficiency figures are computed, and for better repeatability of measurements over an extended period of time. The need also exists for a more accurate breakdown of where the losses are occurring in the structure.

There is also the need for a tool with which to examine the current and voltage waveforms within this highly non-linear device in great detail - not only to suggest improvements in efficiency but also to anticipate failure mechanisms to which the waveforms could contribute. This may best be done by means of computer simulation.

A great deal of progress has been achieved in all of these areas during this technology development program. Much better quantitative data has been obtained in the division between circuit losses and diode losses in the rectenna elements. This data is in the form of both experimental and computer simulation data. In general, there is good agreement between the two kinds of data. The availability of this loss data has made it possible to prepare a balance sheet between the microwave power going into the system and the DC power and the losses coming out of the system. A good balance between the input and the output power and loss measurements, together with an estimate of the error involved in each of the detailed measurements involved, leads to a better confidence in the rectenna element efficiency.

The successful mathematical model and computer simulation program resulting from this study is potentially a tool of great importance. Although used with some effectiveness in this study, its application was limited because of a substantial cost involved in applying it more broadly and because of the greater priority of other items within the contract.

2.2 Techniques for Measuring the Efficiency and Losses of Rectenna Elements

2.2.1 Measurement Equipment

Raytheon Company, in part supported by contracts from Marshall Space Flight Center and Jet Propulsion Laboratory, has established a number of experimental techniques which were used to advantage in this technology development contract.[9] One of these techniques is the measurement of individual rectenna element performance in an expanded waveguide fixture which tends to simulate its behavior and performance within the cell area that it occupies in the rectenna. This is a closed system from which there is no microwave leakage. The microwave input to the fixture can be calibrated to within 0.5% of the power standard maintained at Raytheon and periodically checked at the National Bureau of Standards at Boulder, Colorado. A photograph of this set up is reproduced in Figure 2-1. The equipment is used to make accurate impedance measurements with the addition of a movable-probe VSWR indicator.

Another piece of equipment which was effectively used in the measurements program to improve rectenna element design is the unbalanced version of the rectenna element and its associated coax-line test equipment. This piece of equipment is shown in Figures 2-2 and 2-3. The technique is to use a ground plane to simulate one side of a balanced transmission line. This allows a coax line to be connected to the rectenna element so that measurements can be made over a very broad band of frequencies without the introduction of waveguide modes which would occur in the set up of Figure 2-1. This feature can be used to great advantage in the measurement of harmonic power at the input terminals of the low pass filter. Figure 2-2 shows a directional coupler placed before the VSWR probe for this purpose. Another useful aspect of the unbalanced set-up is that probes to the microwave current and voltage waveforms in the rectenna circuit of the rectenna element can be set into the ground plane.

The ground plane test fixture can also be modified as shown in Figures 2-4 and 2-5 to accommodate the two thermistors of a thermistor bridge to measure the losses in the diode. This experimental technique is based upon the fact that the heat sink of the diode cannot detect the difference between heat which is generated by microwaves and heat which is generated by DC power. The thermistor bridge can therefore be accurately calibrated with DC power dissipated in the diode. The thermistor bridge technique for measuring diode dissipation was developed under this contract.

A very important test equipment is the complete microwave power transmission system shown in Figure 1-13 in which DC to DC efficiency has been certified[10]. The major use of this equipment was to permit substitution of the two plane rectenna construction developed under this contract into the rectenna to determine its behavior in a full rectenna environment.

2.2.2 Calibration of Microwave Power Input

In a rectenna element development program it is essential that the value of microwave power input to the rectenna element under test be accurately

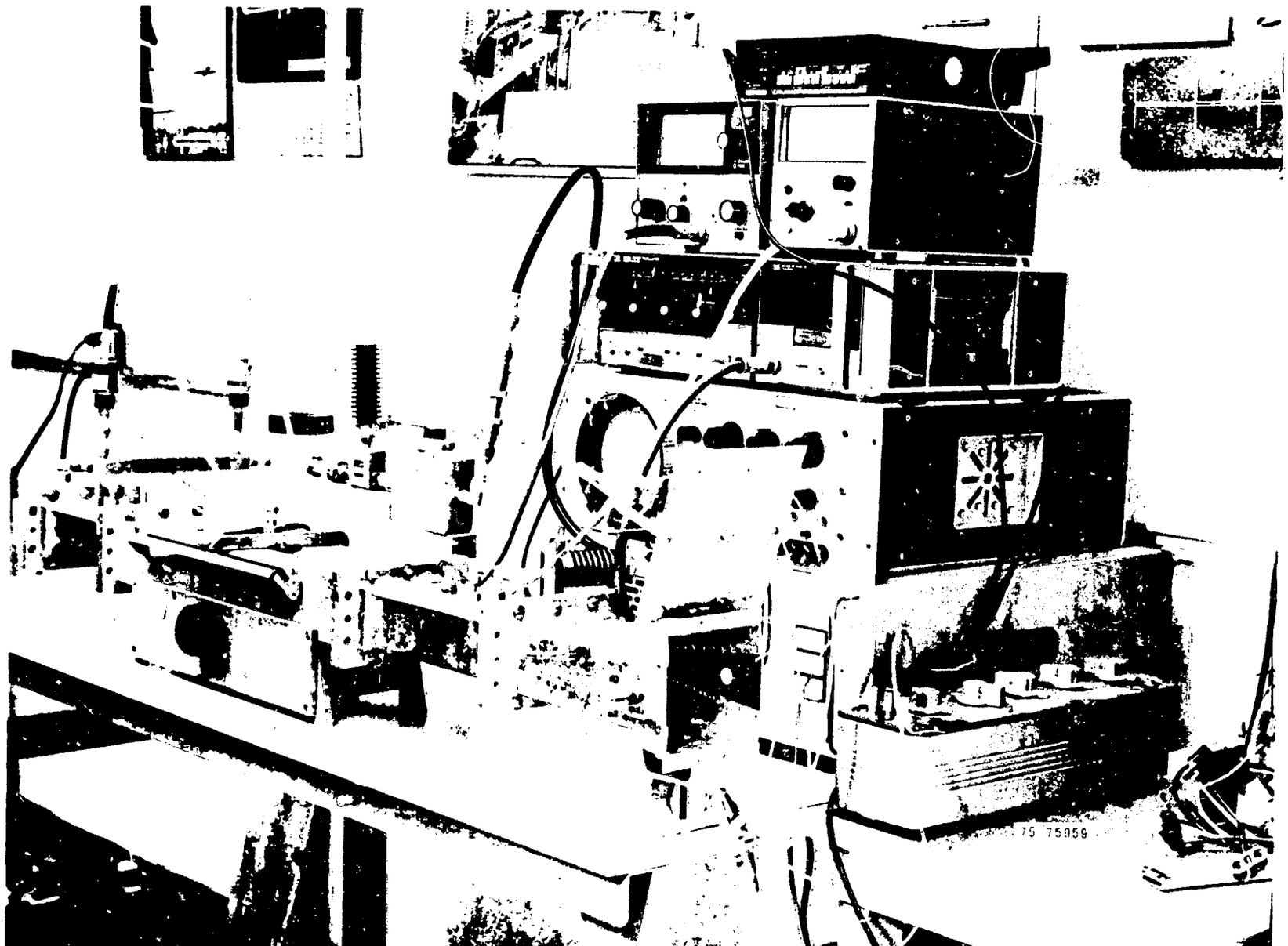

Figure 2-1. The Rectenna Element Test Arrangement Utilizing the Expanded Waveguide Test Fixture.

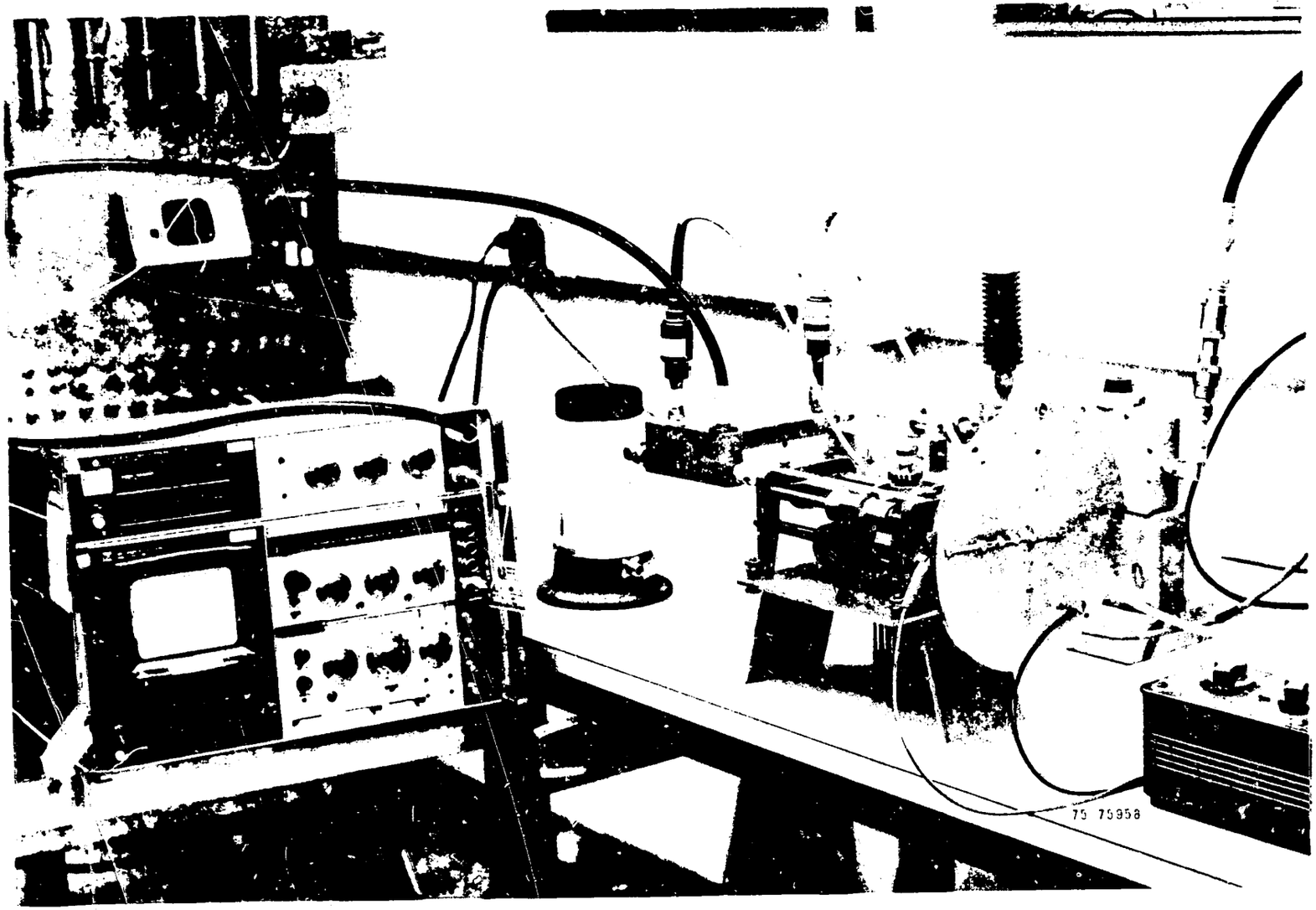

Figure 2-2. The Rectenna Element Test Arrangement Utilizing the Test Fixture with RF Ground Plane. Also shown is added directional coupler and HP analyzer to measure harmonic power level.

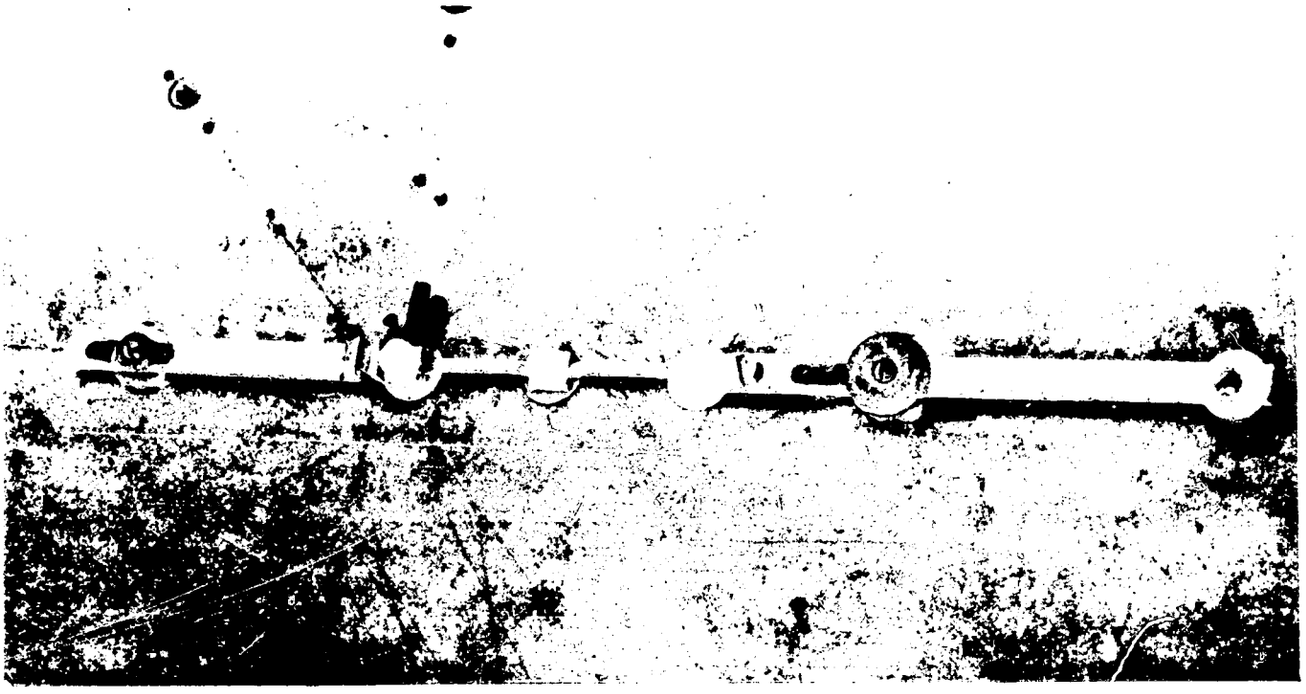

Figure 2-3. Close-up View of the "Split" Rectenna Element Mounted on the Ground-Plane Test Fixture.

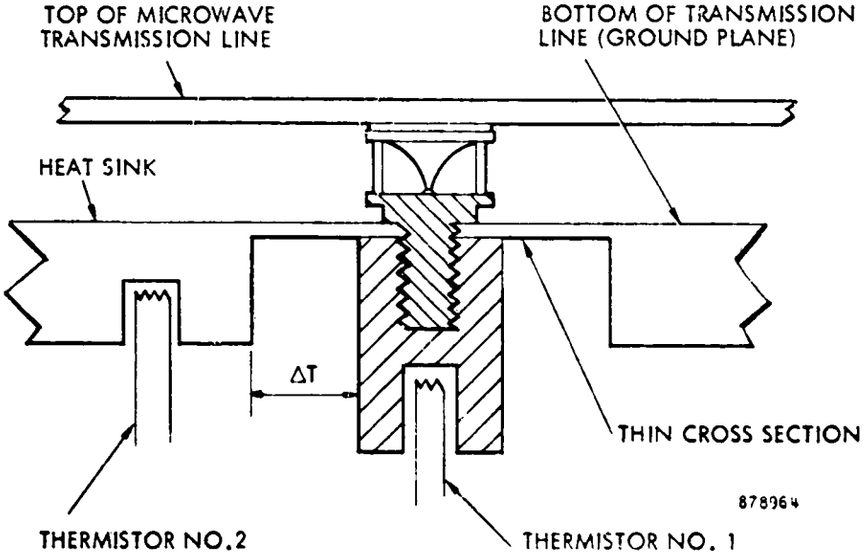

Figure 2-4. Diagram of the Arrangement for Measuring Diode Losses

Figure 2-5. View of the Back Side of the Ground-Plane Test Fixture Showing the Mounting of the Two Thermistors Which are Used in a Bridge to Measure the Diode Losses. The Thermistors Measure the Temperature Drop Across the Heat Flow Path from the Diode Heat Sink to the large Heat Sink of the Heavy Brass Plate.

established. The efficiency of the rectenna element as given by the ratio of DC power output to microwave power input depends upon it. Moreover in this development dealing with refinements in efficiency, an efficiency improvement of 1% is important. It is therefore necessary that the measurement sensistivity be considerably less than 1%, and it is desirable that repeatability in the measurement of efficiency be within a small fraction of 1%.

The microwave power standard that is used at Raytheon was calibrated at 2450 MHz at the National Bureau of Standards in Boulder, Colorado in the summer of 1975. The probable error in this calibration was ±0.34% *

It is estimated that another probable error of 0.5% is involved in the calibration of the test set-ups at the two to ten watt level where the use of a calibrated attenuator is necessary, and about 0.3% at the 100 milliwatt level. The 100 milliwatt level is the same level as the calibrated standard so it is not necessary to use calibrated attenuators at this power level. Calibrations were made for both the expanded waveguide test fixture and for the fixture with the RF Ground plane.

The block diagram for the calibration of the incident microwave power upon the rectenna element test fixture with the use of the Raytheon microwave power standard calibrated by the Bureau of Standards is shown in Figure 2-6. The power standard is placed at the point where the test fixture attaches and the 432A power meter or other suitable power meter is calibrated against this standard. This arrangement eliminates the errors in the calibration of the directional coupler and in the power meter itself. A digital readout is used on the power meter to eliminate operator error in reading the power meter.

Calibrations at the 90 milliwatt level and at the 4 watt level were made for each of the two test fixtures. The microwave power standard itself is calibrated at the 90 milliwatt level. It is therefore necessary to insert calibrated incident power at the 4 watt level. The block diagram shows this attenuation to be 15.95 dB.

Precaution is taken to eliminate errors in the calibration of incident microwave power, and errors in subsequent efficiency measurements on rectenna elements, caused by reflections of power at various interfaces in the system. The reading of power in the forward direction is affected by any reflection of reverse directed power from an impedance mismatch at the source. By means of the three port circulator and the coax matching section, this reverse directed power can be absorbed so well that the resulting forward directed power can be held to less than one percent of the reverse directed power. The result of this adjustment is that a change from a match condition to a full short at the input

---

* The uncertainty of the accuracy of the microwave power standard will be a major factor in obtaining an accurate efficiency measurement on the rectenna element. For this reason, the present calibration of the Raytheon standard has been discussed with Mr. Paul Hudson, Program Chief, RF Power, Current and Voltage Section of the National Bureau of Standards, Boulder, Colorado. His statement to me was that if a perfectly matched termination is used on the standard, a 2-sigma confidence level corresponds to a ± 1% error. It follows that the probable error is ± 0.34%.

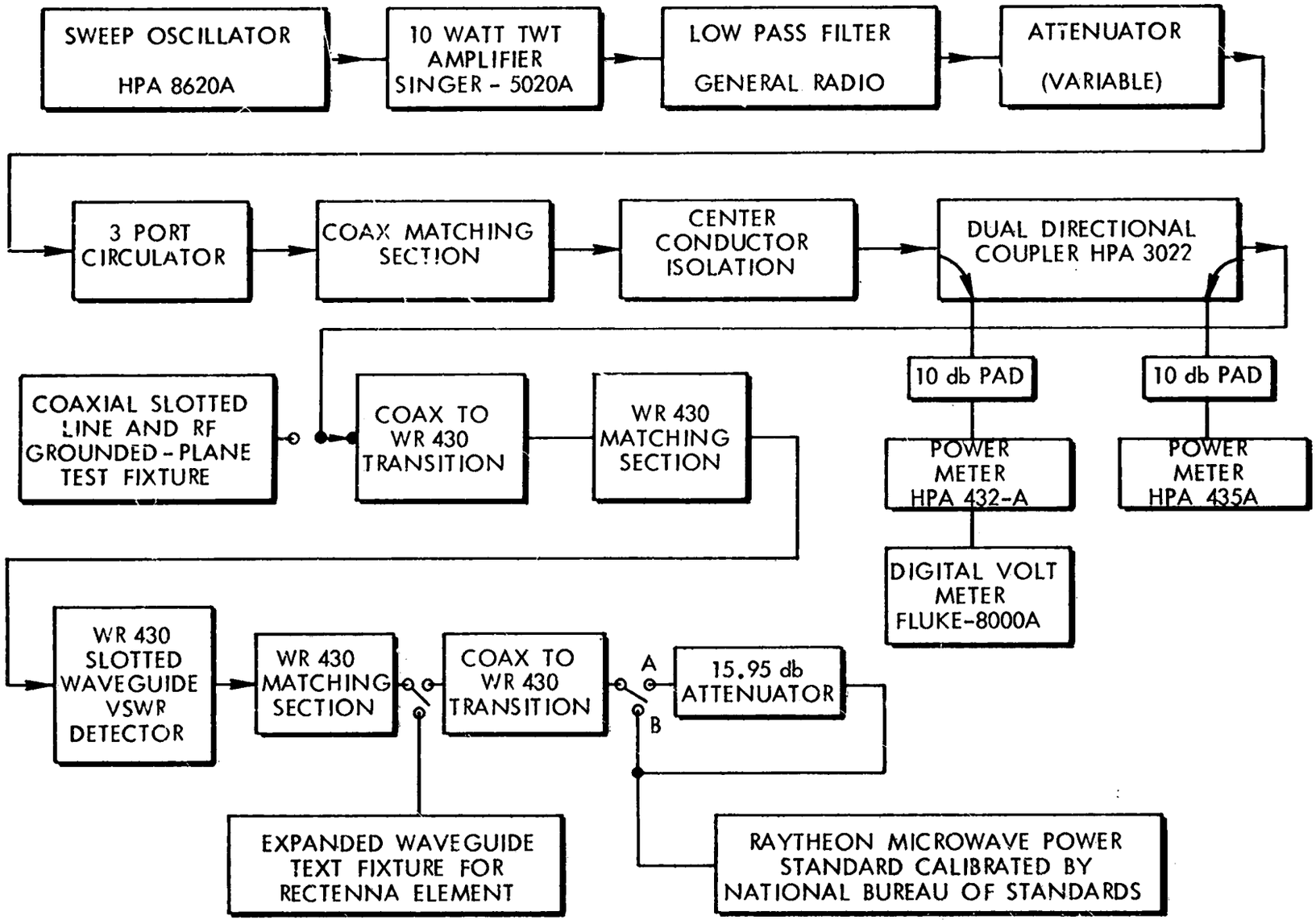

Figure 2-6. Schematic Arrangement of Test Equipment for Calibration of Incident Microwave Power at the Input to the Rectenna Element Test Fixture.

to the rectenna element test fixture will cause the measurement of incident power to vary by only 1%. Since the measurement of rectenna element efficiency takes place under reasonably well matched conditions, we can be well assured that the measurement of incident power is affected to less than 0.1% by reflected power during any efficiency measurement of rectenna elements.

Likewise, any errors in the measurement of reflected power from the expanded waveguide test fixture that might be caused by a mismatch in the coax to waveguide transmission unit is eliminated by terminating the WR 430 waveguide at the normal point of attachment of the expanded waveguide test fixture with a precision-matched waveguide termination load and then adjusting the waveguide matching section near the coax to waveguide transition so that a minimum of reverse power is indicated by the directional coupler.

In the use of the microwave power standard for calibration purposes, any reflected power from the standard and from the waveguide-to-coax transition is matched out to a reflection of less than 0.02% as measured by the slotted waveguide VSWR detector by adjustment of the matching section located on the outboard side of the slotted waveguide detector.

Finally, in order to eliminate any measurement error caused by 2nd and 3rd harmonic output from the 10 watt TWT Amplifier, a low pass filter was inserted between the TWT and the input to the measurement system.

2.2.3 Measurement of Diode Losses

The basis for being able to make accurate measurements of microwave losses in the diode is that the heat flow geometry for getting rid of the heat from dissipation losses in the semiconductor chip in the diode package is the same whether the heat comes from insertion of DC power or from microwave power. (It is assumed that all of the microwave losses and all of the DC losses taking place within the diode envelope originate in the semiconductor chip.) If it is then possible to build a sensitive sensor to indicate the heat flow from the diode, one can calibrate this sensor by the injection of accurately measured DC power into the diode. The sensing arrangement for doing this is shown in Figures 2-4 and 2-5.

The bridge consisting of two thermistors was used primarily because of the great sensitivity of the thermistors to a change in temperature. One thermistor was placed adjacent to the heat sink of the diode while the other thermistor was placed in the larger system heat sink across an impedance to the heat flow.

A number of factors are of interest in this arrangement. One of these, of course, is the sensitivity of the system or how small an increment of heat dissipation it will resolve. Another is the system noise. The response of the system to a change in the heat input to the diode is of interest. Still another is the linearity of the system and its sensitivity to a change in the ambient temperature of the heat sink.

In discussing the data that was taken to respond to these areas of interest it should be realized that the object was to develop this method to the point of usefulness in our measurements and not to refine it to its fullest capability.

The sensitivity of the arrangement is best indicated by the measurements that were made in the calibration process and by the residual drift in the system. Figure 2-7 shows a typical calibration curve of output of the thermistor bridge as a function of DC power dissipated in the diode.

The slope of the curve shown in Figure 2-7 is 0.188 millivolts per milliwatt. On the other hand as Figure 2-8 indicates, the drift of the zero on the thermistor bridge shows that a variation of as much as 0.4 millivolts can occur within a time period of a minute. Thus it would appear that the resolution of the system is in the range of two milliwatts. Larger variations that occur over a time period of several minutes can be eliminated by rebalancing the thermistor bridge.

Figure 2-9 indicates the typically fast response time of the measuring system to a step function of applied or removed power. The time constant is nine seconds, so that the steady state is reached in less than a minute. About one minute was allowed for taking a point of data if a high degree of accuracy was wanted.

The ambient temperature of the system heat sink has an impact upon measurement accuracy and should be taken into consideration by taking the experimental data at the same ambient temperature at which the thermistor bridge is calibrated. The mass of the heat sink is about 2000 grams and its heat storage is about 160 calories or about 670 watt seconds. Hence, if there were no other means of dissipating the heat than absorbing it in the mass of the brass plate, about 20 minutes would be required for the plate to increase its temperature by one degree Centigrade.

2.2.4 A Check on Measurement Accuracies by Balancing Measurements of Input Microwave Power Against the Sum of the Measurements of DC Power Output, Diode Losses, and Circuit Losses

A primary objective of the measurement portion of this technology development program has been the development of measurement techniques which will provide high confidence in the measured rectenna element's overall efficiency and which will also provide an accurate measurement of the major losses in the system. This objective has been achieved by measuring the microwave power input as accurately as possible and comparing this with the sum of the DC power output, the diode losses, and the circuit losses.

All of these measurements have some error associated with them. The DC power output measurement has a relatively small error associated with the measurement of voltage across a known resistance. The probable error of these measurements is estimated to be ±0.20% of the absorbed microwave power.

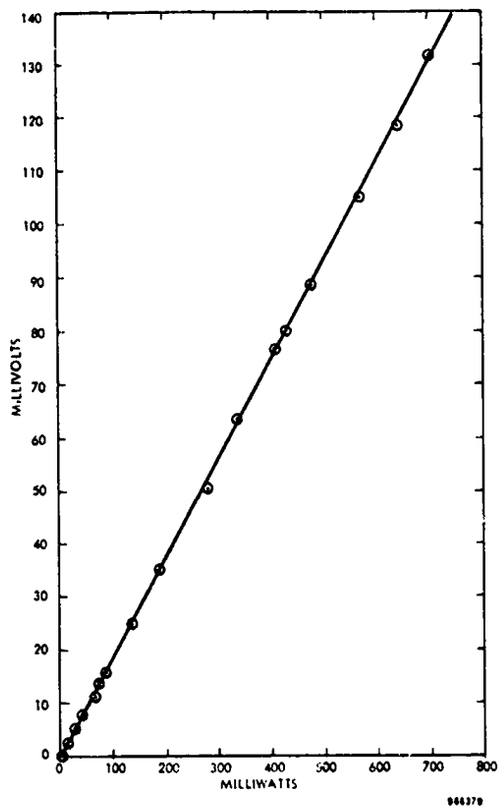

Figure 2-7. Typical Calibration Curve

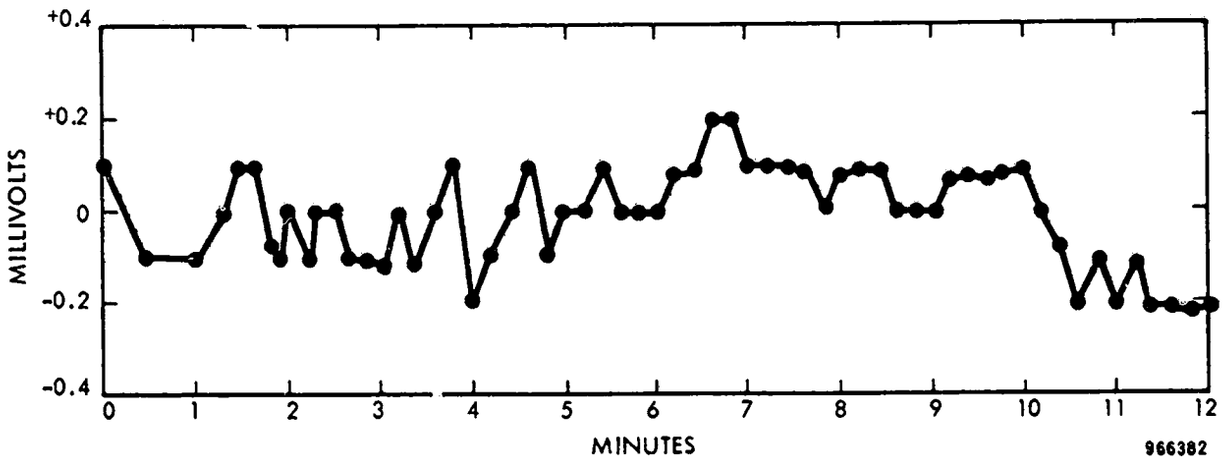

Figure 2-8. Zero Drift on Thermistor Bridge

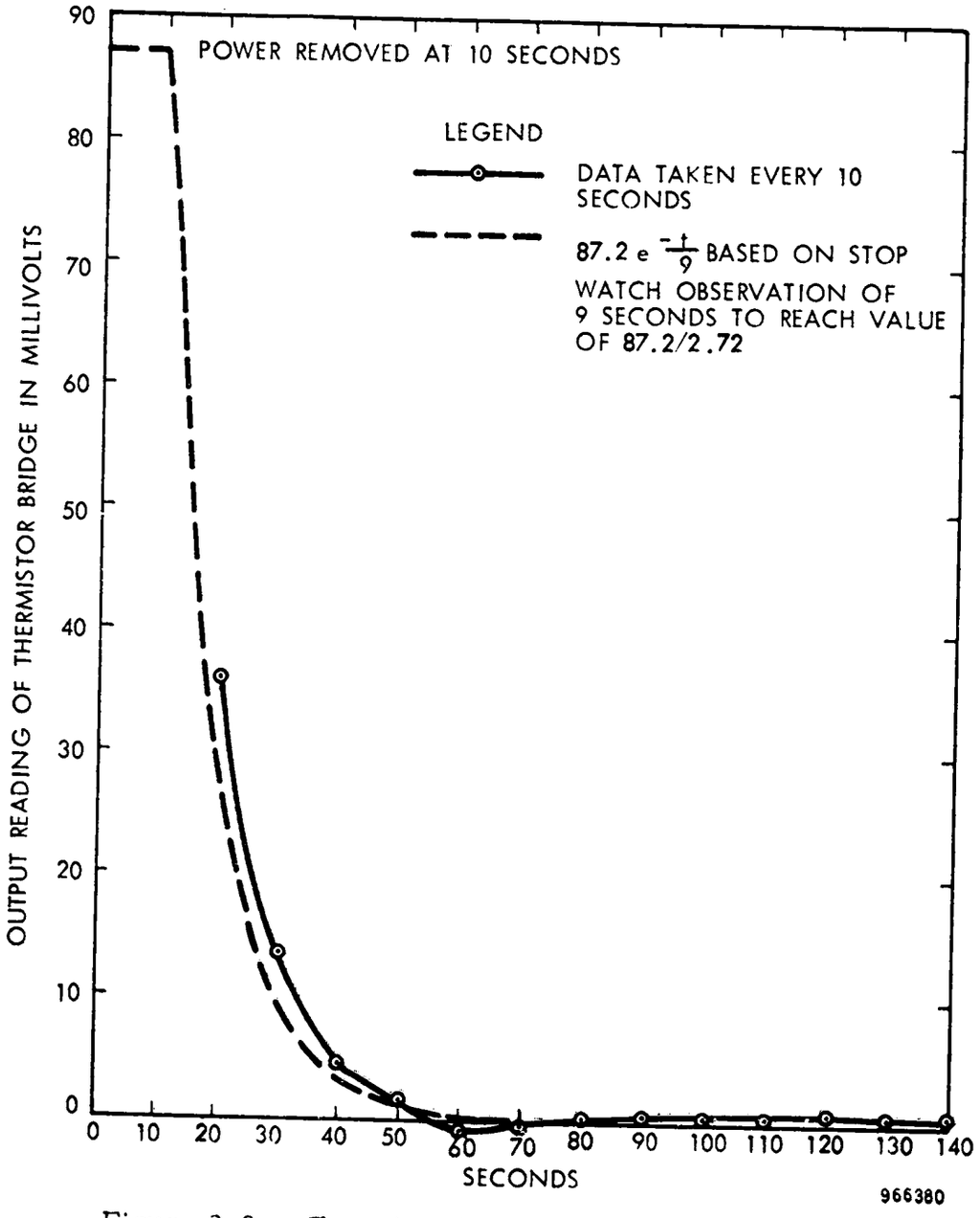

Figure 2-9. Transient Response of Thermistor Bridge to step function of DC Power Input.

The diode losses are accurately measured by the technique described in Section 2.2.3. The measurements themselves are accurate to within 2% at diode loss levels corresponding to incident power levels of two watts or more. Since the diode losses at these power levels are typically less than 10% of the absorbed microwave power, the measurement uncertainty with respect to the absorbed microwave power corresponds to a probable error of 0.2%. This of course, is considerably better than the measurement of the microwave power input and no further refinement is necessary.

The measurement of the circuit losses (other than those in the diode itself) represent the remainder of the energy output of the system. Getting an estimate of these losses can be approached in two ways. One of these is by computer simulation to be discussed in Section 2.3. In the mathematical model the skin resistances in the circuit are modeled and given a value. An accurate computation of power losses is then provided by the computer simulation of the overall functioning of the rectenna element. Typically, all of the circuit losses amount to 2.15%, of which 1.9% represents circuit losses in the microwave input filter, and 0.25% is the remainder. However, the validity of the results from computer simulation depend upon the assumptions made with respect to skin resistance.

Another approach to establishing these losses is to make an insertion loss measurement upon the input filter which the computer simulation (as well as simpler analysis) indicates is the major portion of the circuit losses. These losses were measured to be 2.37% ± 0.3% at the fundamental frequency, and seen to be 0.47% higher than those obtained by computer simulation. They are believed to be more valid because no assumptions of the skin resistance were needed. We have decided to use the measured value of 2.37% for the input filter losses and to add to this the 0.25% for the rest of the circuit losses as determined by computer simulation. Thus, the circuit losses are established as 2.62% and the probable error associated with this is 0.4%.

The probable error of the individual measurements is listed below:

P.E. of microwave power input measurement	±0.6% of absorbed microwave power
P.E. of diode dissipation losses	±0.2 of absorbed microwave power
P.E. of circuit losses	±0.4% of absorbed microwave power
P.E. of D.C. power output measurement	±0.2% of absorbed microwave power

From the listing, the composite probable error of balancing microwave power input against the sum of dc power output, diode losses, and circuit losses may be computed. It is found to be ±0.75%.

In Table 2-1, the DC power output, diode losses, and circuit losses are given in terms of their ratio to the absorbed microwave power in the

TABLE 2-1

DC Power Output, Diode Losses and Circuit Losses as % of Absorbed Microwave Power *

A Incident Microwave Power Level	B DC Load Resistance (ohms)	C Absorbed Power in Element Watts)	D Reflected Power (Watts)	E DC Output as % of C	F Diode Losses as % of C	G Measured and Computed Circuit Losses % of C	H Total Measured Losses and DC Power Output E + F + G	I 100% - H
0.100	80	0.085	0.015	56.50	36.0	2.62	95.12	4.88
0.200	80	0.180	0.020	66.70	28.26	2.62	97.58	2.92
0.400	80	0.375	0.025	74.30	21.86	2.62	98.78	1.22
0.600	80	0.573	0.027	77.80	18.84	2.62	99.26	0.74
0.800	80	0.772	0.028	80.00	17.34	2.62	99.96	0.04
1.000	80	0.991	0.009	82.30	14.30	2.62	99.22	0.78
2.000	80	1.997	0.003	86.12	11.33	2.62	100.07	-0.07
3.000	80	3.000	0.000	87.60	10.17	2.62	100.39	-0.39
4.000	80	3.998	0.002	88.45	9.24	2.62	100.31	-0.31
5.00	80	4.992	0.008	89.06	8.77	2.62	100.45	-0.45
6.00	80	5.984	0.016	89.50	8.39	2.62	100.51	-0.51
7.00	80	6.972	0.028	89.95	8.11	2.62	100.68	-0.68
8.0	80	7.957	0.043	90.26	7.93	2.62	100.81	-0.81
8.0	90	7.938	0.062	90.59	7.51	2.62	100.72	-0.72
8.0	100	7.850	0.150	90.54	7.40	2.62	100.56	-0.56

* Test made use of grounded-plane test fixture and diode No. 40593 - CPXIG No. 13, a GaAs-Pt standard reference diode.

** This value is a composite of following measured and computed inputs.

Measured loss at fundamental frequency in microwave input filter is 2.37% ± 0.3%

Computer simulation of loss including harmonics in input filter is 1.83%.

Computer simulation of other circuit losses is 0.25%.

Computer simulation of all circuit losses is typically 2.08%.

The decision was to add the measured input filter loss at 2.37% to the 0.25% "other circuit losses" computed by computer and add an uncertainty factor to give 2.62 ± 0.4%.

rectenna element over a wide range of power levels. The efficiency of the rectenna element as measured by the ratio of DC power output to microwave power absorbed is seen to vary from a low of 56% at 100 milliwatts of incident power to 90.5% for a power input of 8 watts. The diode losses are observed to vary from 36% to 7.4% of the absorbed microwave power. The circuit losses are assumed to remain constant at 2.62%. When the DC power output is added to the sum of the diode losses and circuit losses the total sum as represented as a percentage of the absorbed microwave power is seen to be very close to 100% and within the probable error of 0.75% previously established, over an appreciable portion of the range of input power levels examined.

All of the data given in Table 2-1 was obtained with the use of the ground-plane test fixture shown in Figure 2-2, since the diode loss measurements can only be made with the aid of this test fixture. The measurements were also made with the use of diode 40593-CPX1G #13 which was one of the standard reference diodes obtained from the RXCV program. The Schottky barrier was platinum on Gallium Arsenide. A metallic shield was placed over the rectenna element to improve the efficiency.

Most of the information given in Table 2-1 is given in graph form in Figure 2-10.

Of especial interest is the manner in which the diode losses are shown to vary in Figure 2-10. The diode losses follow very accurately a curve described by the equation:

$$\text{Diode Loss } \% = \frac{A}{\sqrt{P_{in}}} + B \quad \text{as a function of input power level.} \tag{1}$$

where for the curve of diode losses in Figure 2-10

$$A = 10.04$$
$$B = 4.212$$

The first term in the expression also closely approximates the following relationship

$$\frac{0.90 \text{ Volt}}{0.90 \text{ Volt} + \text{DC voltage across load resistor}} \tag{2}$$

in which 0.9 volt represents a fixed voltage drop in the forward direction independent of current level and is analogous to the brush drop in a DC generator or motor. Therefore, it is seen that the diode loss in the particular diode observed has a constant term B which amounts to 4.22% of the absorbed microwave power and a variable term $\frac{A}{\sqrt{P_{in}}}$ which reflects the relationship of a fixed voltage drop across the Schottky barrier to the total dc voltage developed. For good efficiency it is obvious that this voltage drop should be as low as possible, and this is the prime reason for shifting to a GaAs-W barrier in the Schottky diode.

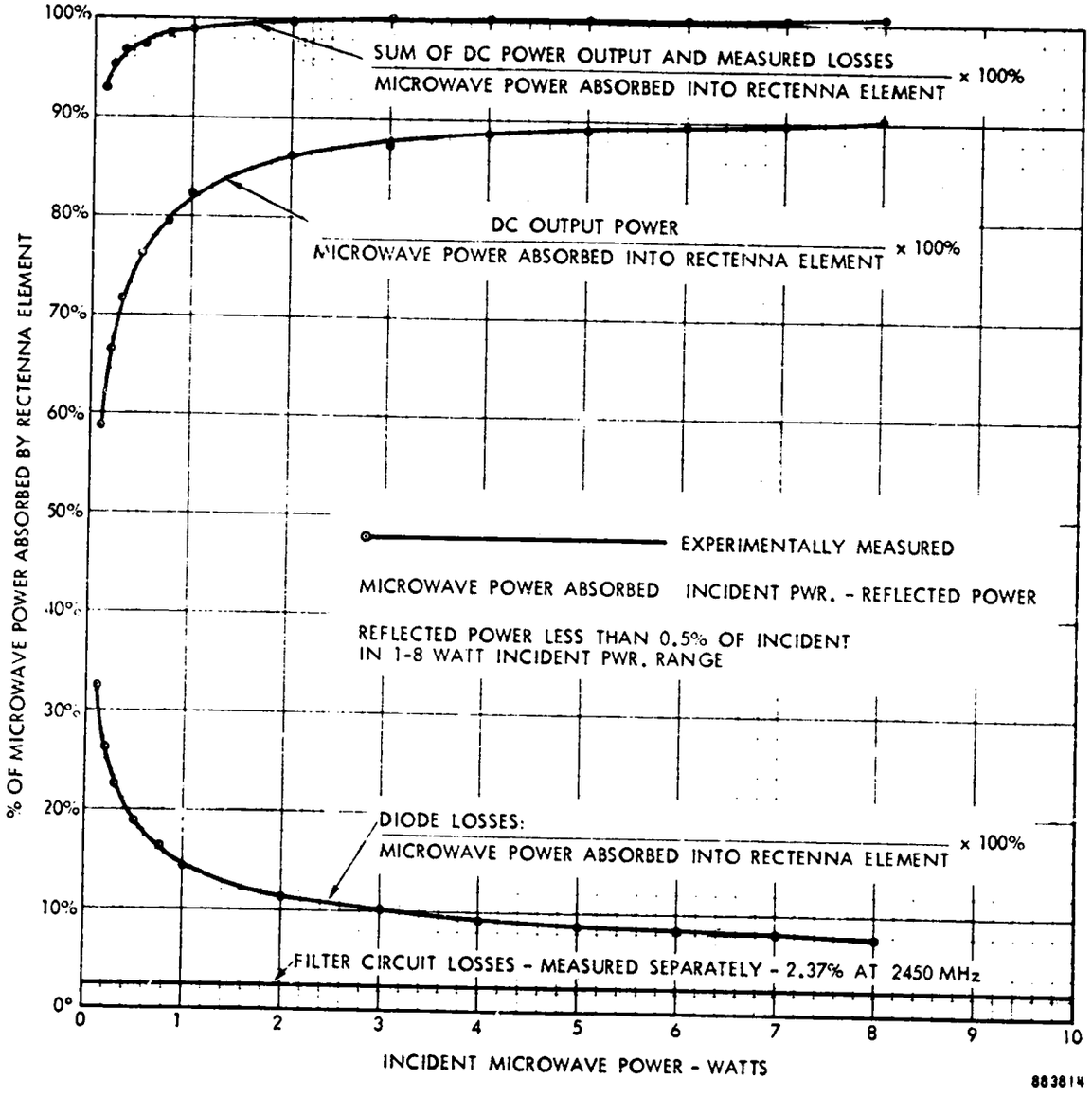

Figure 2-10. The DC power output, losses in the microwave diode, and losses in the input filter circuit are shown as a percentage of the microwave power absorbed by the rectenna element as a function of incident microwave power level. The sum of all of these is then compared with the absorbed microwave power.

In conclusion it is observed that the balancing procedure just described and used in one example greatly improves confidence in the accuracies of all the measurements. The establishment of probable errors for each of the individual measurements eliminates the possibility of two or more gross measurement errors offseting each other to provide false confidence. Even greater confidence results from including further results of computer simulation to be described in Section 2.3.

In the quest for higher efficiency, it is noted that the diode itself is the greatest source of loss particularly at the lower power levels. The circuit loss at approximately 3% is relatively small and tends to be independent of power level. However, at the lower power levels, it may be found that a circuit which greatly reduces the diode losses may significantly increase the circuit loss.

2.3 The Development of a Mathematical Model of the Rectenna Element Together with Computer Simulation Program and its Use

2.3.1 Introduction

A major feature that characterizes the present standard design of the rectenna element that has been used in the establishment of 54% DC to DC microwave power transmission efficiency and in the successful JPL demonstration of power transmission over a distance of 1.6 km is the use of a single diode shunted across a transmission line and used as a half-wave rectifier. This approach was adopted in 1972 and represented a distinct departure from the full wave bridge rectifier design that had been used up to that time with a high degree of success. A principle reason for the departure was a simultaneous recognition of the need for a better understanding of the functioning of the rectenna element and the difficulty of analyzing the device because of the complexity introduced by its high non-linearity and harmonic contect for the wave forms. Obviously, if an analysis were to be attempted, the initial effort would be made easier by the simpler math model afforded by the half-wave rectifier approach. A substantial start on such a mathematical model and computer simulation program was made by E. E. Eves of Raytheon at that time but the contractual support was not sufficient to finish the work. [9]

Meanwhile, many advantages afforded by the rectenna element with a half-wave rectifier had become evident. Acceptable efficiencies were being measured, and it was recognized that for the "power from space" application a single GaAs diode would adequately handle the power requirement placed upon a single rectenna element.

With the realization of an apparently efficient and practical rectenna element the role of a computer simulation program has shifted to an exploratory tool for further optimization of the efficiency and to help expose any phenomena that might be a source of trouble at some time in the future but which had thus far not been detected experimentally. It is of interest that one such phenomena seemed to have been uncovered. This will be discussed later in this section. In this connection, it has been generally noted that many subtle problems are encountered in the production of items that were never encountered in their development, simply because the production situation presents a better chance

for an unusual mix or an unusual alignment of factors necessary for the occurrence of the phenomena.

From the viewpoint of optimizing efficiency, the computer simulation program will become very valuable in the future, because it is possible to change one parameter and observe its effects upon efficiency while the other parameters remain constant. This is often difficult to do experimentally if we are dealing with a resolution of 0.1% in efficiency. It is also probable that the chance alignment of parametric factors becomes more important as efficiency refinements deal with small improvement in efficiency, say from 91% to 92%. Obviously such computer simulation becomes very valuable in a quality assurance program where the objective is to maintain efficiency within very tight tolerences and above all to avoid highly destructive mechanisms.

In 1975 Dr. Joseph Nahas [28, 29] reported upon Math modeling and computer simulation that he had successfully carried out for a rectenna element modeled after the standard RXCV rectenna element in many respects. The contract for which this final report is being written was issued in 1975 and contained a task in which the RXCV element was to be math modeled and its operation simulated with a computer program. This aspect of the contract was assigned to E.E. Eves of Raytheon. He was assisted by Phil Knight. They requested and obtained a copy of Nahas's computer simulation program, which was of considerable aid to them.

Although Nahas's basic approach to the problem was very similar to that which had been taken by Eves in the earlier time period [9], Dr. Nahas's program was not used directly or modified for two reasons. It did not directly model the RXCV element, and the detail of the math modeling was so great that the computer time to obtain performance data represented an expense that the present contract could not support. Further, we wanted to compare the results of the computer simulation with experimentally measured values of diode dissipation and the latter could be obtained only with the use of the ground-plane fixture which omits a consideration of the half wave dipole input. Hence, the modeling of the antenna was eliminated. This provided considerable simplification. The skin losses were modeled only for the fundamental frequency and the number of filter sections to be modeled was two rather than five in the Nahas model. This represented additional simplification. However, every effort was made to simulate the diode characteristics and function very accurately, starting with the most basic characteristic of the junction itself. Further precautions were taken in setting up the program to eliminate computer errors at points of sharp discontinuity. Predictor-corrector routines were incorporated as they were in the Nahas program.

Both the Nahas and the Eves-Knight computer simulation programs depend upon watching the buildup of the current and voltage waveforms from a transient to a steady state condition in the rectenna element after the step application of microwave power input. The convergence to a steady state condition for the Eves-Knight program requires about 20 cycles. The number of steps within a cycle is 8192 and a printout is made of designated parameters 128 times at equal intervals in the last cycle. The computer time required to obtain the results from one set of input parameters is 3 minutes on a CDC6700 computer. The cost is about $20.00 per set of data.

The Eves-Knight computer simulation program records the losses within the rectenna element, divided up into approximately twenty locations. It computes harmonic coefficients up to the fifth harmonic in a Fourier analysis of five different wave forms. It prints out several key currents and voltages as a function of time.

The complete description of the Eves-Knight math-modeling and computer simulation program and one example of its use and print out of data is shown in Appendix A. In the remainder of this section a brief introduction to the modeling and some typical results of the computer simulation will be presented. The results of the computer simulation will then be compared with the experimental data obtained from the ground plane test set up.

2.3.2 Mathematical Model of the Rectenna Element

The electrical schematic model of the rectenna element in its simplest form is shown in Figure 1-11. The element is seen to consist of half-wave dipole antenna, a two section low-pass filter, and a rectification circuit consisting of a Schottky-barrier diode in shunt across the circuit, an inductive section of line to resonate with the diode capacitance, and a capacitance to store energy and to remove harmonic content in the DC output power. The dipole antenna is matched to space, and the characteristic impedance of the filter is matched to the terminal impedance of the dipole. The input low pass filter, in addition to attenuating harmonic power, also acts as a buffer between the sinusoidally periodic input and the abrupt switching action of the diode.

This simplistic model is not at all adequate for a computer simulation program. The behavior of the diode needs to be modeled in great detail. The sections of transmission line which are a portion of the low pass filter need to be broken down into short sections so that the lumped-network equivalent of these sections will suitably handle the higher harmonic currents which will flow in the filter sections. The computer simulation program is completely in the time-domain. The manner in which this is done, the number of divisions made, and the assignment of values of R, L and C to these divisions is clearly explained in Appendix A.

2.3.3 A Representative Set of Data Resulting from the Use of the Computer Simulation Program

Figure 2-11 represents a simplified schematic of the circuit elements of the mathematical model for the computer simulation program presented in Appendix A. The chief purpose of Figure 2-11 is to indicate the current and voltage parameters which are presented as a function of time during the rf cycle in Figures 2-12 and 2-13 respectively.

The particular set of data corresponds to the test arrangement for the RXCV circuit element and diode on the ground-plane test fixture. The dc power output level is 2.969 watts and the load resistance is 80 ohms - the value usually used for tests in the ground-plane test fixture. The complete set of data is given in Appendix A together with the graphs replotted in this section as Figures 2-12 and 2-13.

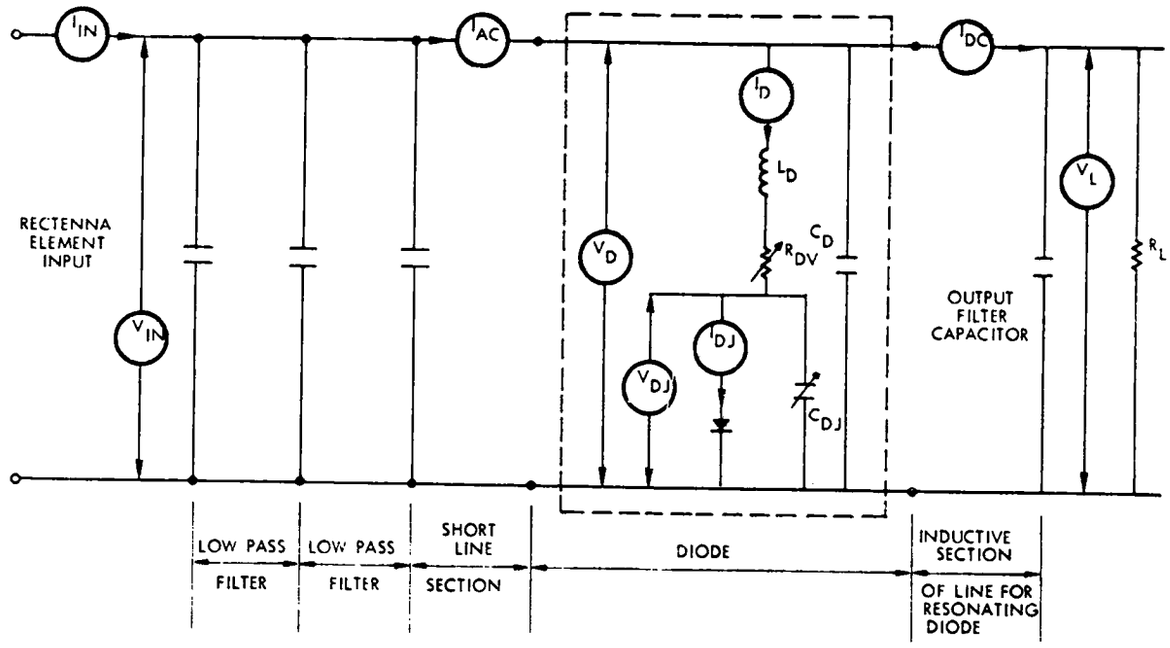

Figure 2-11. Simplified Math-Model Schematic Diagram for Interpreting Computer-simulation results presented in Figures 2-12 and 2-13.

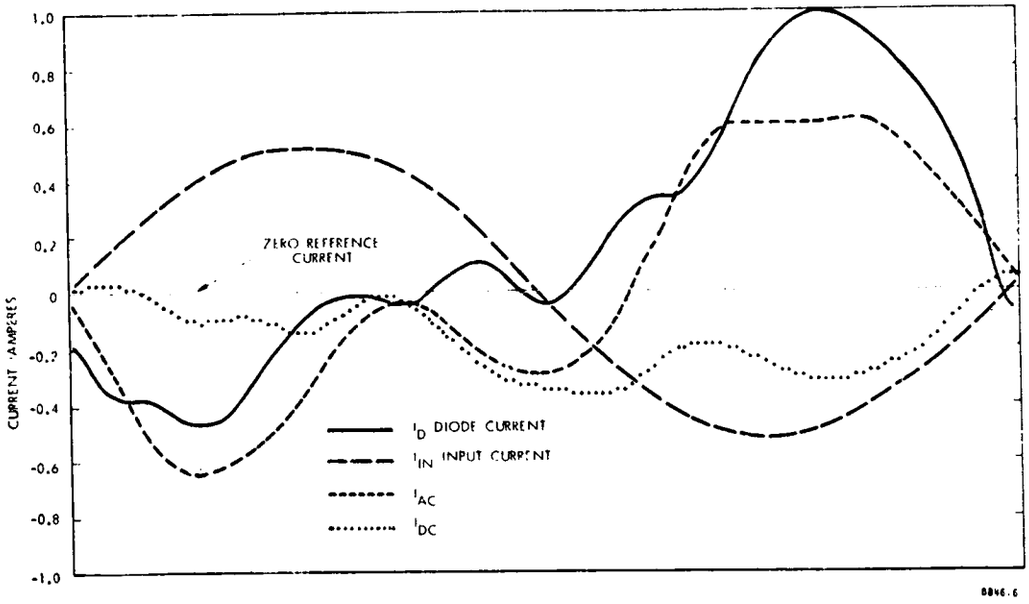

Figure 2-12. Time Behavior of Input Current to Rectenna Element, Diode Current, Microwave Filter Output Current, and Input Current to Rectifier Tank Circuit, as Computed.

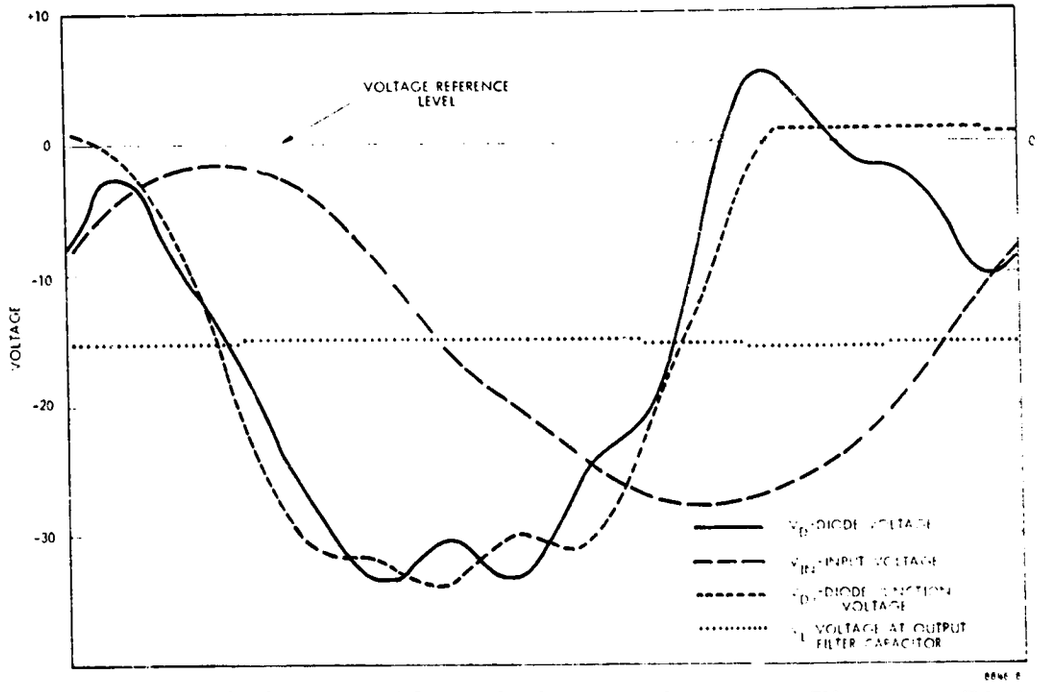

Figure 2-13. Time Behavior of Input Voltage to Rectenna Element, Diode Voltage, Diode Junction Voltage, and Voltage Across Output Capacitance Filter, as Computed.

Figures 2-12 and 2-13 in conjunction with other readouts from the computer simulation program, permit a number of statements to be made about the behavior of the rectenna element.

1. There are no current or voltage spikes whose presence, if severe, is usually associated with a life failure mechanism.

2. In Figure 2-13 it will be seen by observing the diode junction voltage V_{DJ} as it swings into the positive voltage region, that the conduction period is about 105°.

3. There is a large amount of diode current flow during the non-conduction period which is caused by the charging and discharging of the diode capacitance. This represents a loss as the charging current must flow through the series resistance of the diode. It will be recalled that the series resistance in the forward direction remains constant during the forward conduction cycle but decreases considerably as the voltage swings away from the zero-bias value. The total loss in the series resistance integrated over the entire cycle as printed out is 121.7 milliwatts or 3.73% of the input power. Of this, 82 milliwatts or 2.52% is represented by losses in the series resistance of the diode in the forward conduction period; while 40 milliwatts or 1.23% represents a loss through this resistance in the reverse direction. The loss in the Schottky junction itself is 170 milliwatts or 5.22% of the input power. Finally, the skin losses in the rectenna element amount to 68 milliwatts or 2.08%. The total losses as given by the computer simulation program are therefore 11.03% of the power input. This compares well with 12.8% obtained experimentally as noted in Table 2-1. It compares more closely if a Schottky junction voltage drop of 0.9 volts observed experimentally is used in place of the 0.65 volts assumed theoretically. Under these circumstances the Schottky junction loss becomes 7.22% and the total losses become 13.03% - very close to the 12.8% observed experimentally.

4. It will be noted that there is a small amount of ripple on the output filter capacitance. The maximum voltage is 15.8 volts and the minimum is 15.1. When this ripple is broken down into the harmonics, the first harmonic is found to have an rms value of 0.246 volts, representing a power in the load resistance of 0.75 milliwatts. The second harmonic is down by almost a factor of 100 from this value.

2.4 Agreement of Computer Simulation Data with Experimental Measurements.

2.4.1 Comparison of Simulated Efficiency and Losses with Those Measured Experimentally.

Figure 2-14 compares the data obtained by math modeling and computer simulation with that obtained experimentally. It will be noted that there are two kinds of computer simulation data. One kind uses the theoretical characteristics of an ideally designed Schottky barrier diode and the other uses the voltage drop across the diode as determined by DC measurements. The difference in these two measurements may not necessarily be at the Schottky barrier whose properties have been theoretically characterized but may be a voltage drop associated with the back ohmic contact which may not be purely ohmic but is partially a Schottky barrier.

The circuit losses as determined by the computer in Figure 2-14 tend to check the experimentally measured losses at values of microwave power input of 1 watt or more as discussed in more detail in Section 2.2.4. However, it is of interest that at the 300 milliwatt input level the computed losses are about 2.5% higher than at high levels. If this computation is valid it could account for the failure to obtain a power balance at the 300 milliwatt level by about 3%. The circuit losses had been assumed constant at all power levels.

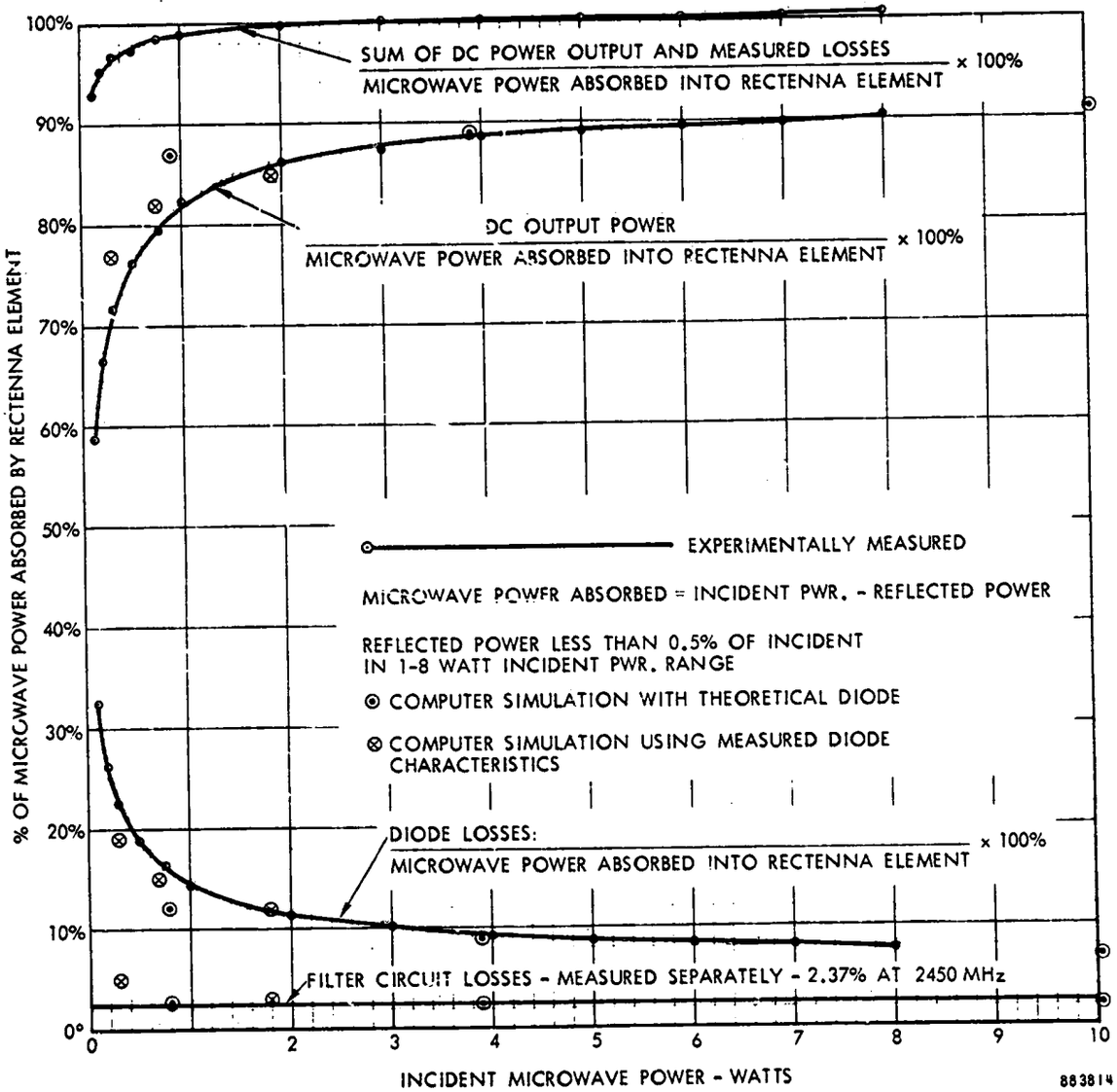

Figure 2-14. Comparison of Computer Simulation Computations of Efficiency, Diode Losses, and Circuit Losses with those obtained experimentally.

3.0 RECTENNA ELEMENT CIRCUIT MODIFICATIONS

3.1 Introduction

The activities reported upon in this section are as follows:

(1) Modification of the circuit of the rectenna element to permit more efficient operation at lower input power levels. This was the principle effort in this section.

(2) The first steps in the integration of the basic RXCV rectenna element into a configuration consistent with the two-plane rectenna construction in which nearly all of the basic functions of the rectenna are carried out in the front plane to facilitate a much more economical form of construction.

(3) Investigations into reducing the second and third harmonic radiation from the rectenna element by the use of stub lines tuned to the harmonic frequencies. One of these stub lines is naturally present in the two-plane rectenna concept.

(4) Investigation of the role of metallic shielding to improve the efficiency and reduce the radiation of harmonic power.

(5) Improvements in efficiency by refinements in the construction symmetry of the RXCV element.

3.2 Circuit Modifications to permit more efficient operation at reduced microwave power input levels.

3.2.1 Introduction and summary of results

The motivation for this activity was the conclusion reached after making a study of the microwave transmission system of a solar power satellite system (26) that most of the area of the rectenna in a full scale SPS would be operated at power density levels that are low compared to those of the RXCV at Goldstone. At these low input power levels, the standard RXCV rectenna element gave considerably lower efficiency than that obtained at the higher power levels. It was therefore logical to direct a portion of the effort under this contract to improving these efficiencies.

The efficiency objective of this technology development contract was 85% at an input power density level of 1 to 100 mW/cm^2 (2450 MHz). Since the cell area occupied by a rectenna element is very close to 50 square centimeters, this objective translates into a power input range to an individual rectenna element of 50 milliwatts to 5.0 watts.

Prior to the undertaking of work under this contract an approximate expression had been developed for diode efficiency in terms of important diode parameters, and the value of the load resistance. These led to an

understanding that more efficiency could be obtained at lower power levels by doing three things: (1) reducing the junction capacitance of the diode, (2) reducing the drop across the Schottky barrier and (3) operating at a higher value of load resistance. Items (1) and (2) involve the design of the diode and item (2) represents a change in the basic metallurgy of the diode and was the basis for considerable effort under this contract.

The implementation of a program to bring about these changes resulted in considerable improvement in efficiency at the lower microwave input levels. This is shown in Figure 3-1, in which the efficiency achieved from the new effort is compared with that obtained from a representative RXCV rectenna element.

The newly achieved efficiencies are associated with a large range (four orders of magnitude) of power input level and are obtained from several diode and circuit configurations since it has been found impractical to cover the entire power range with a single diode and circuit configuration.

A more detailed description of the data in Figure 3-1 is provided in Table 3-1 for cross referencing to Section 4.0 to better identify circuit arrangements and diodes and to indicate efficiencies better.

One of these circuit and diode configurations (No. 5 in Figure 3-1) gives remarkably higher efficiencies at very low values of power input than does the standard RXCV element. On the other hand, the new efficiency of 80% obtained at the 50 milliwatt level is disappointing in that it did not reach either the contract objective or the efficiency predicted from previous studies.

It is believed that there are two reasons for this reduced efficiency from that anticipated. The first one is that it was necessary to add an impedance transforming section between the low-pass input filters and the diode and its tank circuit to match the dipole antenna into the rectification circuit to minimize reflected power. There was undoubtedly some additional circuit loss in this section. A more important cause of the reduction in efficiency from that anticipated is the relatively high loss that occurs in a diode with a small junction area because of the high back contact resistance. The back contact resistance can be reduced but in doing so the effective spreading resistance is increased. These losses were not taken into consideration by our earlier analysis. It is believed that these losses are from 5% to 10% in absolute terms. It is believed that these losses can be reduced to 2% to 6%.

3.2.2 The Design and Construction of Circuits for more efficient operation at lower power levels

There were three different circuits used to obtain data on more efficient operation at lower power levels. However, they were all based on the RXCV element type circuit - that is the half-wave rectifier circuit, with two low pass filter input stages.

1. GaAs - P_t IN GROUNDED PLANE FIXTURE, REGULAR FILTER
2. GaAs - W IN GROUNDED PLANE FIXTURE, REGULAR FILTER
3. GaAs - W, 50 V_{br} MTL, C_{to} = 1 pf, REGULAR FILTER AND λ/4 MATCHING LINE SECTION
4. GaAs - W, 50 V_{br} MTL, C_{to} = 1 pf, REGULAR FILTER AND λ/4 MATCHING LINE SECTION
5. GaAs - W, 20 V_{br} MLT, NO ETCH, C_{to} = 1 pf, REGULAR FILTER AND HIGHER IMPEDANCE λ/4 MATCHING SECTION
6. PREVIOUS DATA ON MSFC - RXCV TYPE RECTENNA ELEMENT WITH SAME DIODE USED THROUGHOUT BUT ELEMENT RETUNED AT EACH POWER LEVEL

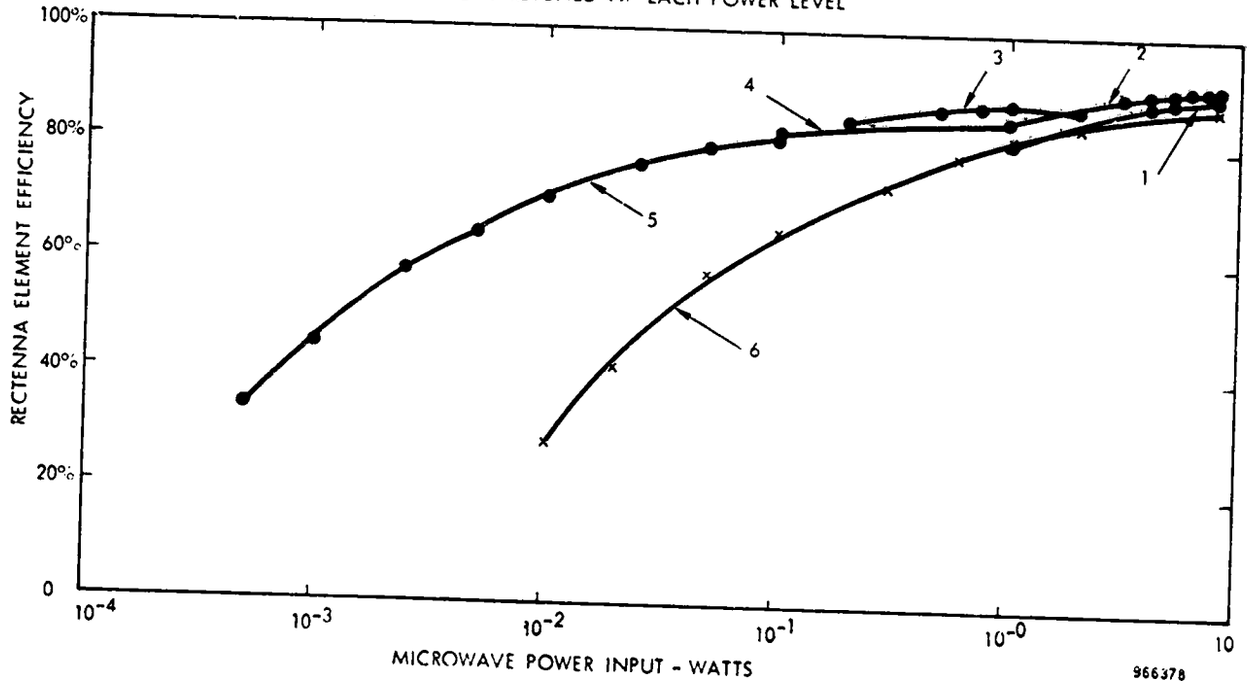

Figure 3-1. A summary of the efficiencies achieved with various new rectenna and diode configurations as a function of power level, compared with performance of a standard RXCV element.

TABLE 3-1

Figure 3-1 Curve No.	* Rectenna Element Circuit Identification	Diode Identification	Diode V_{br} (Volts)	Diode C_{jo} (unfd)	Incident Microwave Power (milliwatts)	Power Reflected %	Load Resistance (ohms)	Efficiency %	Other Reference This Report	Other Reference
1	A	40593 CPXIG No. 13 GaAs-P_t	60	3.6	1000-8000	0-1	80	82.3-90.26	Table 4-1 Figure 3-1	23486-27 Notebook
2	A	50234CX WC-8 GaAs-W	59	3.5	1000-8000	0-2	80	85.8-91.3	Table 4-1 Figure 3-1	23486-47 Notebook
3	B	40904 WB No. 3 GaAs-W	51	0.99	500 750 1000 2000	1 1 0 3.2	600 500 450 300	86.8 87.8 88.1 86.8	Figure 3-1	3-27-76 Diode log Figure 3 - Report No. 8
4	B	40904 WO No. 4 GaAs-W	30	1.01	100 200 500 1000	1 1 1 5.5	600 600 400 300	82.3 83.9 85.1 85.2	Figure 3-1	3-27-76 Diode log Figure 3 - Report No. 8
5	C	40477 3PXI WA-3	19.5	0.80	0.5 1.0 2.5 5.0 10.0 25.0 80.0 100.0	5 5 4 2 0 0 2 2	1000 1000 1000 1000 1000 1000 1000 700	34.3 44.5 56.6 64.9 69.5 75.6 80.0 81.3	Figure 3-1	5-5-76 - Diode log
6	D	Typical RXCV Diode	---	---	1000 - 8000	---	160	78	---	Bibliography Ref. No. 26 Figure 3-8

* RECTENNA ELEMENT CONFIGURATION

A RXCV element adapted to ground plane fixture

B Standard RXCV element with 240 ohm λ/4 transformer added as in Figure 3-2

C Standard RXCV element with 300 ohm λ/4 transformer added as in Figure 3-2

D Standard RXCV element (balanced)

The chief sources of loss in a low power rectenna element are losses caused by the voltage drop across the Schottky barrier diode, and the I^2r losses caused by the passage of the charging current to the diode capacitance through the series resistance of the diode.

The efficiency loss caused by the voltage drop across the Schottky barrier is closely given by $V_b/(V_{dc} + V_b)$ where V_b is the Schottky barrier voltage drop and V_{dc} is the voltage across the load resistor. The voltage drop across the Schottky barrier is fixed so that the loss caused by the barrier can only be reduced by increasing the DC voltage. This can be done for a given microwave power input level by raising the resistance of the DC load. A four-fold increase in impedance will reduce the Schottky barrier losses by a factor of two, approximately. However, raising the voltage will increase the charging current losses into the diode so that decreasing the capacitance and therefore the contact area of the diode will be of some help.

Raising the DC load resistance to decrease the Schottky barrier voltage presents a new problem in that the rectenna element will not be matched into space. The amount of power reflected is approximately:

$$\% \text{ Reflection Loss } = \left(\frac{R_L - R_{LM}}{R_L + R_{LM}} \right)^2$$

where R_L is the DC load resistance and R_{LM} is the load resistance that gives a match to the incoming power.

In the RXCV rectenna element the input impedance to the dipole antenna is approximately 120 ohms as is the characteristic impedance of the low pass filters that are matched to it. The value of R_L that provides a good match into the 120 ohm impedance level is about 160 ohms. Therefore to match into a higher load resistance while still retaining the 120 ohm impedance of the low pass filters requires another matching section which is conveniently supplied by a quarter wavelength line of an impedance level which is the geometric mean of the two.

In the first modification a quarter wavelength line at an impedance level of 240 ohms was used. This provided a reasonable match into a load resistance of 640 ohms. A photograph of the arrangement just described is shown in Figure 3-2.

The data given as Items 3 and 4 for curves 3 and 4 in Figure 3-1 were obtained with the use of the rectenna element shown in Figure 3-2.

At values of incident power below 100 milliwatts there was an appreciable amount of power reflected with the circuit shown in Figure 3-2. To explore the impact of a higher impedance transformation upon operation the impedance of the $\lambda/4$ section of line was raised by a factor of 1.25 to raise the matched impedance level for the DC load resistance by a factor of 1.56. This

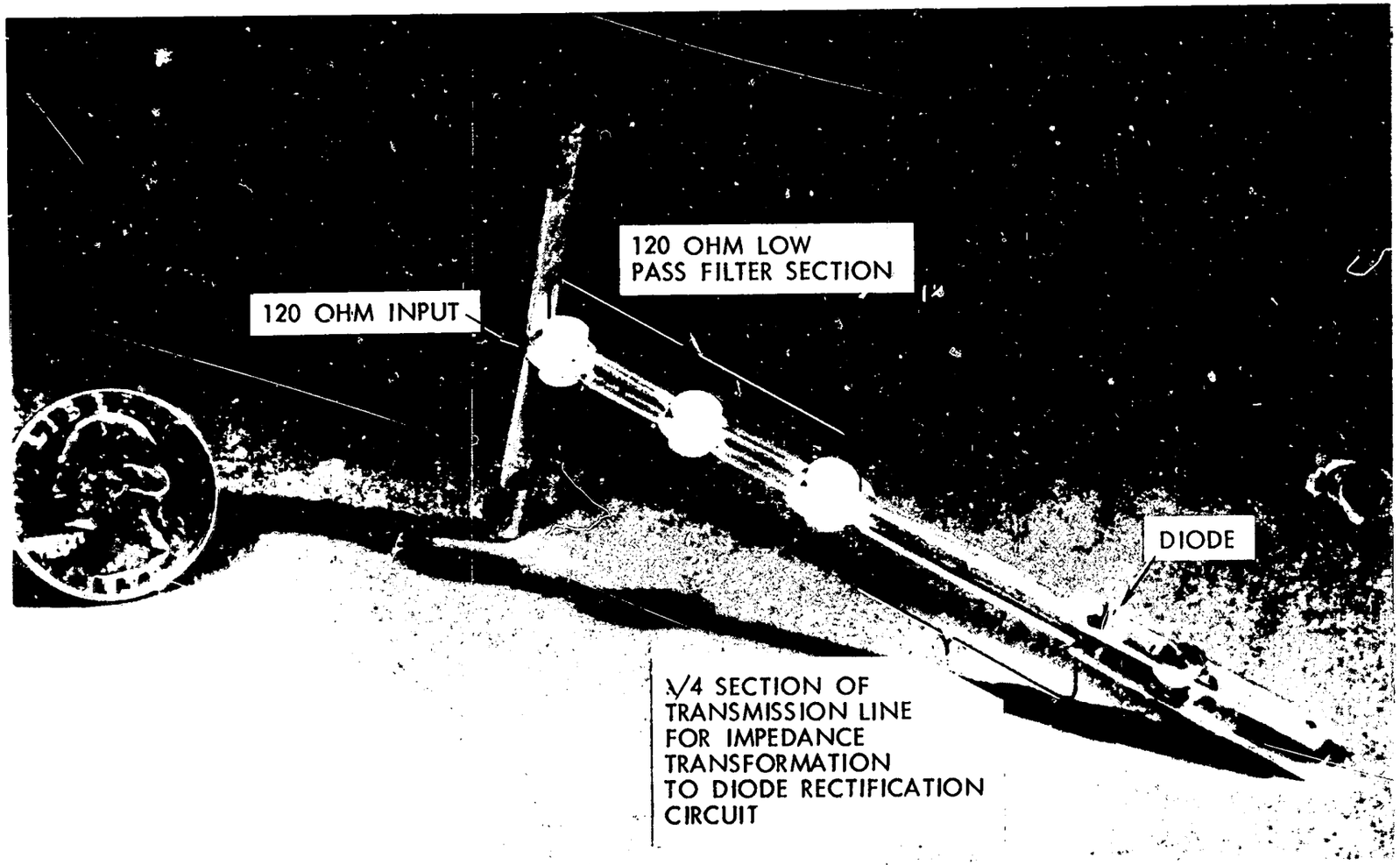

Figure 3-2. Rectenna Element Test Vehicle

change coupled with the use of a different diode made from a different wafer resulted in less reflected power at the 50 milliwatt level (corresponding to the one milliwatt per square centimeter lower limit specified in the work statement). It was further found that very good efficiencies could be obtained at even lower power levels while operating into DC load resistance of 1000 ohms and that the reflected power remained low percentagewise. As curve 5 in Figure 3-1 indicates, seventy percent efficiency was achieved at the 10 milliwatt input level with a reflection of less than one percent. The efficiency at the 1 milliwatt level was still 45% with a reflected power of 5%.

One of the practical problems in the use of the $\lambda/4$ impedance transformer is that it makes the element too long to incorporate into the two-plane construction preferred because of its much more economical construction. This led to an approach in which the second filter section of the RXCV type element was converted into a matching transformer of lower impedance than the $\lambda/4$ length of line. It is not possible to obtain as high a characteristic impedance in this section as in the $\lambda/4$ length of line because of limitations imposed by the fragility of the inductive section of the filter.

However, when attention is focused upon data that has been taken in the 500 milliwatt to 1.5 watt region where a great deal of the SSPS rectenna action is slated to occur, it is noted that a dc load resistance of the order of 300-500 ohms seemed appropriate when used with a diode having a C_{to} capacitance of 1 picofarad. Matching into this requires only the increase of the characteristic impedance of the second filter section by a factor of $\sqrt{2}$ rather than 2 and this is consistent with what can be accomplished in a physical structure. Consequently we constructed a rectenna element which incorporated a second stage filter with a characteristic impedance approximating $\sqrt{2} \times 120$ ohms or 170 ohms as shown in Figure 3-3. A comparison of the performance of this rectenna element with that of the two filter section plus $\lambda/4$ impedance transforming line and utilizing diode 40904 X WB3 for both sets of measurements is given in Table 3-2 for 1 watt of power input.

The above data indicates that the two-section filter with a 170 ohm second stage is as efficient as the standard two section filter with an additional $\lambda/4$ section of line. Moreover, this same diode was found earlier to have had an 88.1% efficiency into a 450 ohm load, or 1.6% higher than reported in Figure 3-4. It is believed that the diode may have changed since another diode 40904 X WB4 was found to be more efficient than diode 40904 X WB3 in a new set of measurements whereas the reverse had been true when the diodes were checked several weeks previously.

The conclusion is that the two section filter with the second section modified may be acceptable for operation of the 1 picofarad diodes at the 1 watt level into a resistive load of a nominal resistance of 400 ohms; thereby resulting in a better efficiency than with the 140 to 180 ohm load resistance normally used and in a design compatible with the two-plane construction.

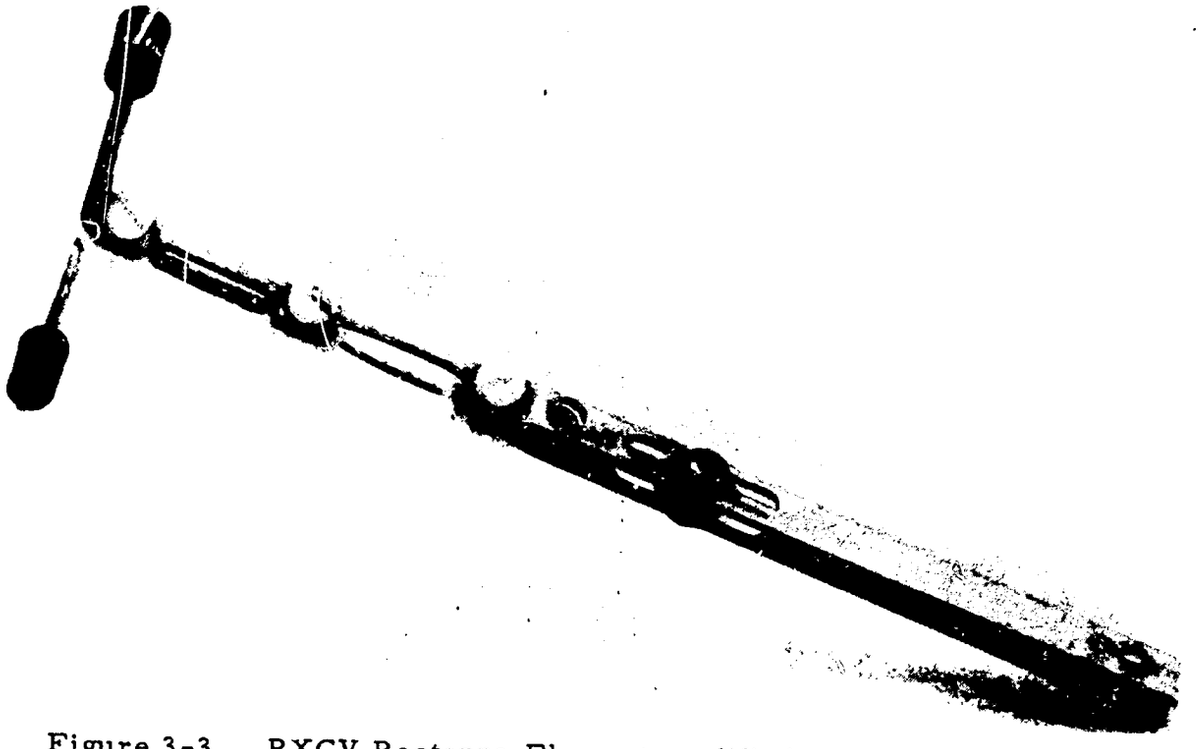

Figure 3-3. RXCV Rectenna Element modified to provide higher characteristic impedance of second section of the input filter which serves as a $\lambda/4$ matching section for higher impedance operation of the rectifier circuit.

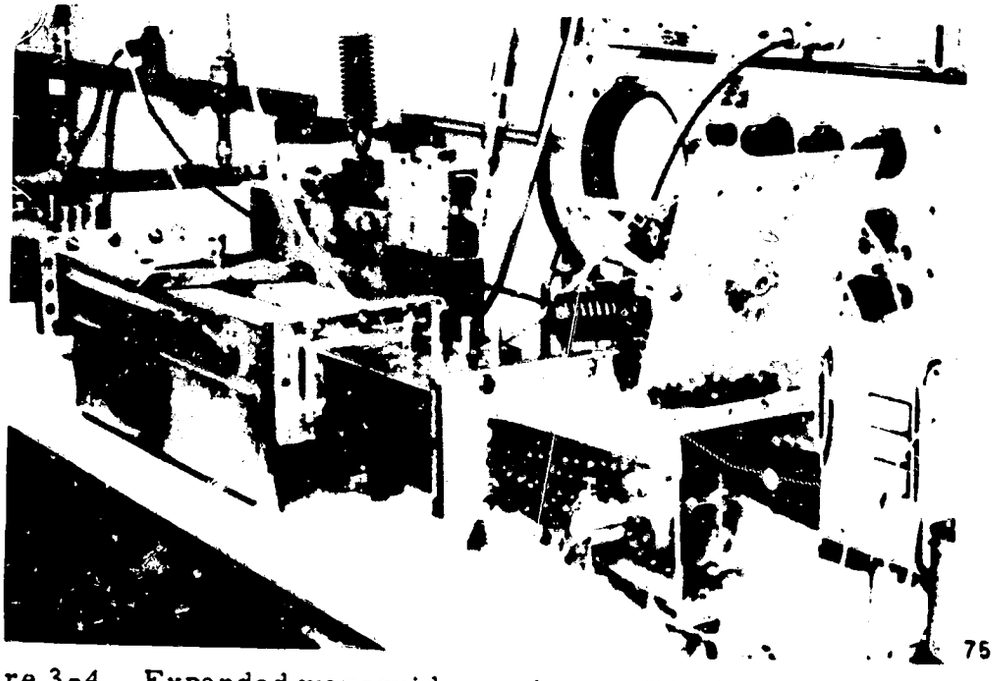

75 75959

Figure 3-4. Expanded waveguide section modified to permit testing of rectenna element with axis normal to regular position. New orientation corresponds to that in the two-plane rectenna construction format.

Power Input	DC Load Ohms	Rectenna Element with 170 Ohm 2nd Stage Filter		Rectenna Element with Additional λ/4 Length of 240 Ohm Line	
Watts		Power Reflected %	Element * Efficiency %	Power Reflected %	Element * Efficiency %
1.00	250	3.3	85.89		
	280	2.0	86.42		
	300	1.4	86.32	5.9	84.88
	320	1.1	86.44	4.7	85.31
	340	0.9	86.78	3.7	85.68
	360	0.8	86.54	2.8	86.02
	380	0.9	86.70	2.1	86.22
	400	1.0	86.52	1.5	86.39
	420	1.3	86.62	1.05	86.44
	440	1.6	86.70	0.7	86.49
	460	2.0	86.61	0.4	86.52

* Element efficiencies are DC Output/Absorbed Power

Table 3-2. Comparison of efficiencies achieved with the rectenna element configuration of Figure 3-3 with that achieved from the configuration of Figure 3-2.

3.2.3 Other Approaches to Efficient Operation at Lower Power Levels

In looking at the design of circuits for more efficient operation at lower power levels a number of approaches were passed over. The first of these was the use of either a full wave rectifier circuit or a pseudo-full wave circuit. In view of the fact that the circuit losses have been demonstrated by experimental measurement and by computer simulation to be very low for the half-wave rectification circuit, it was felt that this approach would not be fruitful.

Another approach was to feed more than one dipole into a diode. This would probably favorably impact the efficiency at the very low power input levels. Figure 3-1 would seem to indicate an improvement in efficiency from 80 to 82% by just doubling the input power from 50 milliwatts to 100 milliwatts, and an improvement from 45% to 56% by doubling the power from 1 milliwatt to 2 milliwatts. The latter power level is, of course, a factor of 50 below the lowest level at which the full scale SSPS rectenna is anticipated to be operated.

It is observed that a rectenna array rapidly takes on the directivity characteristics of a conventional phased array when an attempt is made to operate many dipole elements into one rectifier element. There may be instances where this is desirable for experimental reasons but the desirability in the full-scale SSPS application is questionable. Since the experimental investigation of this approach requires an elaborate new test arrangement it was not felt to be cost-effective within the present contract.

Another approach that was not investigated was the elimination of the input filter sections completely and the use of a $\lambda/4$ impedance transformer between the terminals of the dipole and the rectification circuit. Under this proposed arrangement the 2nd harmonic and 3rd harmonic would be shorted out at the terminals of the dipole by stub lines. This approach would seem to place a burden upon the critical adjustment of the stub lines to prevent excessive harmonic radiation, but would, nevertheless be a worthwhile investigation to determine how efficient such an arrangement would be.

3.3 Initial Effort in Integration of Rectenna Element into a Two Plane Structure

An initial investigation of the performance of a rectenna element when it was mounted in the waveguide test fixture at right angles to its normal position as shown in Figure 3-4 was carried out. It was found that there was no significant change in performance for the unshielded case as shown in Figure 3-4. However, there was a reduction in efficiency of about 1% when a short circuited quarter wavelength line was added to the structure to simulate a connection to the next rectenna element.

The further integration effort is discussed in detail in Section 5.0.

3.4 The Reduction of Second and Third Harmonic Radiation with the use of Stub Lines

Another area of activity involved taking steps to decrease the amount of second and third harmonic power radiated from the antenna. In this case the grounded plane fixture was used and the input impedance of the antenna was simulated by a matched 50 ohm line. This, of course, is an accurate simulation of the properties of the dipole antenna only at the fundamental frequency since the dipole antenna will appear as a different impedance at the two harmonic frequencies. However, data on dipole antennas whose arms have a high ratio of thickness to length indicate a fairly good match (that is, not more than 75% of the power reflected) over a frequency range that includes the fourth harmonic. On this basis an attempt to reduce the harmonic content by placing open and short circuited stubs of appropriate length in parallel with the input terminals of the dipole antenna seemed worthwhile.

There is a natural opportunity in the two-plane rectenna construction to short out the second harmonic at the dipole antenna terminals because the section of transmission line that extends to the next rectenna element in the two plane construction must look like an open circuit. It therefore looks like a short circuit for the second harmonic. Using the ground-plane construction it was found that this section of line could indeed be adjusted to greatly reduce the second harmonic content that got into the 50 ohm line. As shown in Table 3-3, experiment No. 5 indicated a 30 dB reduction in the second harmonic level. The experimental set up for this is shown in Figure 2-2. The connection to the 50 ohm line is made through a small hole in the geometric center of the ground plane.

Figure 2-3 also shows a short stub which acts as an open circuit at a quarter wavelength at the third harmonic frequency. The data indicates a 15 dB improvement in harmonic level as shown in experiment 6 in Table 3-3. It is interesting to note that in comparison with other data in Table 3-3 there was no appreciable change in efficiency caused by the reduction of the second and third harmonics. However, it was found in later work as reported upon in Section 5 that the adjustment for the reduction of the second harmonic in the foreplane of the two-plane rectenna structure by this means may be so critical as not to be practical. More investigative work needs to be done since the structures being worked with were not identical, and in the foreplane case the physical length of the $\lambda/4$ section is shortened by capacitance loading.

The method by which the harmonic content at the input to the rectenna element was measured is indicated in Figure 2-2. The relative levels of the forward directed fundamental power and backward directed harmonic power can be measured with the use of an HPA spectrum analyzer and a directional coupler which is designed to operate at the frequency of the harmonic power.

No observation of harmonics greater than the third harmonic were obtained although the analyzer could have seen harmonics down by a factor of

TABLE 3-3

MEASURED EFFICIENCY AND HARMONIC LEVEL RESULTING FROM CIRCUIT CHANGES IN RXCV ELEMENT DIRECTED TOWARD 2-PLANE RECTENNA CONSTRUCTION AND HARMONIC REDUCTION. MEASUREMENTS MADE ON FIXTURE WITH RF GROUND PLANE

Sequence of Experiment	Description of the experiment	Load Resistance	Absorbed Microwave Power (Watts)	Reflected Microwave Power (Watts)	DC Output as % of Absorbed Power	2nd Harmonic Power Level Related to Incident Power	3rd Harmonic Power Level Related to Incident Power
1	Unshielded RXCV element adjusted for minimum reflected power. 3rd Harmonic Filter installed.	100	4.074	0.042	86.30%		
2	Add shield over entire structure	100	2.980	0.135	87.19%		
3	Change load resistance to minimize reflected power	80	4.089	0.028	87.53%		
4	Rise input power level to 5 watts nominal	80	5.107	0.038	88.17%		
5	Add 10 dB 4-10 GHz directional coupler to measure harmonics. Compensate for insertion loss (1.052). Measure harmonic levels.	80	5.116	0.029	88.73%	-25 dB	-55 dB
6	Add transmission line section which would connect one rectenna element to its neighbor in 2-plane construction and which doubles as 2nd harmonic filter.	80	5.059	0.086	88.67%	-50 dB	-55 dB (-40 dB with filter removed)
7	Take out 10 dB 4-10 GHz directional coupler. Same as sequence No. 3 but w/conn. trans. line (2nd H/F) incl.	80	5.123	0.022	88.1%		

Conditions - Thermistor Bridge Calibration as of 10-8-75
RF Input Power Calibration as of 10-6-75 - 1.029 x 432A Power Supply Reading
Diode used was 40593CPX1G No. 13 (Diode Std. No. 11)

70 dB from the fundamental. It is therefore concluded that the fourth harmonic is down by at least this factor from the fundamental. The fourth harmonic was later observed in the rectifier tank circuit by means of a special probe which was coupled into the rectifier tank circuit in the ground plane test fixture.

In connection with the measurement of harmonic power at the second and third harmonics, it is of interest to compare the level with that predicted by computer simulation. For both the experimental case and the simulated case the input to the rectenna element was terminated in a 50 ohm line. In the experimental case no stub lines were being used when the measurements were made.

HARMONIC LEVEL WITH RESPECT TO FUNDAMENTAL

	Measured at Input on Ground - Plane Fixture	Predicted at Input Computer Simulation
2nd Harmonic	-25 dB (at 5 watts)	-27.5 dB
3rd Harmonic	-40 dB (at 5 watts)	-37.4 dB
4th Harmonic	<-70 dB (at 5 watts)*	---

* Sensitivity of equipment to 4th harmonic was -70 dB from fundamental. However, no 4th harmonic was observed.

3.5 Reduction in radiated harmonic power by metallic shielding

A considerable amount of harmonic power is radiated from the rectifier tank circuit directly into space unless some metallic shielding is placed around the tank circuit. Experiment No. 2 in Table 3-3 shows that the addition of a metallic shield over the rectenna element resulted in an improvement in efficiency by nearly 1%; this despite the fact that there must be some skin losses in the shield.

The second and third harmonic power being radiated from the unshielded structure was easily detected by monitoring equipment fifty feet away. The addition of the shield reduced any radiation to a level that the monitoring equipment could not detect.

The radiation of harmonic power from the rectifier tank circuit should not be confused with radiation of harmonic power from the dipole antenna which must be transmitted through two or more low pass filter sections.

3.6 Improvement in the efficiency and in the consistency of efficiency measurements by refinements in the construction of the RXCV rectenna element.

It was found that there was a considerable variation in the efficiency of some RXCV rectenna elements depending upon whether they were inserted into

the waveguide test fixture in the "up" or "down" position. The "up" and "down" positions corresponded to the position of the aluminum nuts which were used in conjunction with teflon machine screws to hold the side rails of the rectenna element together. The test procedure was to make an efficiency measurement in the "up" position, take the element out of the test fixture and reinsert it in the "down" position, take another efficiency reading, and to repeat this enough times to obtain reliable statistical data. The efficiency measurements in either position showed only a small amount of dispersion but the difference in the average efficiency obtained for the two positions was 0.64%.

It was then found possible to reduce this difference to 0.2% by substituting teflon nuts for the aluminum nuts. There was also a net gain of .15% in efficiency in the higher efficiency position indicating that the aluminum nuts themselves were a minor source of efficiency loss, independent of their unbalancing impact.

The reason for the impact of the orientation of the rectenna element in its test position upon operating efficiency is traceable back to an interaction between the rectenna element and the metalic cylinder which surrounds a portion of the rectenna element. Ideally, the two-wire transmission line should be electrically centered in the metallic cylinder. If it is not, a plus-plus mode contamination superimposed on the normal plus-minus mode of the transmission line will result. The harm that this does depends both upon the amount of the imbalance and what impedance the plus-plus mode couples into.

If the rectenna transmission line itself is electrically symmetrical and if it is mechanically centered in the metallic cylinder, the amount of imbalance will be negligible. However, the old design was not electrically symmetrical in that aluminum nuts were used on one side of the transmission line while the heads of the teflon screws protrude on the other side.* The 3-48 thread on the diode also protrudes from one side which is the same side that the metallic nuts are on. Now, when the rectenna element is inserted into the fixture, and if the center line of the rectenna element corresponds to the center line of the metallic cylinder, the side of the transmission line with the nuts will couple more closely to the cylinder and set up an imbalance which will produce an efficiency loss. Presumably if the rectenna element is taken out, rotated 180°, and replaced, the nuts will be on the other side of the cylinder, and the imbalance and efficiency impact will be the same. But if the axis of the cylinder and the rectenna element do not coincide, then the results of the 180 degree rotation will be different; there will be more electrical imbalance in one position than for the other and the result in efficiency measurements may be noticeable.

---

* The use of aluminum nuts in the design of the RXCV rectenna element was based upon better delivery and lower cost of aluminum nuts and tests which were not refined enough to detect an appreciable difference in operating efficiency of the aluminum and teflon nut designs.

In conclusion it is observed that good electrical symmetry should be incorporated into the design of the rectenna foreplane if mode conversion with consequence loss in efficiency is to be avoided.

4.0 SCHOTTKY BARRIER DIODE DEVELOPMENT

The material discussed in this section is closely associated with the material described in Section 3.0. Section 3.0 stresses the work done in modifying the circuits to a higher impedance level and the results of the total circuit and diode modification efforts in terms of higher efficiency obtained for the lower levels of microwave power input. It was acknowledged in Section 3.0 that the diode modifications were an important part of the effort. In this section the work on the diode will be stressed.

Historically, much of the improvement in rectenna element performance has been attributable to improvements in diodes. (Figure 1-16.) The major improvements in diodes have resulted from reducing the series resistance of the diode. This reduction was accomplished in part by using GaAs as the semiconductor material. GaAs has a much higher mobility which results in much lower series resistance. Another major improvement was making the thickness of the epitaxial layer as thin as possible consistent with thickness required for the reverse breakdown voltage, V_{br}, specified. Most diodes are constructed with excess thickness of the epitaxial layer to obtain greater yield. A quality control problem is basically involved in making them thinner. Another important improvement in diode construction, the plated heat sink design, reduced the contribution of the resistance of the substrate to the total series resistance by greatly reducing the substrate thickness.

But even after these improvements it was known that the losses in the diodes were considerably greater than circuit losses; therefore, further improvements would most likely come from improvements in diodes. Confirmation of the source of losses of a more quantitative nature has resulted from the present work as described in Section 2.2.3. Diode losses have now been measured quite accurately, and the circuit losses sufficiently so by experiment and computer simulation. These measurements indicate that the diode losses are significantly greater than circuit losses. Circuit losses other than those represented by the diode itself tend to be 3% or less of the power input, while diode losses range from a minimum of 6% to much higher values.

Rectenna element efficiency with the diodes available from the RXCV program were found to be close to 90% at the power levels corresponding to such optimum efficiency. [12] These levels were in the three to ten watt region. However, at lower power levels of 50 milliwatts the RXCV rectenna elements would perform at only 58%. (Figure 3-1 .) Since the circuit losses tend to remain relatively constant, such low efficiency must be associated with the diode or the manner in which it is used.

Prior to this technology development program it had been established that most of the loss in the diode at such low power levels was associated with the voltage drop across the Schottky barrier itself and that the extent of this loss relative to the microwave power input was roughly given by the ratio of the drop across the Schottky barrier to the DC output voltages as discussed in Section 2.2.4. To improve the efficiency the DC load resistance could be increased or the drop across the barrier reduced.

An approximate analysis of losses in the diode as it is used in the rectenna element also indicated that the capacitance across the junction should be reduced if the diode were to be operated at higher impedance level. Two major modifications in the diode were therefore indicated if it were to be used at a lower power level - a decrease in the junction capacitance and in the voltage drop across the junction. Another area of interest was the further progressive reduction of the epitaxial layer thickness into the "punch through" region to establish the impact of this upon the efficiency of the diode.

A search of other possible junctions reveals that the Schottky barrier voltage for a GaAs-W barrier is about 25% lower than that of the GaAs-Pt barrier. An objective of this contract was to build some diodes with the GaAs-W barrier and to evaluate them. Now tungsten is a desirable material from most viewpoints but it is more difficult to get it to bond to GaAs than it is platinum. Fortunately, the development effort concerned with getting a satisfactory mechanical and a satisfactory electrical bond between GaAs and Tungsten was the subject of an ongoing effort supported by another contract. [31] The diode development work for this contract benefited from that experience.

The voltage current characteristic of a GaAs-W diode constructed under this contract is compared with that of a GaAs-Pt diode specified for the RXCV element. (Figure 4-1.) Both diodes had approximately the same reverse breakdown voltage and the same junction capacitance so a direct comparison can be made. The GaAs-Pt diode was a diode that had been used as a standard during the construction of the JPL RXCV rectenna. It is noted that the slope of the voltage-current characteristic in the forward direction of the two diodes are essentially the same, indicating that the series resistance of the diodes are very similar. The essential difference in the two diodes is in the Schottky barrier voltage and that this difference as measured by the intercept of the tangents of the voltage-current characteristic with the zero-current axis is about 0.2 volts. This is the value that one would expect.

The impact that the reduced junction voltage would have upon improvement in efficiency of the rectenna element was examined by putting the diodes in the ground-plane test fixture (Table 4-1) and then running a comparison test of overall efficiency and diode losses. The results indicate that the reduction in diode losses are just about what would be anticipated from the reduction in the Schottky-barrier voltage.

The major importance of the comparison tests between the GaAs-W and the GaAs-Pt diodes is to confirm what was expected - a slight improvement in efficiency at the higher power output levels with a greater improvement as the DC voltage output was reduced. There were no surprises.

As we sought to improve the efficiency at the lower microwave input levels, however, some unexpected difficulties were encountered. As the DC voltage on the diode is increased for a given input power by using a higher value of DC load resistance, the loss in the series resistance during the conduction period goes down while the loss in the series resistance during the non-conduction period increases rapidly due to the charging current flowing into the junction capacitance.

Table 4-1. Comparison of GaAs-Pt * and GaAs-W ** Diodes in Ground-Plane Test Fixture

	A	B	C	D	E	F	G	H	I
Microwave Power Input	Diode Being Tested	Microwave Power Reflected	Microwave Power Absorbed by Element	DC Power Output	Efficiency of Element D/C	Measured Diode Losses	Inefficiency of Diode F/C	Inefficiency of Filter Circuits	Total of DC Output and Losses E+G+H
Watts		Watts	Watts	Watts[1]	%	Watts	%	%[2]	%
1	GaAs-Pt	0.009	0.991	0.816	82.3	0.140	14.15	2.37	98.82
	GaAs-W	0.023	0.977	0.838	85.81	0.120.9	12.37	2.37	100.55
2	GaAs-Pt	0.003	1.997	1.719	86.12	0.226	11.33	2.37	99.82
	GaAs-W	0.020	1.980	1.750	88.42	0.198	10.03	2.37	100.82
3	GaAs-Pt	0.000	3.000	2.628	87.60	0.305	10.17	2.37	100.14
	GaAs-W	0.017	2.983	2.670	89.56	0.265	8.90	2.37	100.83
4	GaAs-Pt	0.002	3.998	3.536	88.45	0.369	9.24	2.37	100.05
	GaAs-W	0.016	3.984	3.591	90.14	0.332	8.33	2.37	100.84
5	GaAs-Pt	0.008	4.992	4.446	89.06	0.438	8.77	2.37	100.20
	GaAs-W	0.016	4.984	4.522	90.73	0.394	7.92	2.37	101.02
6	GaAs-Pt	0.016	5.984	5.356	89.50	0.502	8.39	2.37	100.26
	GaAs-W	0.017	5.983	5.454	91.17	0.455	7.61	2.37	101.15
7	GaAs-Pt	0.028	6.972	6.272	89.95	0.565	8.11	2.37	100.43
	GaAs-W	0.019	6.981	6.378	91.37	0.524	7.50	2.37	101.24
8	GaAs-Pt	0.043	7.957	7.180	90.26	0.631	7.93	2.37	100.56
	GaAs-W	0.022	7.978	7.284	91.30	0.605	7.58	2.37	101.25

1. DC Load Resistance Used was 80 Ohms
2. Measurement of Filter Circuit Loss was a Separate Measurement.

Standard Diode S.n. 11 from RSCV Contract - Diode identified as 40693-GPSIG No. 13.

5-2140X-WC No. 4 made under LeRC technology development contract.

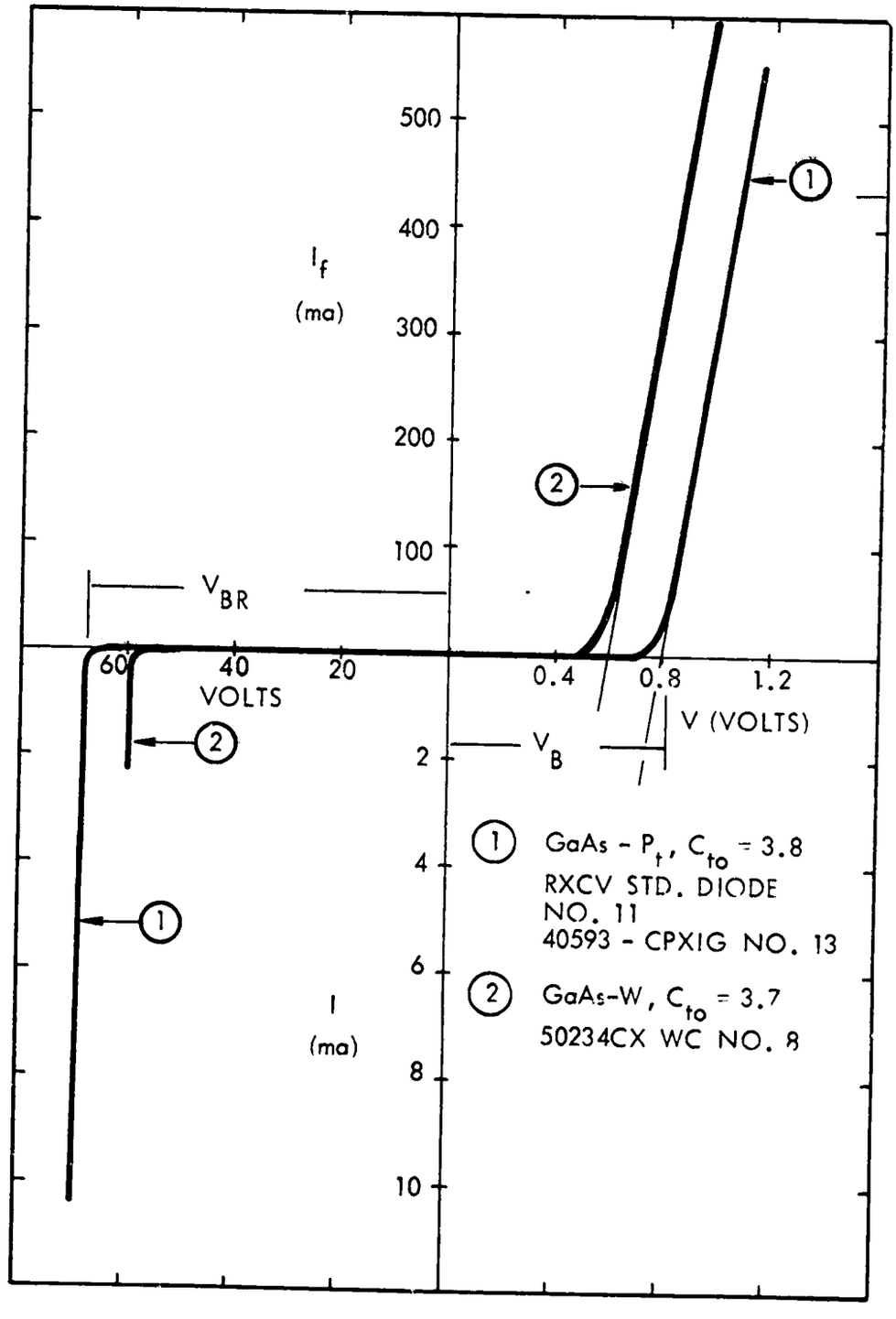

Figure 4-1. Comparison Between Voltage Current Characteristics for GaAs-P_t and GaAs-W

The distribution of losses is such that the junction capacitance and therefore the area of the junction should be reduced.

The reduction of the capacitance across the diode did not improve the low power performance of the diode as much as anticipated. This was because of a complication caused by the emergence of the back contact resistance as a significant portion of the series resistance when the active area associated with a low capacitance junction is small. The resistance in the depletion layer is very low in a diode designed for low reverse breakdown voltage, even in a small junction area associated with a small capacitance. The back contact resistance increases greatly, however, because the distance between the junction and the back contact is so small in a plated heat sink diode that the current does not have a change to spread out. This suggests making the base material out of a heavily doped material to keep the spreading resistance low and of sufficient thickness to allow spreading to a large area to cut down on the back contact resistance. Unfortunately diodes made in this fashion do not perform as predicted because current at the microwave frequency flows close to the surface, resulting in significant skin resistance between the active junction and the back contact. There are ways to reduce this skin resistance by evaporating a metal deposit over most of the surface flow path and thereby reducing its length. However, this is a recommended activity for the future since such diodes were not made under this study.

4.1 The Diode Design and Construction Matrix

The approach to the design and construction of the diodes took the following objectives into consideration:

1. To use the RXCV diode and rectenna element as a base and performance reference. To this end the RXCV diode has been included as one of the end items in the matrix.

2. To permit a systematic evaluation of the impact of various parameters and to note any inconsistencies in results or departures from expected behavior.

3. To use two types of barriers, GaAs-Pt and Ga-As-W, to investigate differences in their efficiencies. And also to investigate GaAs-W barrier construction techniques.

4. To investigate the performance of diodes having a low value of zero-bias capacitance and to confirm the design prediction that a lower value of capacitances would improve the efficiency of the diode and rectenna element at low power levels.

5. To compare the performance of diodes having greatly different values of reverse breakdown voltage, particularly at low power levels.

6. To investigate the performance impact of reducing the thickness of the epitaxial layer.

To implement these objectives a matrix plan for diode fabrication was derived, as shown in Figure 4-2 .

Figure 4-2 indicates various kinds of diodes that result from such a construction matrix. The matrix produces 16 different kinds of diodes from each wafer. Two diodes of each kind, or a total of 32 diodes from each wafer, were generally made available for testing.

A brief description of the manufacturing sequence may be of interest.

The epitaxially grown surface of each wafer was covered with a material resistive to etching. The resistive coating from a portion of the wafer was then removed, and the thickness of the epitaxial layer was reduced by the application of an etch. Then the resistive coating was removed from another area, and the etch was applied to both areas. Then the resistive coating was removed from a third area, and the etch was applied to all three exposed areas. In this manner, the four different thicknesses of the epitaxial layer corresponding to the designations A, B, C and D on Figure 4-2 were established. The designation A corresponds to the unetched portion of the wafer.

The wafer was then divided into two parts. Tungsten was deposited as an interface with the epitaxially grown active area on one part while platinum was deposited on the other part. A heat sink in the form of a gold-plating deposit about three mils thick was then attached to the metallic deposition and was lapped down to flatness. Then most of the substrate was removed by grinding.

An ohmic contact was made on the back of each piece of material. A photomask technique was used to define the area occupied by the ohmic contact for each individual diode. After the etching process, the ohmic contact was about six mils in diameter. The mesa of the diode was then defined and etched to a diameter of about eight mils. The diodes were then separated from each other by an etch applied to the outboard side of the heat sink. After etching and diode separation each heat sink was about twenty by twenty mils in size.

The individual diodes were then mounted by a brazing technique to the package heat sink. The diode mesas of half of the assembled units were then subjected to an etching process until the zero-bias capacitance was close to 3.7 picofarads. The remainder were etched down to a value of about 1 picofarad.

4.2 Life Test on Rectenna Elements and Diodes

Prior to the work undertaken under this contract there had been a life test started on rectenna elements and diodes utilizing the 199 element rectenna array development under an earlier MSFC contract. Because of the importance of the information being obtained from the life test, the life test was continued. Although the work was not a portion of the present contractural effort a summary of the results of the life test are being included here for documentation and reference purposes.

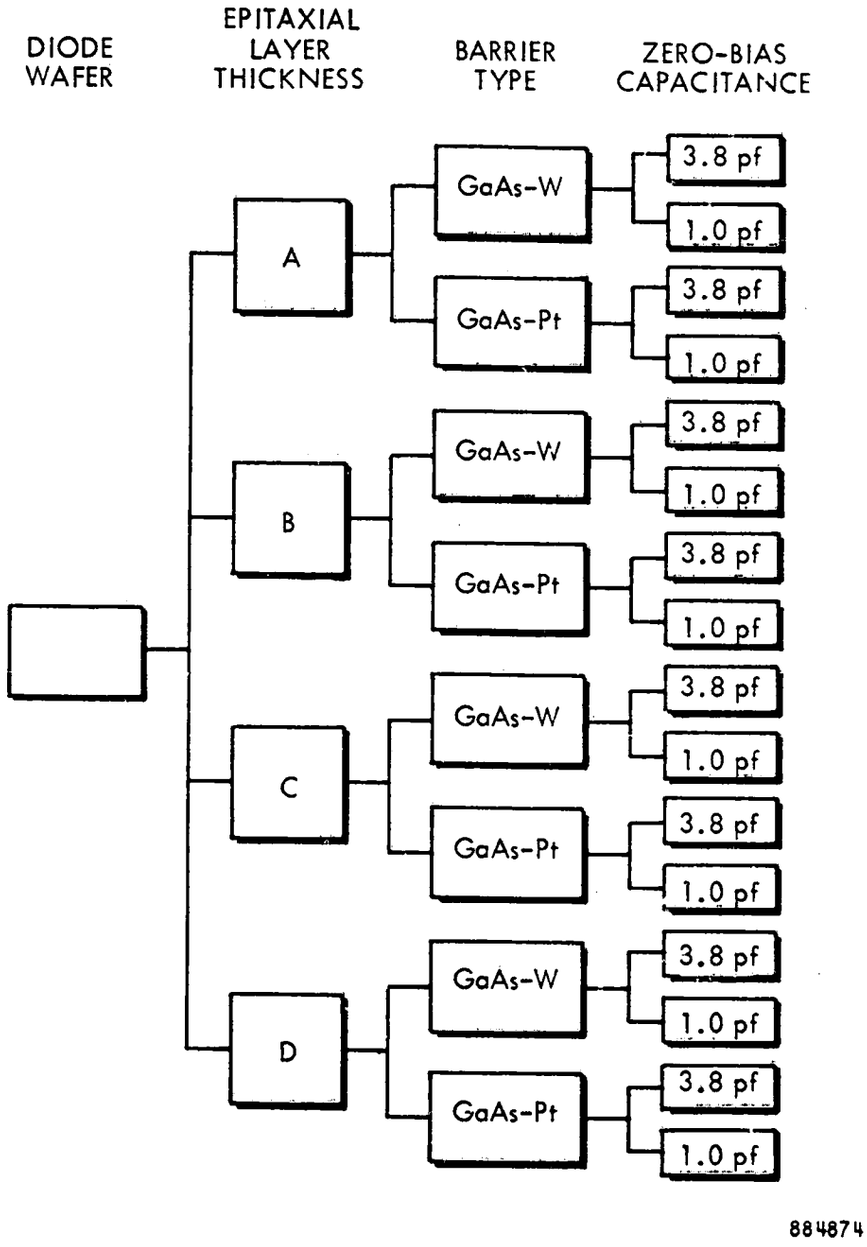

Figure 4-2. Diode Matrix and Manufacturing Sequence

The life test that was run is important because it was the first and only life test that has been run on Schottky barrier diodes used as high power microwave rectifiers. Normally these devices are used in Impatt applications. It was appreciated that the dissipation level in the Schottky barrier diode when used as a microwave rectifier would be considerably below the dissipation level when it is used as an Impatt device and that the dc bias on the diode would be less than half that in an Impatt device. These were factors which would normally enhance the life of the device. Still the microwave power rectification was a new application for the device and there had been no life experience.

Fortunately the rectenna designed as part of a complete microwave power transmission system (shown in Figure 1-13) for Marshall Space Flight Center made a natural test rack and panel for the evaluation of diodes used in RXCV rectenna elements. 199 rectenna elements could be inserted into the rectenna test panel. These elements were the same ones used in the certified demonstration illustrated in Figure 1-13. Further, the radial Gaussian pattern of illumination made it possible to vary the operating power level of the diodes over a wide range and provide a step stress kind of life test. The rectenna elements were combined into sets, each set being comprised of those elements which had a common radius from the center and therefore similar power illumination as indicated in Figure 5-13. The dc output terminals of all the rectenna elements in a set were connected in parallel across a common load for that set. If only one diode shorted out, there would be zero voltage across the load which would extinguish a light normally continuously on. In the case of an open diode, a reduction in power output of the set would be found when the total current in a set was periodically checked.

It was convenient to break the total number of elements down into seven groups depending upon the incident power. The power level and set numbers included in a group is given below.

Group Designation	Set numbers	Power Range of Group	No. of Units in Group
A	15, 16, 17, 18, 19, 20	0.2-0.5 Watt	78
B	12, 13, 14	0.5-1.0 Watt	30
C	9, 10, 11	1.0-2.0 Watt	30
D	6, 7, 8	2.0-4.0 Watt	24
E	4, 5	4.0-6.0 Watt	18
F	1, 2, 3	6.0-8.0 Watt	18
G	0	8.0-10.0 Watt	1
			199

It is therefore seen that the life test is conducted with a power range of over 20, making it possible to observe if the diodes in the high power range degrade more rapidly than those in the low power range.

Using this equipment a life test was started on 17 March 1975 and with occasional interruptions had reached 2913 hours by 22 Sept. 1975. During

the first 150 hours there were three failures. There were no more failures. If we regard these early failures as of an infant mortality type, a total of 2763 hours without a failure or noticeable degradation in efficiency performance had been achieved. Thus, 549,837 diode hours have been accumulated without a failure or noticeable efficiency degradation.

If we apply MTBF tables to this life test data, and request a 90 percent confidence factor, we find that the MTBF is 239,059 hours or 27.3 years. If we relax the confidence factor to 50 percent, an MTBF of 785,481 hours or 91 years is obtained.

The efficiency of the diodes in a set was monitored by periodically checking the current which flows into the common load resistor for each set, when the RF power which flows into the illumination horn is precisely set at a pre-established value. The data in Table 4-2 indicated negligible drift in efficiency performance after 1800 hours of life test operation. The average ratio of the last measured currents to the initial measured currents is 0.9982, representing a very small change and one which is easily attributable to measurement error. The average deviation of the ratios from unity is 0.0123. Of special interest is the fact that no degradation was noticed for the rectenna elements operating at high power levels. These power levels are several times what would be antifipated in the SSPS rectenna.

Figure 4-3 provides a summation of the life test data taken up to a total of slightly over 800,000 diode hours. After the 2913 hours of life test just reviewed an operator accidentally applied much higher microwave power to the test set and four diodes failed in Group F. The first life test failure not to be confused with operator error occurred at 3078 hours. It occurred in Group F. The life test was continued without additional failure to 4178 hours when it was shut down for two weeks. In restarting the life test the single center element failed. It is believed that the applied microwave power was at an excessive level. The life test was discontinued on 24 March 1976, a little more than a year after it had started.

In summary, a great deal was learned from the life test. The test was not a continuous life test and there were substantial periods of time in which the set up was not operating. Hence there was also a kind of shelf life evaluation to help rule out a "sleeping sickness" type of syndrome. Many of the groups of elements were run at power levels several times that anticipated in the rectenna for the SSPS and no degradation in efficiency was noted for these elements after a running time of 1800 hours. The life test results were marred by operator error but there was a continuous period of time with no failures of any kind which indicated a mean time between failure of 27 years with a confidence factor of 90%

TABLE 4-2

EFFICIENCY PERFORMANCE

Set #	No. of Elements in Set	Initial Current 151 Hrs	Current 1428 Hrs	Current 1800 Hrs	Ratio of Current (1800 Hrs) to Current (151 Hrs)
0	1	251	251	254	1.0120
1	6	1363	1360	1360	0.9978
2	6	1258	1261	1268	1.0079
3	6	1198	1194	1199	1.0008
4	12	*	*	*	
5	6	1010	1012	1014	1.0040
6	6	939	934	933	0.9936
7	12	1783	1768	1776	0.9961
8	6	792	790	791	0.9987
9	12	1306	1299	1298	0.9939
10	12	1190	1180	1189	0.9992
11	6	547	544	548	1.0018
12	6	524	509	509	0.9714
13	12	935	910	920	0.9840
14	12	818	813	825	1.0085
15	6	362	358	358	0.9890
16	12	654	668	682	1.0428
17	12	639	628	631	0.9875
18	12	558	548	556	0.9964
19	6	220	235	240	0.9600
20	18	678	681	701	1.0339
21	12	431	420	424	0.9838

* Beyond current range of monitor meter. Average Ratio: 0.9982

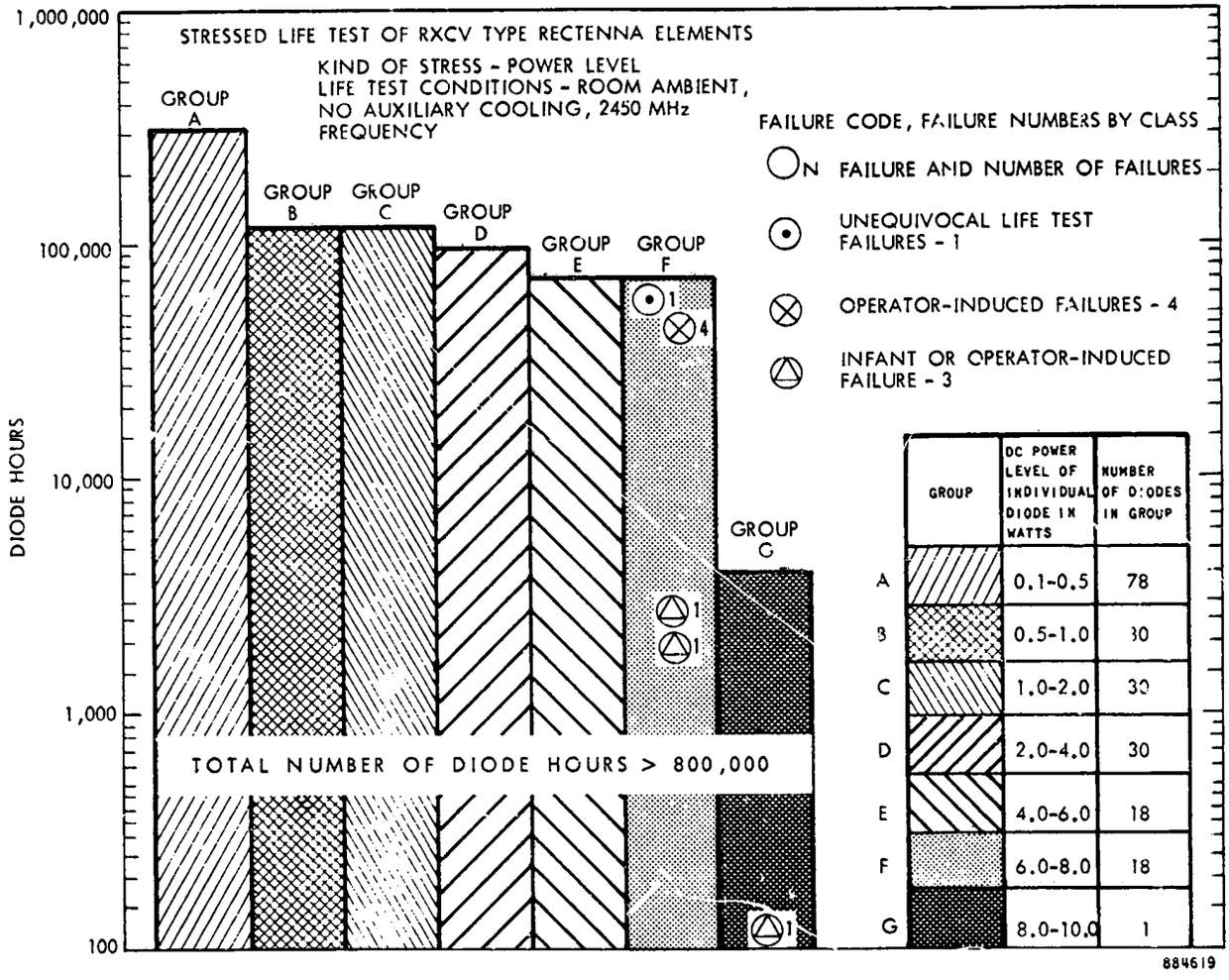

Figure 4-3. Diode Life Test Results Using Test Arrangement Shown in Figure 1-13.

5.0 INTEGRATION OF IMPROVED DIODES AND CIRCUITS INTO A DESIGN COMPATIBLE WITH THE LONGER RANGE OBJECTIVE OF A LOW-COST RECTENNA SUITABLE FOR SSPS DEPLOYMENT

5.1 Introduction

Prior to this contract, there had already been an appreciable base established for a low-cost design. Early rectenna designs had employed a two-plane construction in which one plane was merely a metallic reflector of some kind while the other plane contained the half wave dipole, the rectification circuit, and the DC collecting busses. However, in an attempt to better understand the behavior of the rectenna array, as well as to incorporate some necessary harmonic filtering into the system, the development had subsequently gone in the direction of a three-plane system in which the DC power was collected in a third plane which was behind the reflecting plane. This development sponsored by MSFC support led to better performing rectenna hardware as well as to a better understanding of its behavior. It was then very logical to use the design of the MSFC hardware as a base for fulfilling the NASA sponsored JPL contract calling for the efficient reception and rectification of substantial amounts of microwave power (30 kw) that was to be transmitted over a distance of approximately 1.6 kilometers.

At the successful conclusion of that effort it was logical to think in terms of returning to the two-plane construction and to incorporate the best features of the three-plane rectenna development into it. The present study has successfully pursued this conversion while taking these pertinent factors into account: (1) the need for protecting the active portion of the rectenna from the weather environment (2) the need to minimize radiation of unwanted harmonics (3) the desire to utilize the front active plane of the structure as a structural element to reduce the cost of materials and the cost of fabrication, and (4) the need to develop an output voltage of at least 1000 volts to establish efficient DC to 60 cycle inversion. It is believed that the design approach that has resulted from the present contract fulfills all of those requirements as well as lending itself to a low-cost high speed construction. There are many details, of course, that need to be filled in.

The general design approach that has resulted from this study is shown in Figures 5-1 and 5-2. The construction shown in Figure 5-2 is identical to that tested out in the 199 element array for compatibility evaluation except for the addition of the teflon caps over the half wave dipoles and the replacement of the solid metallic reflector with the electrically equivalent wire mesh.

The exploded view of the foreplane structure shown in Figure 5-3 clearly differentiates between the basic core structure and the external metal shield which also doubles as a major structural element.

In the material that follows we will discuss various aspects of the development and how it should integrate into further development programs and the final manufacturing process for the SSPS. The description of the testing and electrical data are given in Sections 5.5, 5.6, and 5.7.

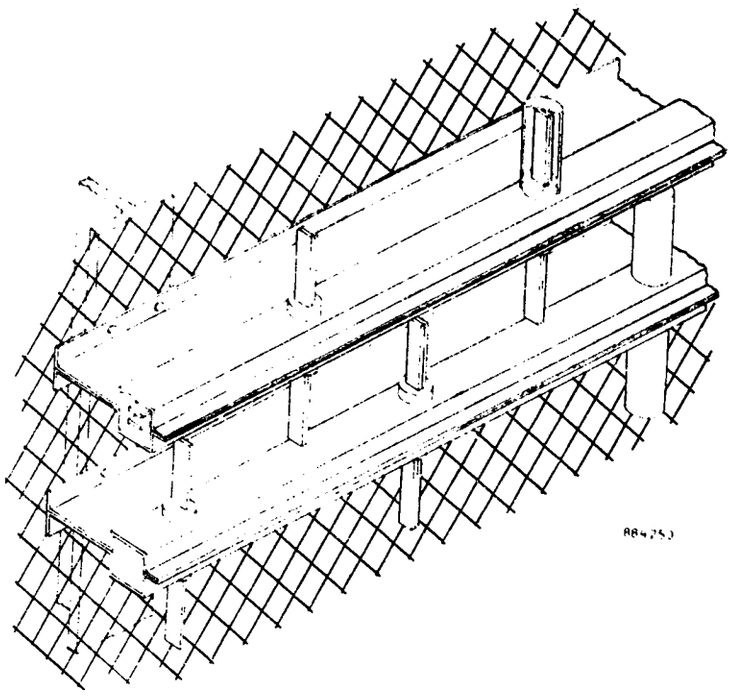

Figure 5-1. Proposed design of Rectenna motivated by environmental protection and cost considerations.

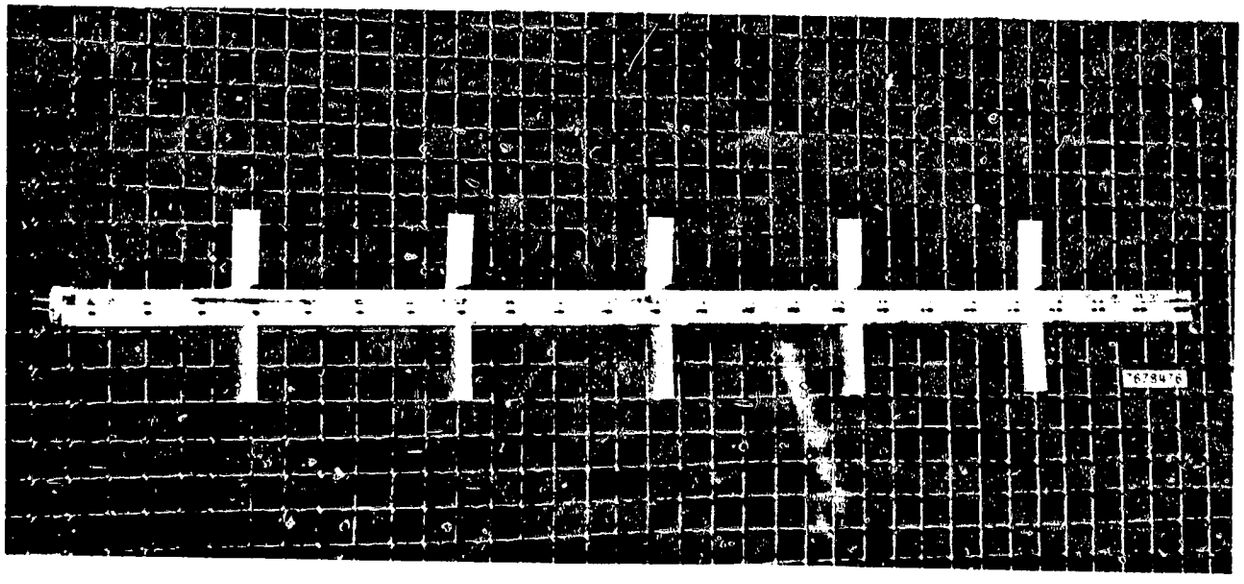

Figure 5-2. Physical construction of two-plane rectenna. With the exception of covers (white teflon sleeves in photograph) this is the same five element foreplane that was electrically tested in Figure 5-12. Reflecting plane made from hardware cloth is representative of what could be used in SSPS rectenna.

5.2 Outline of a Production Process for the SSPS Rectenna

A logical revision of the design of the core structure shown in Figure 5-3 lends itself to a high speed fabrication method which starts out with rolls of flattened wire and insulation material as suggested in Figure 5-4. The wire is rapidly and continuously formed into the side rails of the core structure. These side rails double as microwave transmission lines and busses for collecting the DC power. The two side rails flow together and are fastened to each other in such a way as to form the needed capacitors and the inductive sections of line. The diode is also incorporated at some point. This core-assembly flows continuously together and then the metal shield flows around the core assembly as suggested in Figure 5-5, and is joined together in some manner. (Note the form of the field in the assembly of Figure 5-5 was an earlier variant). The material from which the shield is fabricated is as thin as possible consistent with the strength that is needed for structural purposes.

At this point of development, the subsequent production assembly methods have not been defined, but one can imagine the output of many fabrication machines flowing out over a reflecting plane made up of wire mesh and being joined to it. The reflecting plane in turn is joined to a supporting structure as suggested in Figure 5-1. The entire prefabricated assembly then rolls off the back of a continuously moving factory such as that shown in Figure 5-6.

In this advanced concept materials are hauled into the front of the moving factory and the finished assembly flows out the back. An alternate approach to the moving factory is a fixed factory at the site of the rectenna; in this case the finished rectenna sections would be hauled to the site by specially made trucks. However, the argument for the moving factory is that continuous lengths of rectenna several hundreds of meters long will be needed; this would complicate the hauling process.

In any event, some high-speed, on-site production method will be necessary because of the large scale of the SSPS rectenna as indicated in Table 5-1. Because of the economic desirability of fast erection of facilities, it would probably be desirable to install a complete rectenna in about one year's time. This means that for a rectenna with ten billion elements the rate of production of rectenna elements would be about 318 per second in order to construct the rectenna within the 8760 hours of a year's time. If the rectenna panels were 6 meters wide the moving factory would have to move at the rate of 0.265 meters per second to cover the area with rectenna panels in one year. Undoubtedly the use of more than one machine would be found to be cost effective.

There are a number of changes that will have to be made in the present core-assembly design in order to make it more compatible with a low material cost and high speed assembly. The use of teflon machine screws, nuts and washers to form the capacitors and to hold the structure together is of course incompatible both from a cost and assembly point of view. An alternate approach

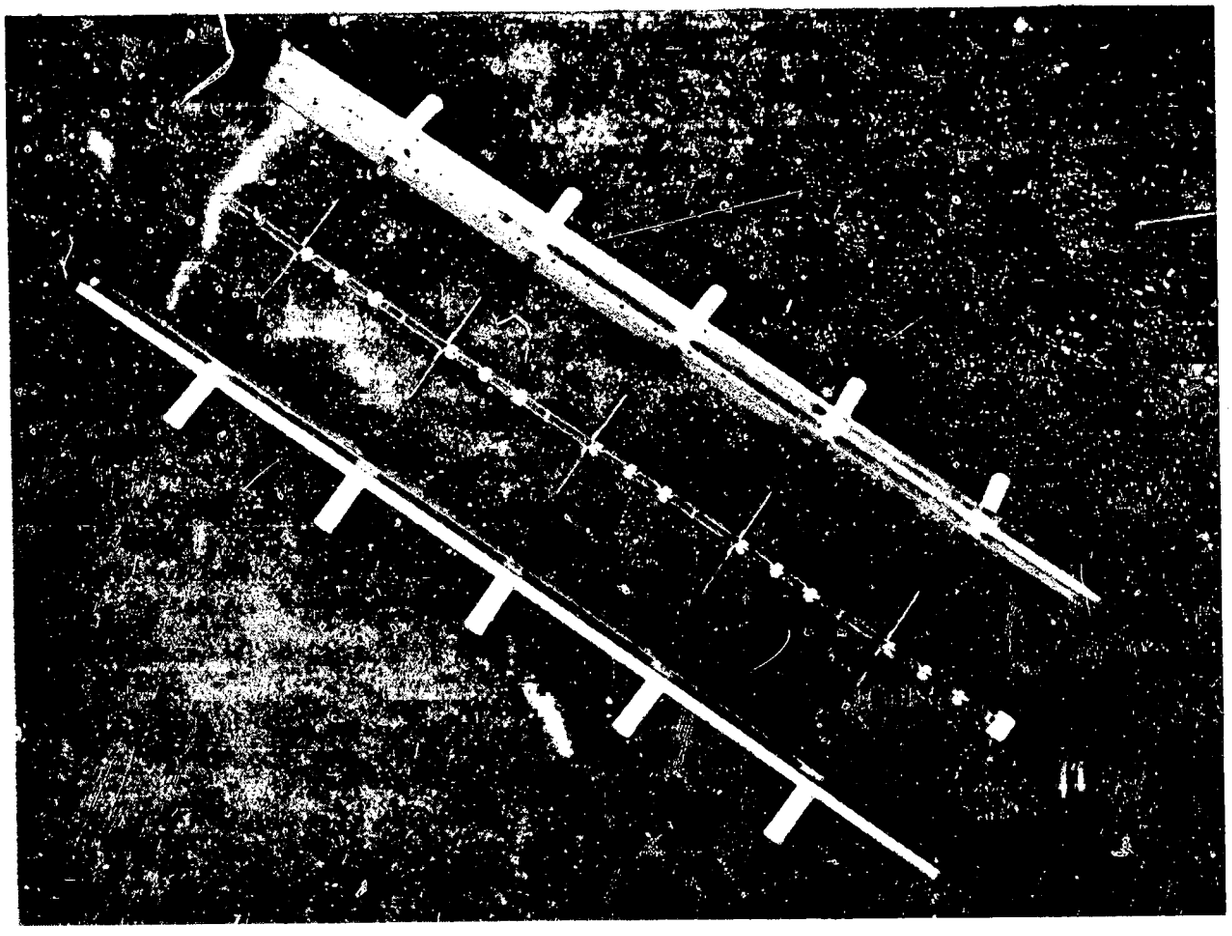

Figure 5-3. Basic core structure design illustrating the joining of individual rectenna elements to each other to form a linear, easily-fabricated structure performing the functions of DC power bussing and microwave collection and rectification

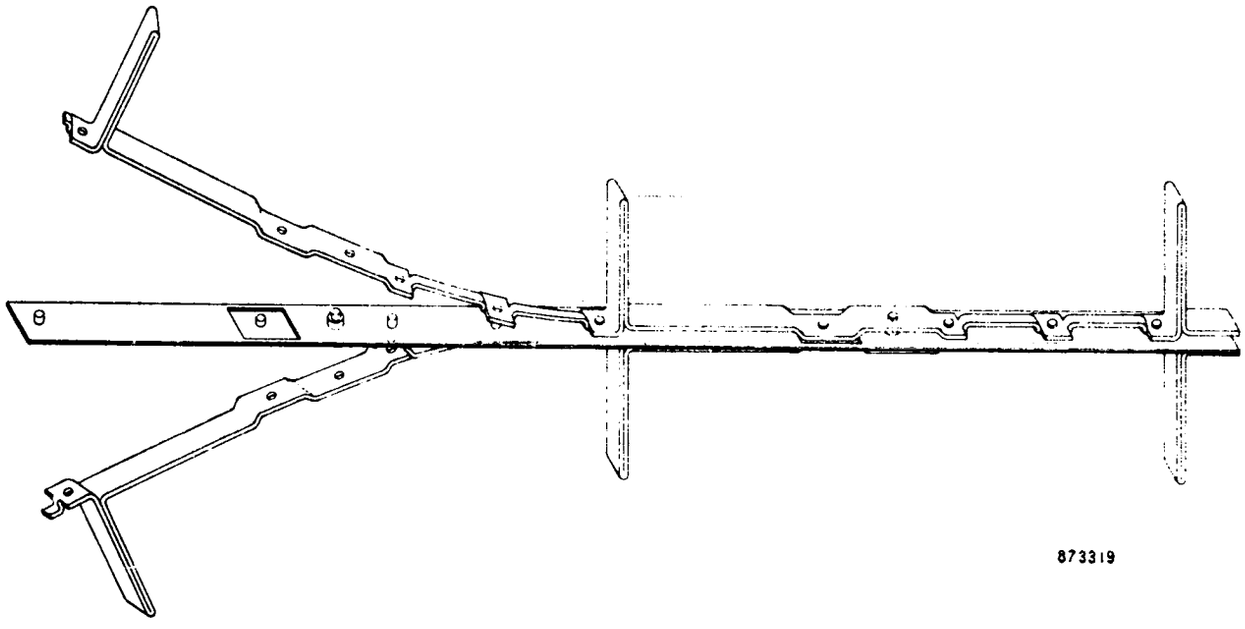

Figure 5-4. Proposed method of continuous fabrication of the core assembly of rectenna elements.

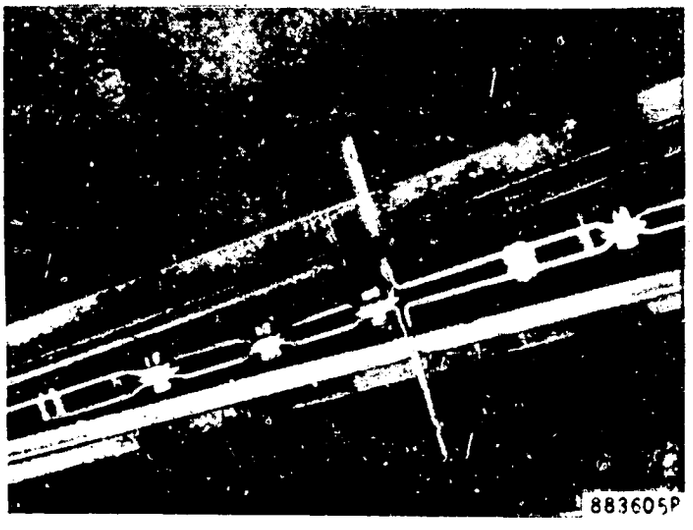

Figure 5-5. A mechanical mockup of the proposed design of Figure 5-1 showing how the metal envelope can be assembled to the core rectenna in a continuous-flow type of manufacturing assembly. The metal envelope is an early design and has been superceded.

TABLE 5-1

STATISTICS ON RECTENNA

Wavelength	12.25 cm
Rectenna Diameter	9.2 Kilometers
Total Area	66×10^6 Square Meters
Average Power Density	
10,000 Megawatts DC	151 Watts/Square Meter
5,000 Megawatts DC	75 Watts/Square Meter
Total Number of Rectenna Elements	1.32×10^{10}
Rectenna Element Density	200/Square Meter
Maximum Power Per Element	
10,000 Megawatts DC	2.8 Watts
5,000 Megawatts DC	1.4 Watts

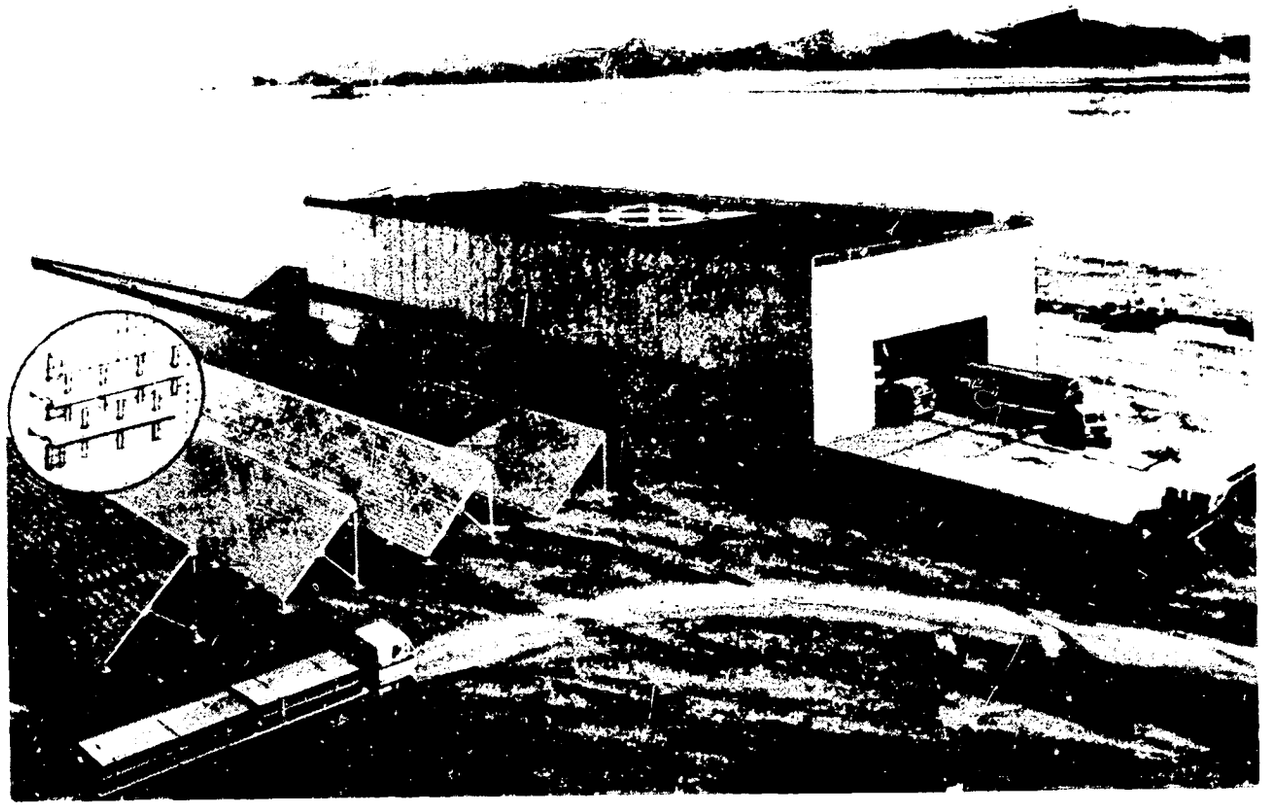

Figure 5-6. Artists' concept of a moving rectenna factory. Materials brought in at one end of factory are basic ingredients to high speed automated manufacture and assembly of rectenna panels which flow continuously from other end of factory. Panels are placed on footings also placed in the ground by the moving factory.

that appears to be attractive is the use of staked-in alumina pins which supply the needed capacitance as well as the means of holding the structure together and spacing the core structure from the metal shield. A preliminary assembly that has withstood some initial thermal shock testing is shown in Figure 5-7.

5.3 Interrelationships Between the Losses in DC Bussing, the Cross Section of the DC Busses, the DC Power Collected by Each Element, the Density of the Rectenna Elements, and the Required DC Output Voltage Level

It has been recognized that the rectenna DC power must be collected locally at a significantly high voltage for two reasons. The first of these is to avoid excessive expense for collecting busses and the second is that the devices used for inverting dc into 60 cycle power become highly efficient only at voltage levels of 1000 volts or more. How does this requirement tie in with the proposed fabrication technology?

In order to get the required voltage it will be necessary to connect in series sections of rectenna line in each of which the individual diodes are operated in parallel. Also, it will be necessary to have an outbound section as well as an inbound section because of the series connection. This results in the circuit as shown in Figure 5-8. It is noted that the series connection of the sections can be accomplished without any additional expense as part of the fabrication procedure shown in Figure 5-4. The only requirements are that one side of the line be cut between successive sections* and that the direction of the diodes be reversed in successive sections.

With this material as a background we are now in a position to derive a useful formula which relates the length of the structure to (1) the ratio of I^2r loss to the collected dc power, (2) the number of rectenna elements per unit length, (3) the dc power level collected per unit element, and (4) the dc resistance provided by the side rails of a single rectenna element. The formula follows:

$$L = 10^3 \sqrt{\frac{k}{n^2 w r}} \quad , \text{ where:} \qquad (5)$$

L = the total length in meters of two strings of rectenna elements, which represent the outbound and inbound strings, respectively.

k = the ratio of the total I^2R loss to the total dc power collected.

n = the number of rectenna elements per meter.

w = the dc power collected by each element.

* Cutting the sections in this fashion would perturb the performance of the $\lambda/4$ isolating section and needs to be looked at in more detail.

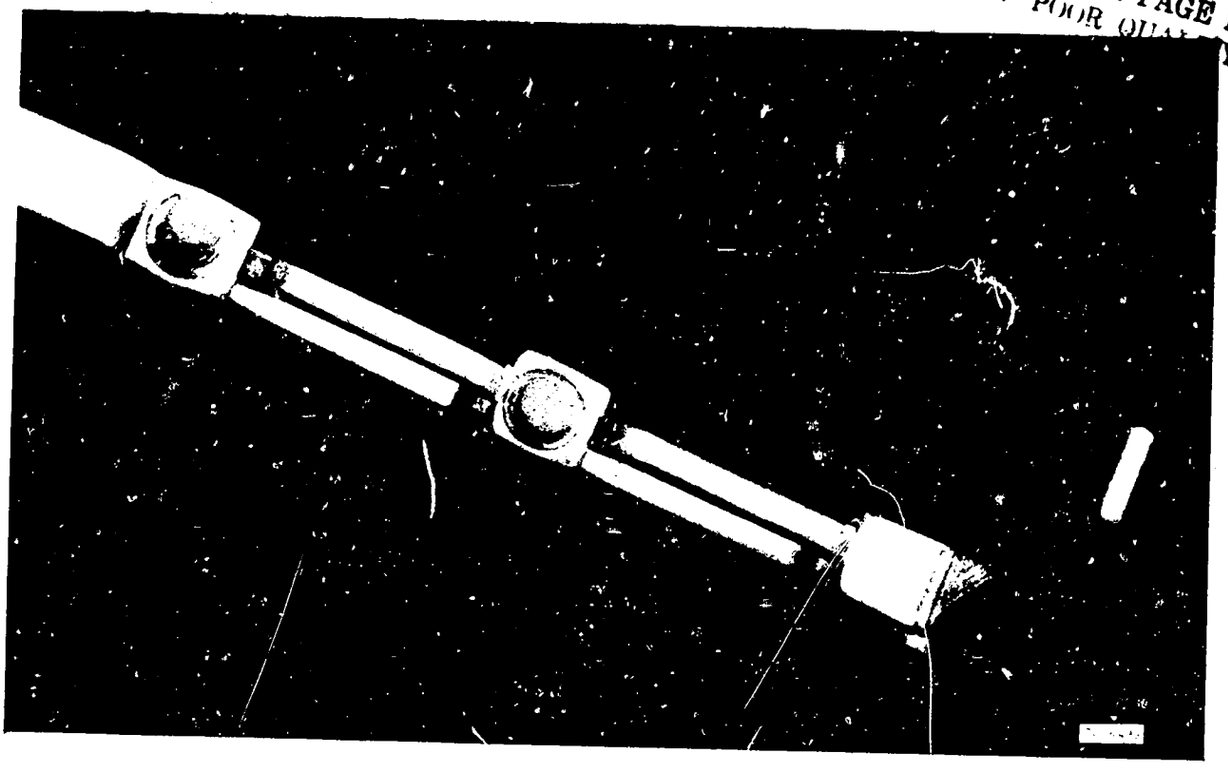

Figure 5-7. Suggested assembly method in which staked-in ceramic pins provide the dual function of assembling the rectenna element and behaving as electrical capacitance in the low pass filter.

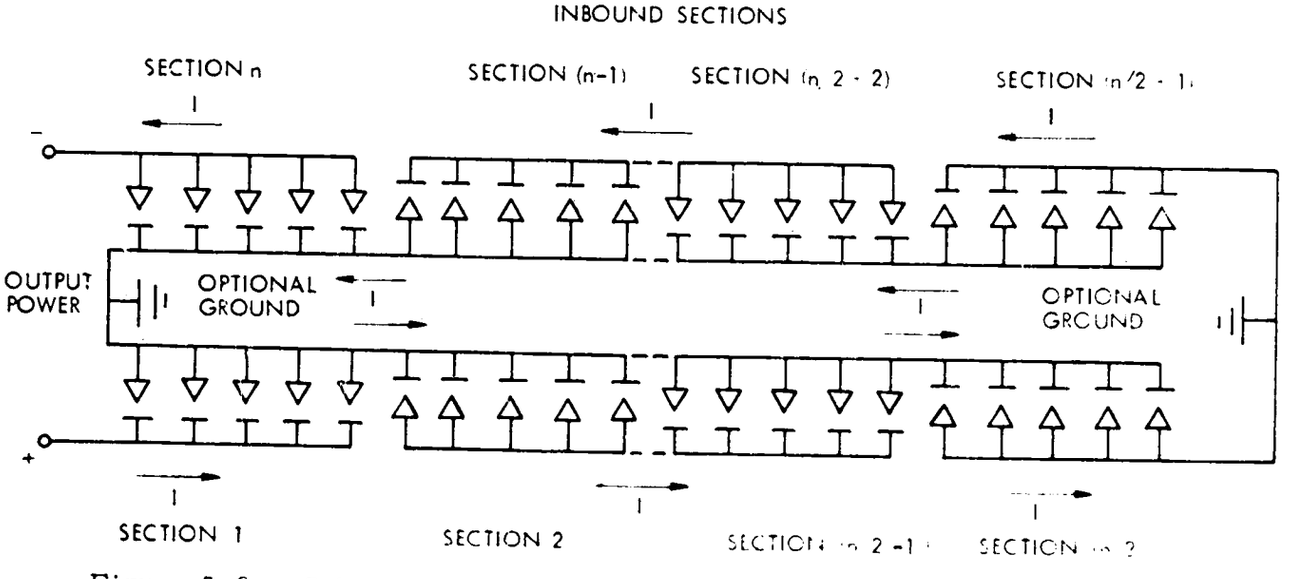

Figure 5-8. Schematic electrical drawing showing how the sections of parallel diodes are connected in series to build up to the desired voltage level at the output.

r = the dc resistance provided by the side rails acting as dc collecting busses for one single element.

If we substitute into this formula the value of n of 13 that is currently being used, and the value of r of 1.72×10^{-3} ohms for the RXCV rectenna element, we obtain the following expression

$$L = 1854\sqrt{\frac{k}{w}} \tag{4}$$

As an example, if the I^2R losses represent 1% of the dc power collected (k = .01), and w is one watt, the total length of the assembly is 185.4 meters. It follows that the number of elements in the string is 2,405, the dc power collected is 2.405 kilowatts and the I^2R losses are 24 watts. Depending upon the proper value of resistive load for each rectenna element, there will be between 40 - 60 sections connected in series. Of course, the total number of elements should be some integral multiple of the total number of sections and will, therefore, not be exactly the number 2.405.

The weight of the aluminum raw material stock from which the rectenna line loop of 185.4 meters is constructed in 5020 grams or 2.09 grams per element. At a current base price of 41¢ a lb for aluminum, this represents a raw material price of 0.183¢ per element, or $1.83 per kilowatt.

If the size of the rectenna requires 10^{10} elements, and the construction remains the same throughout the rectenna, a total of 2.3×10^4 tons of aluminum will be required, or about 0.35 of one percent of the total aluminum produced in the United States in one year.

There is, no doubt, some tradeoff in the value of electrical energy against the investment in conductors for bussing the power. However, the fabrication technique that is shown in Figure 5-3 presents definite restrictions on the cross sectional size of the conductor. It is also noted that rectenna elements made by conventional printed circuit technology would not provide significant self-bussing (or cooling of the diodes) because of the small cross section of the conduction numbers.

5.4 The Design and Construction of the 5-element Foreplane

The 5-element foreplane is the terminology used to describe all of the structures shown in Figures 5-2 and 5-3, with the exception of the reflecting plane. This section will describe the design considerations going into the design and construction of the outer metallic shield and the core-assembly.

5.4.1 Considerations in the Design of the Outer Metallic Shield

In this design, the metallic shield fulfills three requirements imposed upon it: (1) the prevention of direct radiation from rectifier circuit into space, (2) to function as a structural element for the rectenna, and (3) to be fabricated economically.

A photograph of the shield as mechanically fabricated is shown in Figure 5-9. The top and bottom parts are identical. The form of the shield and its appearance when combined with the rectenna core are shown in Figure 5-10.

The choice of the kind of metal and its thickness for the fabrication of the shield received considerable attention. Aluminum was selected as the initial material, primarily because it represents an excellent tradeoff between cost and durability. A secondary factor was its low electrical loss, which is of some importance because some currents will flow in the walls of the shield. Stainless steel might also be considered, but it would be considerably more expensiven even after allowing the use of a thinner material because of the higher modulus of the material.

The requirement for low material cost which will ultimately represent most of the cost of the rectenna indicated that the stock should be as thin as possible since material cost is approximately proportional to thickness.

On the other hand, the strength of the shield as a structural element, the deflection of the shield due to an external force, and the period of vibration will be dependent upon material thickness and upon the size and shape of the cross-section. Further, if the external force is caused by wind pressure, this force will be a function of the size and shape of the structural element. Although this situation would seem to generate a complex tradeoff, matters are greatly simplified because the size of the tubular shield must be at least 1.0 cm for mechanical reasons of housing the rectenna element core and to allow for adequate insulation in the grommet that fits between the shield and the antenna, but no larger than 1.5 cm because of increased wind resistance and non-TEM modes that could exist for high-order harmonics in larger tubes. A good compromise would seen to be a 1.250 cm tube, and to make it rectangular rather than circular in shape because of the increase in moment of inertia by a factor of 5.33 and therefore greater stiffness and strength for a given wall thickness, and because of the much easier problem in designing a suitable grommet.

The problem then narrows down to a selection of the thickness of the material from which the tube of square cross-section will be made. This, in turn, will depend upon an appreciation of how the metal shields fits into the overall rectenna as a structural element. From Figure 5-1 it is seen that the tube is joined onto a foot which would normally be a part of the same continuously formed piece and that this foot, in turn, is joined onto the reflecting plane made from some kind of an expanded metal or interwoven wire (with secured joints at the crossovers). Thus, the moment of inertia of the metal shield arounds its

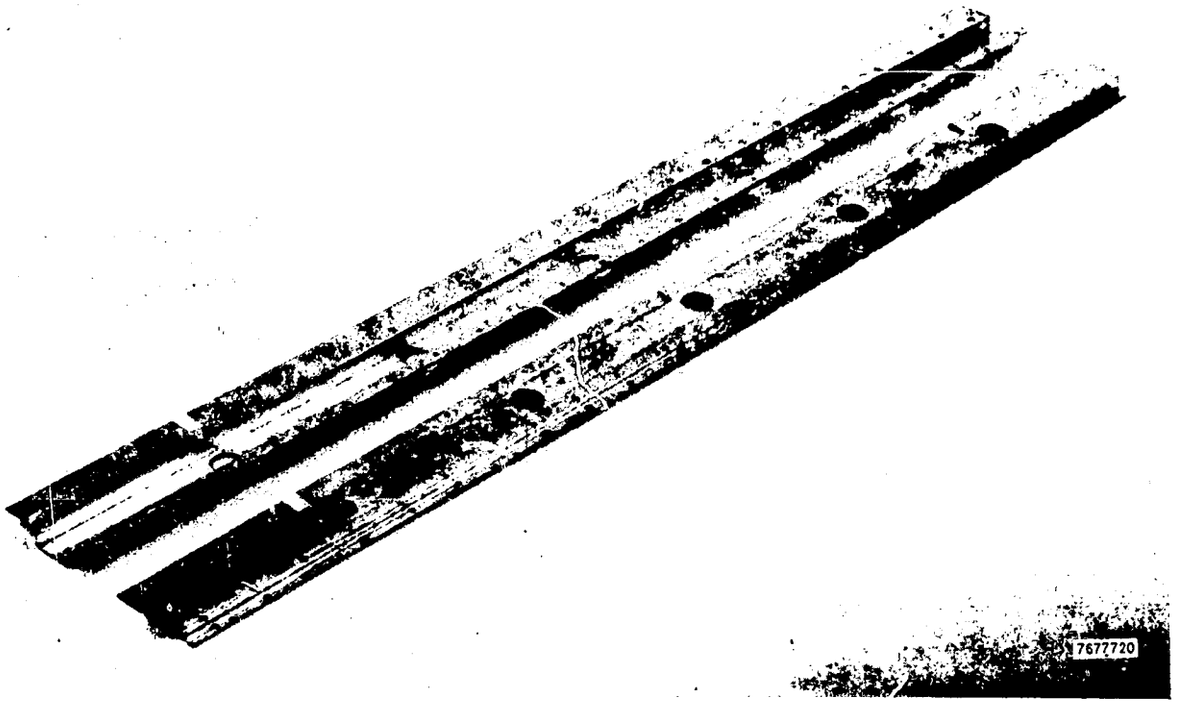

Figure 5-9. Fabricated Metal Shield Halves Which Will Support and Shield, Both Electrically and Environmentally, the Rectenna-Element Core.

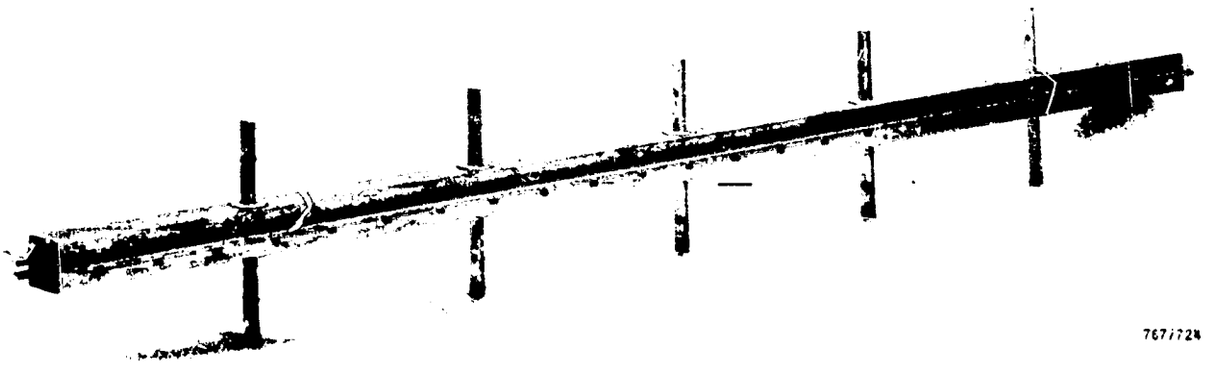

Figure 5-10. Completed rectenna fore-plane assembly consisting of metallic shield and the core assembly of five rectenna elements.

neutral axis parallel to the metal screen and at right angles to the axis of the tubular shape will be much larger than the moment of inertia on the structural member about a neutral axis normal to both the screen and the axis of the tubular shape.

It is noted that the screen itself will prevent the foot of the structural member (that is, the point at which it joins to the metal screen) from deflecting up or down, and the screen itself will add to the moment of inertia because it is joined to the metal shield. This will probably place the neutral axis not too far from the foot of the structural member itself. This all adds up to a very small amount of deflection in a direction normal to the reflecting screen. On the other hand, if Figure 5-1 is examined, the metal shield as a structural element is seen free to flex at the point where its foot joins the metal screening. This could normally be taken care of by inserting some webbing between the foot of the structural member and the square tubular section and welding it to all metal interfaces. The method of continuous fabrication of the shielding member, however, makes the insertion and welding of such a web a difficult undertaking. On the other hand, it would be possible to attach a supporting member to the post (the post is shown in illustration 5-1 as a "T" beam). The supporting member would consist of two parts: an upper part which would prevent any upward motion of the tubular portion of the metal shield and a lower part which would prevent any downward movement of the metal shield. Then, between any two vertical supporting posts (the "T" sections again), the bending of the tubular portion of the shield halfway between the supporting posts would be constrained by the moment of inertia of the tubular section about an axis normal to its own axis and normal to the supporting screen, and by the constraint placed on the foot of the shield where it joins the reflecting screen.

A consideration of all of these factors led to a choice of aluminum material in the range of 0.012 to 0.025 cm. Material in this thickness range is consistent with the material costs that have been estimated for the production rectenna. Rolls of aluminum shim stock in sizes 0.012, 0.020, and 0.025 cm thickness were obtained. An initial selection of 0.020 cm thickness was made.

The 0.020 cm thick material is much thinner than is normally used in the shop and outside the scope of normal shop familiarity and shop equipment. Temporary tools were used, therefore, in the laboratory to form the material as shown in Figure 5-9. Since the material was formed around commercially available ground steel stock, a high degree of precision in forming the pieces was possible. A simple drill jig was also necessary for positioning and drilling the holes for the grommets.

The foot or turned up section where the shield would join the rectifying screen was not formed on the piece. For electrical reasons, we wanted to be able to vary the spacing of the dipole elements from the reflecting plane when it was tested in the central area of the 199 element rectenna.

Because the shield was used for an experimental assembly containing the rectenna core which was modified during the testing period, the edges of the shield have holes drilled in them to permit the use of 0-80 machine screws to hold the pieces together. When the two halves are joined together with machine screws, a surprisingly stiff member results.

5.4.2 Considerations in the Design of the Core Assembly

It was determined early in the work performed under the contract that the individual rectenna element would work satisfactorily in the waveguide test fixture if the axis of the rectenna element was oriented as shown in Fig. 3-4.

Most of the effort in the design of the 5-element foreplane assembly was in connecting the five elements together. This normally simple problem was complicated by the fact that the pitch of the elements (that is the distance between centers of the successive halfwave dipoles) was not great enough to include the shorted quarterwavelength section of air line that is necessary to isolate the elements from each other at the fundamental frequency of 2.45 GHz.

This problem was resolved by adding a capacitance in shunt with the input of the shorted section of line to resonate it at the fundamental frequency. From a physical point of view, this was accomplished by using a thinner Teflon washer at the input of the low pass filter so that there is no additional cost or mechanical complication. The solution is much superior to filling the section of line with a continuous dielectric.

By adding another capacitance of the proper value at the midpoint of the section of line, it was possible to make the section an electrical halfwavelength at the second harmonic while still maintaining a quarter-wavelength at the fundamental with now another value of capacitance having been selected for the input to the line. The half-wavelength line at the second harmonic can behave as a short for the second harmonic at the output terminal, thus in principle decreasing the second harmonic output. However, the adjustment of the value of the midpoint capacitance was found to be very critical; and it was found that a decrease in efficiency and an increase in harmonic content occurred at a point of adjustment only slightly removed from the point at which the radiated second harmonic power was a minimum. It was felt that the reduction in efficiency might correlate with an increase in the generation of second harmonic power in the rectification circuit and suggested an investigation of harmonic power generation as a function of the termination of the low pass filter at the input to the dipole antenna. Although such an investigation was needed, it was identified as a diversion to the main thrust of this task, which was to test the foreplane as part of the 199 element MSFC rectenna. The midpoint capacitance, therefore, was not included in the construction of the core assembly.

Before concluding this discussion it is noted in Section 3.4 that the second harmonic can be reduced considerably by tuning the intervening section of line to the second harmonic. The criticality of the adjustment was not noted although it may well have been there.

5.5 Tests of the Separate Rectenna Elements in the Foreplane Structure with the use of the Expanded Waveguide Fixture

Because the individual elements are isolated from each other in the foreplane structure it should be possible to check the elements individually. Therefore, extensive tests were carried out on the individual elements in the foreplane assembly using a modified expanded waveguide test fixture. The modifications consisted of cutting deep slots into the sides of the test fixture to accept the foreplane. After the foreplane is inserted into the test fixture, the lid is closed and clamped. Secure contact is made between the lid of the fixture and the back of the foreplane section with the use of machine screws, although good contact does not appear to be necessary for proper operation.

Table 5-2 presents the results of the final tests that were made on each of the rectenna elements in the foreplane structure. A set of five GaAs-W Schottky barrier diodes fabricated as part of the diode development program was used. Each of the five diodes was also checked out in an RXCV element to ascertain if there was a substantial difference in efficiency between the RXCV element in the foreplane structure. A slightly lower efficiency (less than 1%) of these elements in the foreplane was noted. This loss was probably caused by the losses in the section of the transmission line that joined the rectenna section to the next within the foreplane construction. The average overall efficiency (the ratio of DC power output to incident microwave power) of the 5 elements in the foreplane was 87.86%. The reflection loss was only 0.26%. An incident power level of 4 watts was used for the test.

Although it was possible to match the foreplane elements so that there was a very small reflection, in the cases of elements 4 and 5 the efficiency decreased substantially when the elements were matched out. This was not the case with the other three elements, and there was no obvious cause of the anomaly experienced with elements 4 and 5.

5.6 Smith Chart Presentation of Reflection Data

A Smith Chart presentation of microwave reflection as a function of incident microwave power level and the ohmic value of DC load resistance, made for a typical element in the foreplane structure is shown in Figure 5-11. This indicates, as had previous measurements of reflected power, that low values of reflected power (less than 1%) can be obtained over a relatively wide range of microwave power input if the proper load resistances are used. However, the reflection can be made to vanish only for a combination of load resistance and microwave power input. An adjustment of the load resistance primarily accommodates a mismatch of the resistance portion of the microwave load, but not the reactance part. The admittance is measured at the point where the half wave dipole input terminals connect to the input of the low pass filter. A temporary short at this point was used to find the corresponding reference point on the moving-probe slotted waveguide standing wave detector. The slotted waveguide standing wave detector is attached to the input of the expanded waveguide test fixture. Figure 5-11 utilizes only the central part of the Smith Chart in order to

Table 5-2. Comparison of the efficiency of the five elements in the foreplane structure with the RXCV element using a set of five GaAs-W Schottky barrier diodes fabricated as part of Task III, diode development

	Diode Identification	50234CX WC-9	50234CX WB-12	50234CX WC-12	50234CX WC-6	50234CX WC-8	Average of 5 Tests
TEST OF DIODES IN RXCV ELEMENT using expanded waveguide fixture 160Ω load 5 watts of rf input	$\%1 = \frac{\text{DC Output Power}}{\text{Incident RF Power}}$	87.32	88.95	89.55	88.80	88.65	88.65
	$\%2 = \frac{\text{DC Output Power}}{\text{Absorbed RF Power}}$	89.14	89.53	89.97	89.49	89.66	89.55
	% of Incident Power Reflected	2.05	0.65	0,47	0.77	1.12	1.01
TEST OF DIODES IN FOREPLANE STRUCTURE using modified expanded waveguide fixture 180Ω load 4 watts of rf input	Rectenna Element Number in Foreplane Array	1	2	3	4	5	
	$\%1 = \frac{\text{DC Output Power}}{\text{Incident RF Power}}$	88.20	88.90	88.20	86.66	87.36	87.86
	$\%2 = \frac{\text{DC Output Power}}{\text{Absorbed RF Power}}$	88.43	88.95	88.68	86.88*	87.49*	88.08*
	% of Incident Power Reflected	0.26	0.07	0.55	0.26	0.15	0.26

* Before rematching to reduce reflected power, %2 for elements No. 4 and No. 5 were 88.31 88.84, respectively — significantly higher. Average %2 before rematching was 88.60.

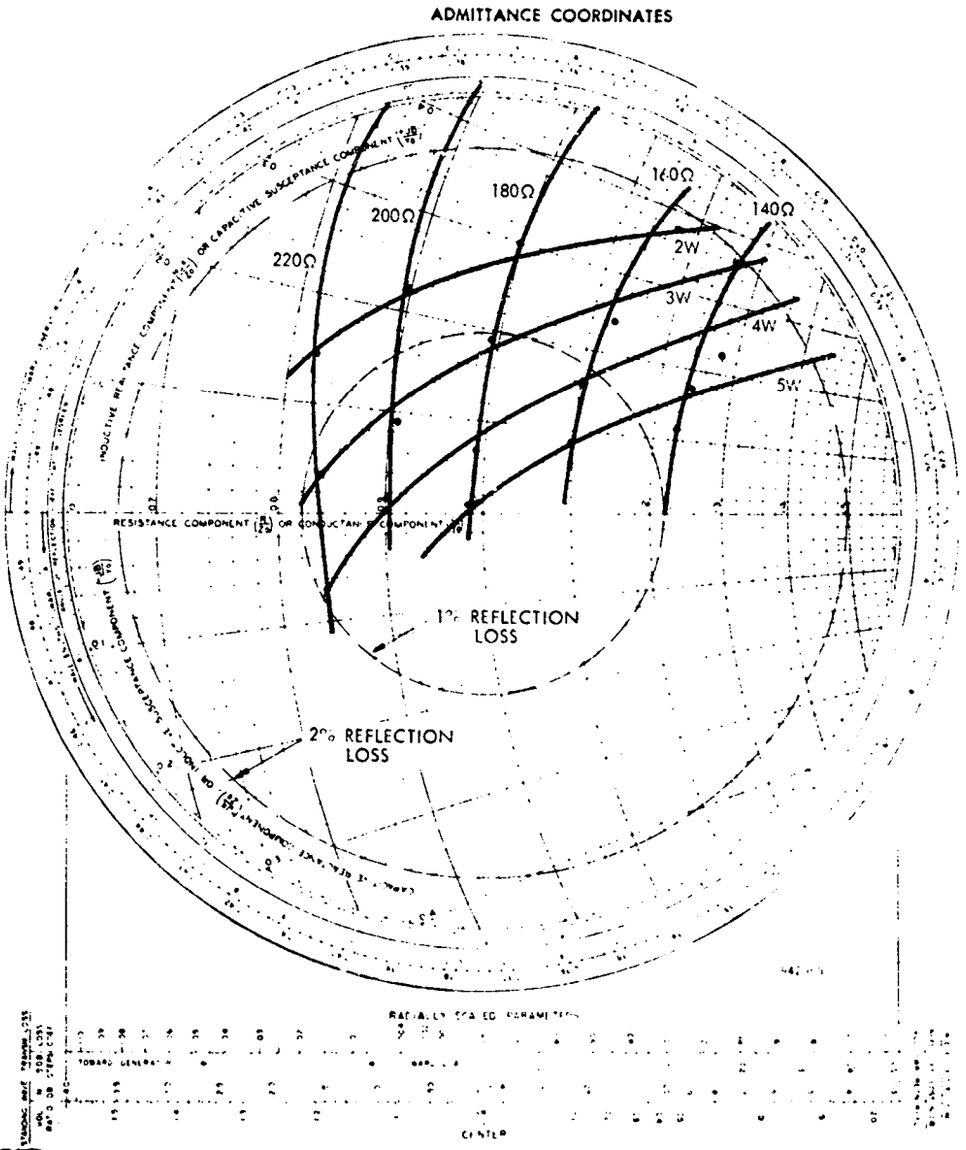

Figure 5-11. Input admittance to the foreplane rectenna element measured at the junction of the half-wave dipole to the low-pass filter section. Input admittance is a function of the input microwave power level and the DC load resistance. Data were obtained using the expanded waveguide test fixture and one of the elements in the foreplane construction. The rectenna element tested was connected in the intended manner to the adjacent rectenna elements. The susceptance component can be varied by resetting the position of the movable short near the diode rectifier. By adjusting this setting and the DC load, it is possible to obtain a zero power reflection for a wide range of incident power. The 5-watt input level was placed at the center of the Smith Chart because this is the intended power level of operation when the foreplane structure is put into the 199-element rectenna for test.

show clearly in the form of concentric circles the relatively small amount of reflected power associated with relatively large variations in admittance from that which matches the generator source. It is noted that a very wide range of input power is associated with a value of reflected power less than 1% of the incident power.

The data in Figure 5-11 are plotted in admittance form. The conductance component tends to remain constant, while the susceptance component varies with the input power level. A variation in the DC load resistance tends to vary both the conductance and susceptance components.

The variation in susceptance as a function of power level undoubtedly comes from the variation in the capacitance of the Schottky barrier diode as a function of the bias voltage which is determined by the power level and the value of DC load resistance. The average value of this capacitance gets reflected back through the two-stage low loss filter to the point at which the admittance is being measured.

5.7 Test of the 5-element Foreplane as an Integrated Part of a Larger Array

The 5-element foreplane structure was integrated into the 199-element rectenna array and an attempt was made to uncover important differences between the behavior of the rectenna prior to such incorporation.

No important differences were discovered. The foreplane assembly consisting of the metallic shield and the core assembly of five rectenna elements was mounted in the central portion of the 199-element rectenna, as shown in Figure 5-12. The output power from the foreplane, as experimentally measured, was then compared with what the power output would have been from the five individual elements that it replaced, according to a formula to be explained later. On the basis of this comparison, the measured power output of the foreplane structure was found to be slightly higher than predicted at lower power and about the same at higher power levels. This behavior could be accounted for by the characteristics of the diodes used in the elements in the foreplane and by other considerations. One of the important possibilities taken into consideration was that the 5 elements in the foreplane were robbing power from their neighbors as the result of operating into a lower dc load resistance. However, a wide variation of the dc load resistance presented to the foreplane structure did not substantially perturb the aggregate power picked up by all the diodes in a central circular area whose diameter was larger than the length of the foreplane structure.

To begin the experimental study of the integration of the foreplane into the 199 element array, it is noted that in the 199-element array all of the rectenna elements lie on sets of circles with different radii but with a common center. The common center is at the center of the array. Starting from the center, there is a single element at the center, designated set "0". There are six elements in Set No. 1 which has the smallest finite radius, six more in Set

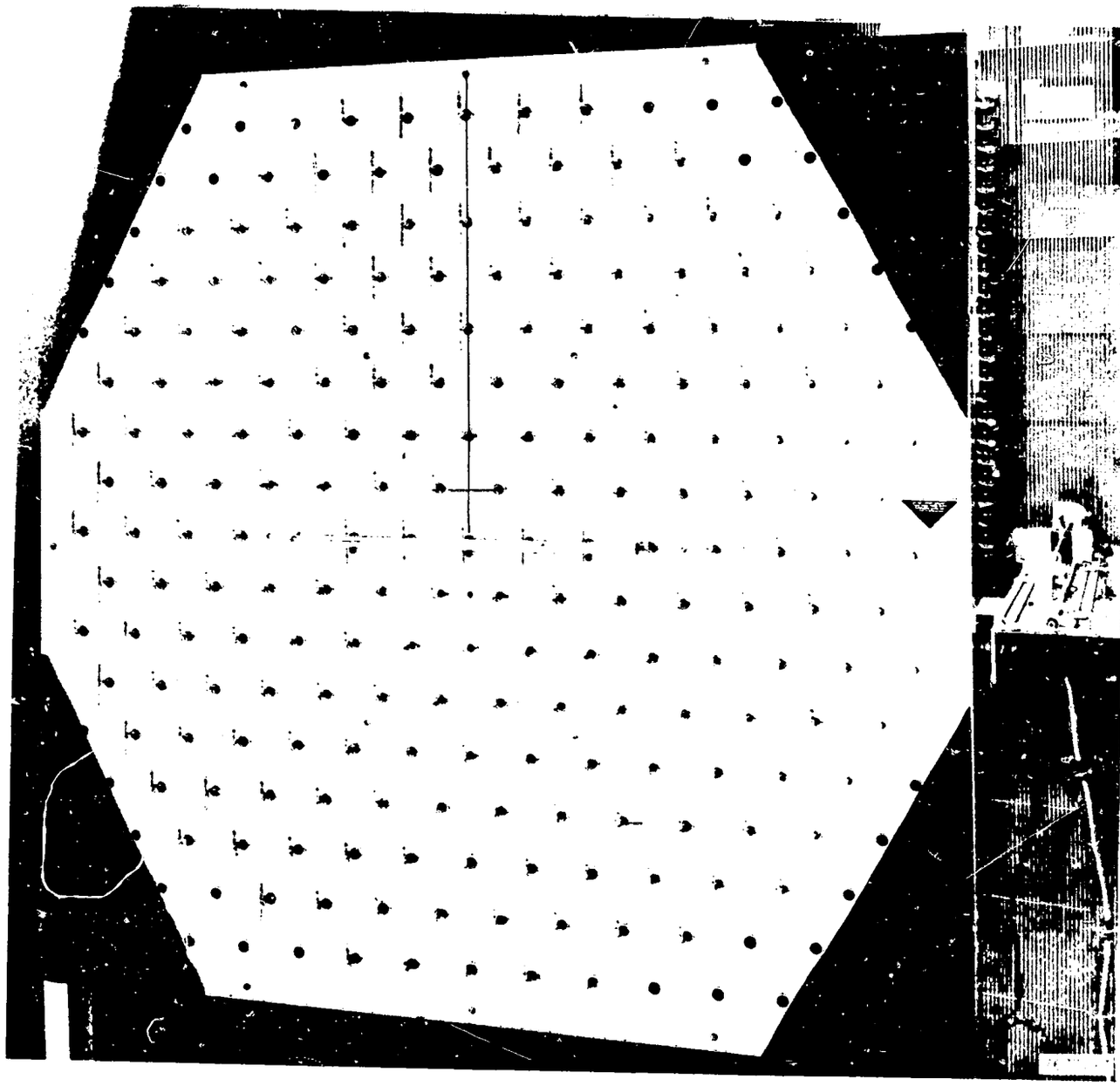

Figure 5-12. The test set-up for checking the foreplane type of rectenna array. The five element foreplane structure is placed at the center of the array as shown. The DC output is dissipated in a resistive load. The collected power from the foreplane can then be compared with the power that would have been collected from the five elements that it replaced by a procedure discussed in the text.

No. 2, six more in Set No. 3, twelve in Set No. 4, six in Set No. 5 etc. This arrangement is made more clear by reference to Figure 5-13 which shows the first fourteen sets of elements and the number in each set.

The average power level in each set is a function of the radius of the circle corresponding to the set. The function is given closely by a gaussian distribution of power density centered at the center of the array. Figure 5-14 shows the correspondence between experimental data and a gaussian distribution for the 199-element array whose performance was verified by the Jet Propulsion Laboratory Quality Assurance Dept. in 1975. [10]

It is noted then that the 5-element foreplane structure as shown in Figure 5-13 replaces two elements of the No. 1 set, two elements of the No. 3 set, and the single element No. 0 set. Now, if the assumption is made that all individual elements in a set have equal power output the prediction of the power in the foreplane structure in terms of the remaining power in sets No. 1 and 3 may be formulated as:

Predicted Foreplane Power = Predicted power in Center Element of Foreplane = Predicted Power of 2 adjacent elements to center element of Foreplane = Predicted Power of 2 outside elements of Foreplane

$$\text{Predicted Foreplane Power} = 1.08\left[\frac{\text{Aggregate Power of 4 elements left in Set No. 1}}{4}\right] + 2\left[\frac{\text{Aggragate Power of elements left in Set No. 1}}{4}\right] + 2\left[\frac{\text{Aggragate Power of 4 elements left in Set No. 3}}{4}\right]$$

The factor 1.08 in the first term above comes from the fact that the density of power at the center as given by the gaussian distribution is 1.08 times the power density at the radius of Set No. 1 consisting of 6 elements.

All the elements in a set operate in parallel into a common load. The effective load per element is approximately 23.5 ohms. To maintain this effective load, it was necessary to reset the common load values of sets 0, 1, and 3.

Figure 5-15 shows experimental data which compare the output of the foreplane structure with the predicted value as given by the preceding formula

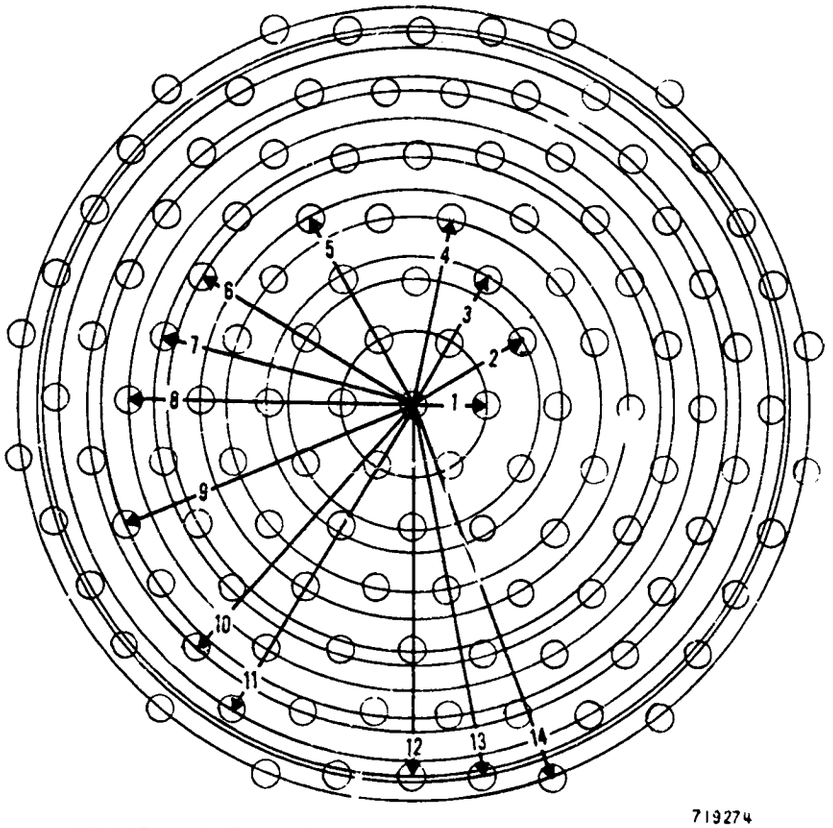

719274

SET NO.	NO. IN SET	SET NO.	NO. IN SET
0	1 (CENTER)	8	6
1	6	9	12
2	6	10	12
3	6	11	6
4	12	12	6
5	6	13	12
6	6	14	12
7	12		

Figure 5-13. Schematic Showing that all Rectenna Elements are Parts of Sets, With Six or Twelve Elements Per Set, Which lie on Circles Concentric with the Rectenna Center. In the 199-Element Array there are 7 additional sets to the 14 of this figure.

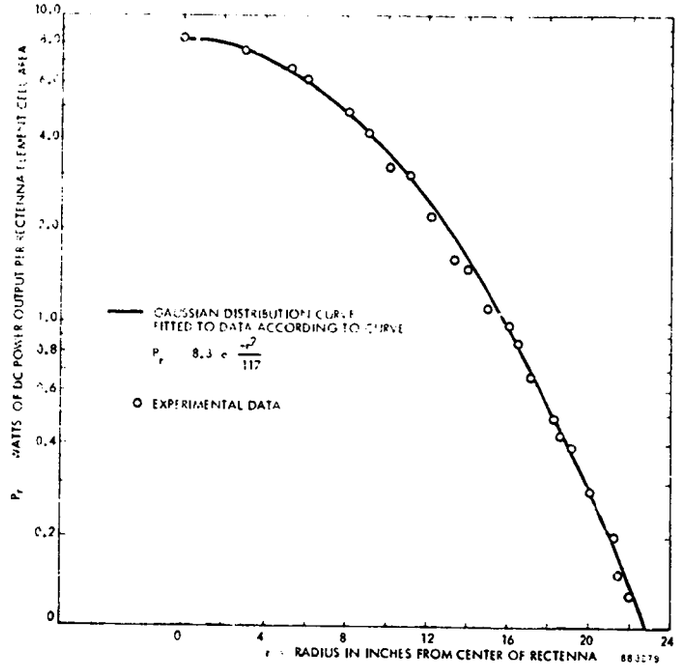

Figure 5-14. The average DC power output per element in a set of elements is plotted as a function of the radial distance of the set. The resulting points of data may be easily fitted to a Gaussian curve which is the approximate power density distribution in the beam.

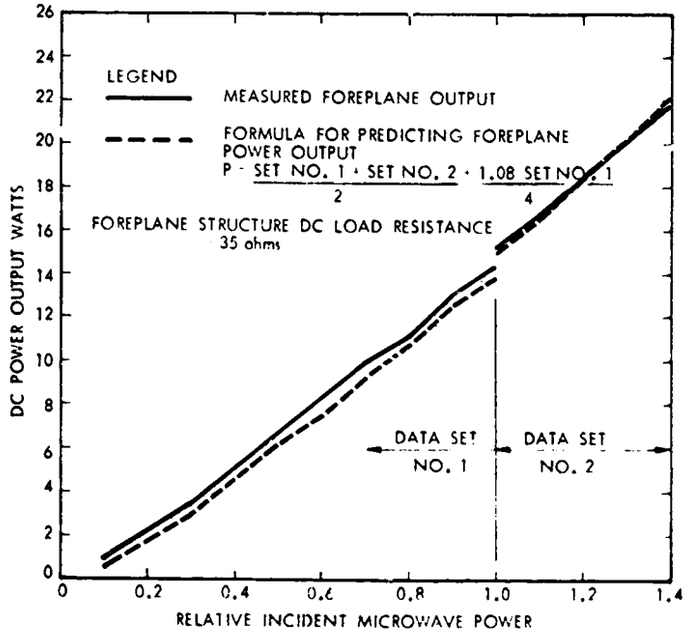

Figure 5-15. Experimentally observed power output of the 5-element foreplane structure is compared with predicted power based upon power picked up by remaining elements in sets whose total number of elements included elements in the foreplane structure. Data set No. 1 and No. 2 were taken at different times. Inconsistency of data at the "relative incident microwave power" value of 1.0 is caused by difficulty in resetting the incident microwave power level from one set of measurements to another.

over a-comparatively wide range of input power levels. The maximum average power level of the elements in the foreplane structure was 4.34 watts. Higher levels were not sought in order to minimize the possibility of diode failure, since these diodes do not have a particularly high reverse breakdown voltage.

The data shown in Figure 5-15indicate that the power output of foreplane structure has a close linear relationship to the incident power level, as does the formula for the predicted power level which is composed of experimental inputs from Sets 1 and 3.

Because portions of Sets, 1, 2, 3, 4, and 5 interact with the foreplane structure, it is of interest to see how the power outputs of these sets behave as a function of the dc load resistance placed upon the 5-element foreplane structure. Figure 5-16 shows the aggregate power output of the foreplane structure plus the power outputs of Sets 1, 2, 3, 4, and 5 all of which have some mutual coupling impedance to the foreplane structure, as the dc load resistance of the foreplane structure changes from 25 to 41 ohms. The aggregate power rises by 2% over this range. The behavior of the individual power in the sets is also shown in Figure 5-16. As the load resistance of the foreplane structure is increased, the power output of the foreplane structure decreases by about 4% while the power in sets 1 and 2 increases by about 4%. Sets 3 and 5 are relatively unchanged. Set 4 has an increase of about 2%.

The qualitative observation is that the perturbation of the aggregate power and the individual set powers is not greatly influenced by the dc load resistance of the foreplane structure. However, it is noted that the agreement between predicted foreplane power and experimentally observed values is a function of the foreplane dc load resistance. This relationship is shown in Figure 5-17.

The total aggregate power increase as a function of the foreplane dc load resistance may be correlated with a decrease in reflected power as determined by VSWR ratio measurements with a probe in front of the center of the 199-element by VSWR ratio measurements with a probe in front of the center of the 199-element array. The validity of this kind of measurement is good if the illumination is gaussian and if the percentage of power reflected is uniform over the array. In the efficient operation of the 199-element array, the elements in each set are trimmed for minimum reflected power at the power level at which they are intended to operate. The reflection loss that is experienced when they are operated at other power levels is suggested by Figure 5-11.

In the illumination of the rectenna in which the foreplane is incorporated, the incident power level is different on the five elements, although they share a common load. Hence, the situation for making VSWR measurements is not ideal, particularly in close proximity to the three central elements of the foreplane structure where these elements will dominate the reflected power. However, if the probe is backed off, the VSWR ratios become more valid. Under these conditions, the VSWR associated with a 25-ohm load is 2.8 dB as compared with 1.5 dB for the 40-ohm load as shown in Figure 5-18. The corresponding

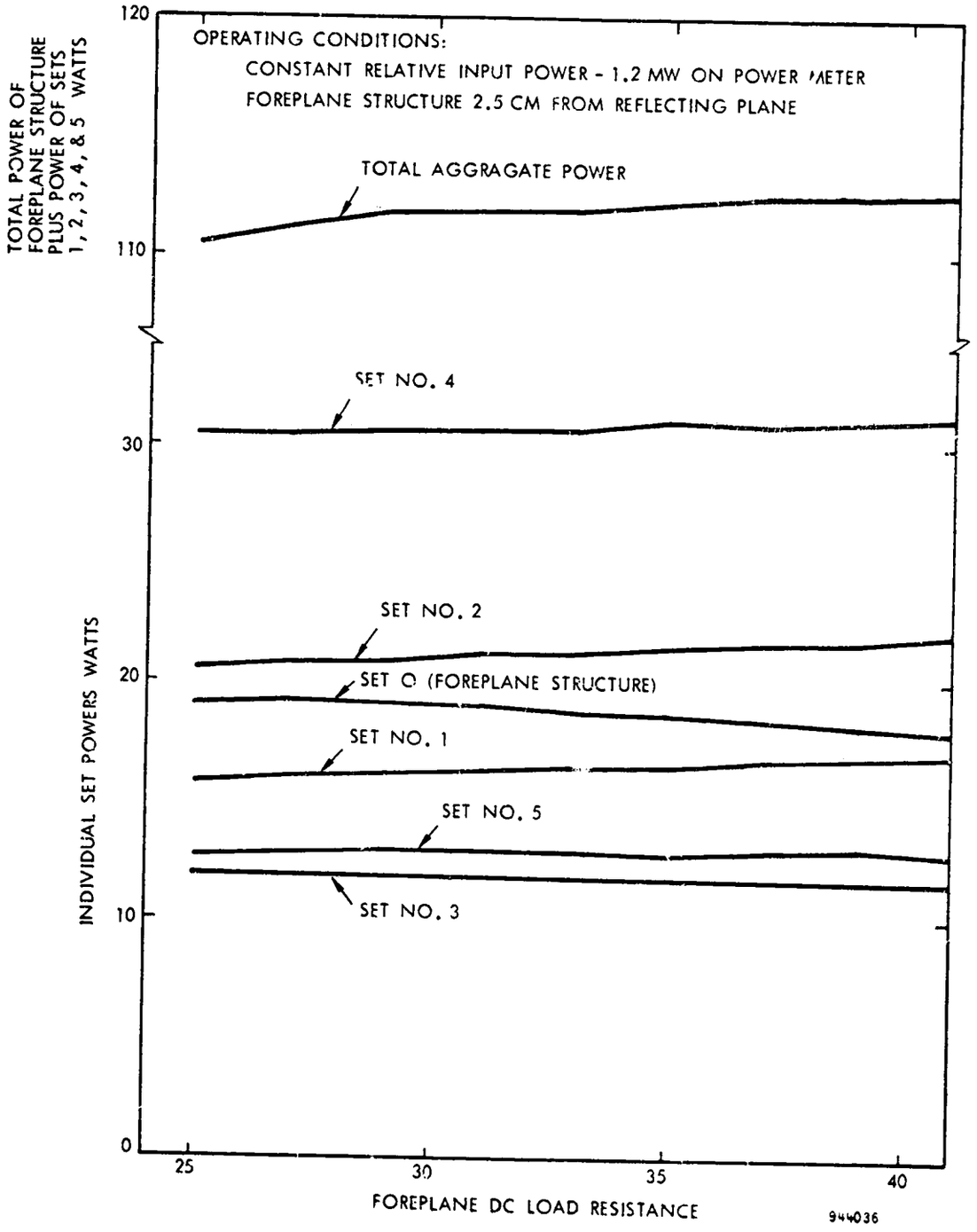

Figure 5-16. The power output of the foreplane structure and other sets of rectenna elements, which contain elements coupled to elements in the foreplane structure, as a function of the foreplane DC load resistance.

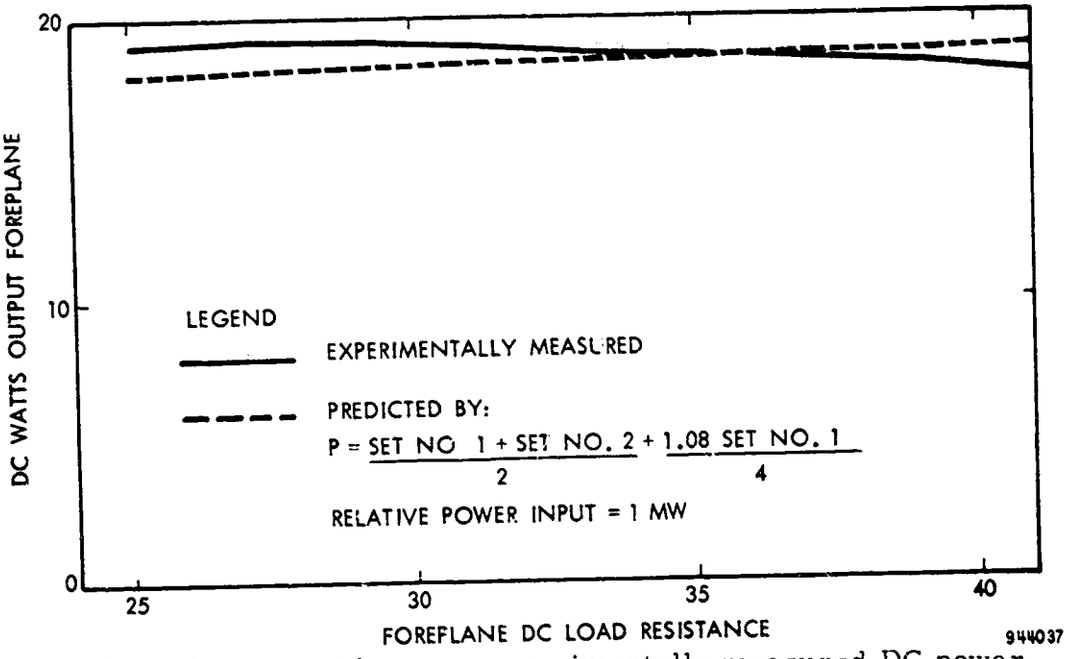

Figure 5-17. Agreement between experimentally measured DC power from the foreplane structure and predicted value as a function of foreplane DC load resistance.

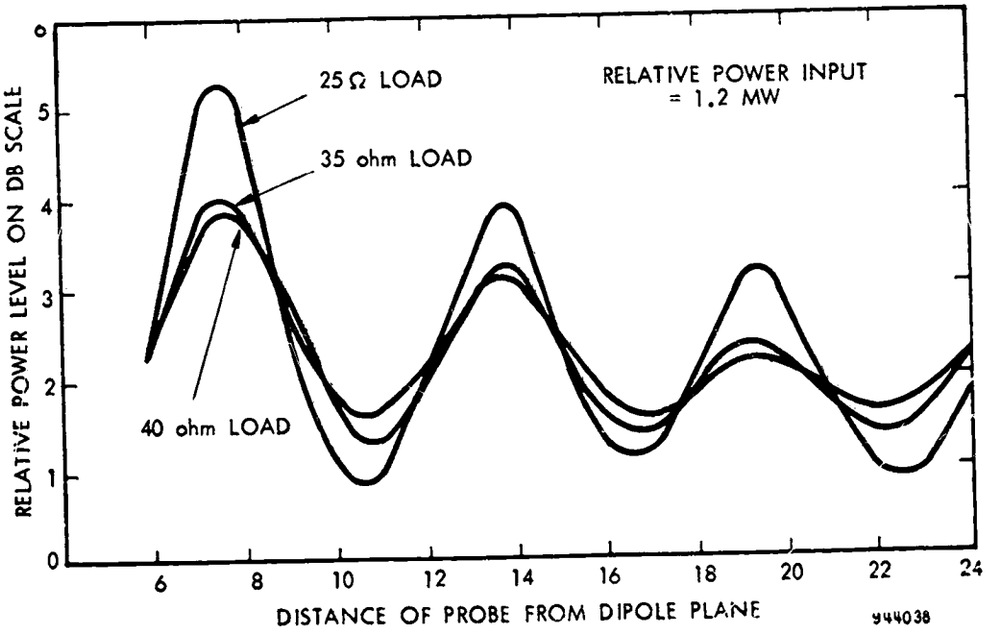

Figure 5-18. VSWR ratio and min position as a function of the DC load resistance of the foreplane construction and of the distance of the probe from the dipole plane.

reflected powers are 2.5% versus 0.7%. The difference of 1.8% in reflected power correlates with the 2% increase in aggregate power. However, the microwave input measurement accuracy and the validity of the reflected power percentage by the VSWR measurements make such good agreement appear to be coincidental.

The type of VSWR measurements that were obtained are shown in Figure 5-18. The 25-ohm load definitely gives a higher VSWR at all probe positions. However, the variation in VSWR as a function of probe position is not characteristic of measurements that had been made previously in this structure without the foreplane structure, as shown in Figure 5-19

The fact that the 5 elements of the foreplane receive different amounts of microwave power but operate into a common load raises the question as to the effective load resistance each one sees. If the assumption is first made that the efficiency of the rectenna element, and therefore its power output is affected to only a minor degree by modest perturbation of its load resistance, it is simple to calculate these load resistances. Thus, out of a predicted foreplane power output of 18.59 watts, 2.94 watts comes from each of the two elements in Set 3, 4.13 watts from each of the two elements in Set 1, and 4.46 watts from the central element. The voltage across the 35-ohm load resistance for 18.59 watts input is 25.51 volts. Since all the elements operate in parallel, the respective load resistances are 221, 157, and 145 ohms respectively. It is possible that the nonuniformity of reflection from these elements may contribute to the difference in VSWR patterns between Figures 5-18 and 5.19. The reflected power that would be associated with these load resistances and these power levels for the individual elements tested in the expanded waveguide fixtures are given in Figure 5-11. According to this figure, 2.94 watts and 221 ohms gives 1% power reflection with an admittance component of 0.8 and very little susceptance; 4.13 watts and 157 ohms gives 1% reflection with an admittance component of 1.1 and a susceptance component of .16; 4.46 watts and 145 ohms gives a power reflection of 1.2% with an admittance component of 1.2 and a susceptance component of about 0.2.

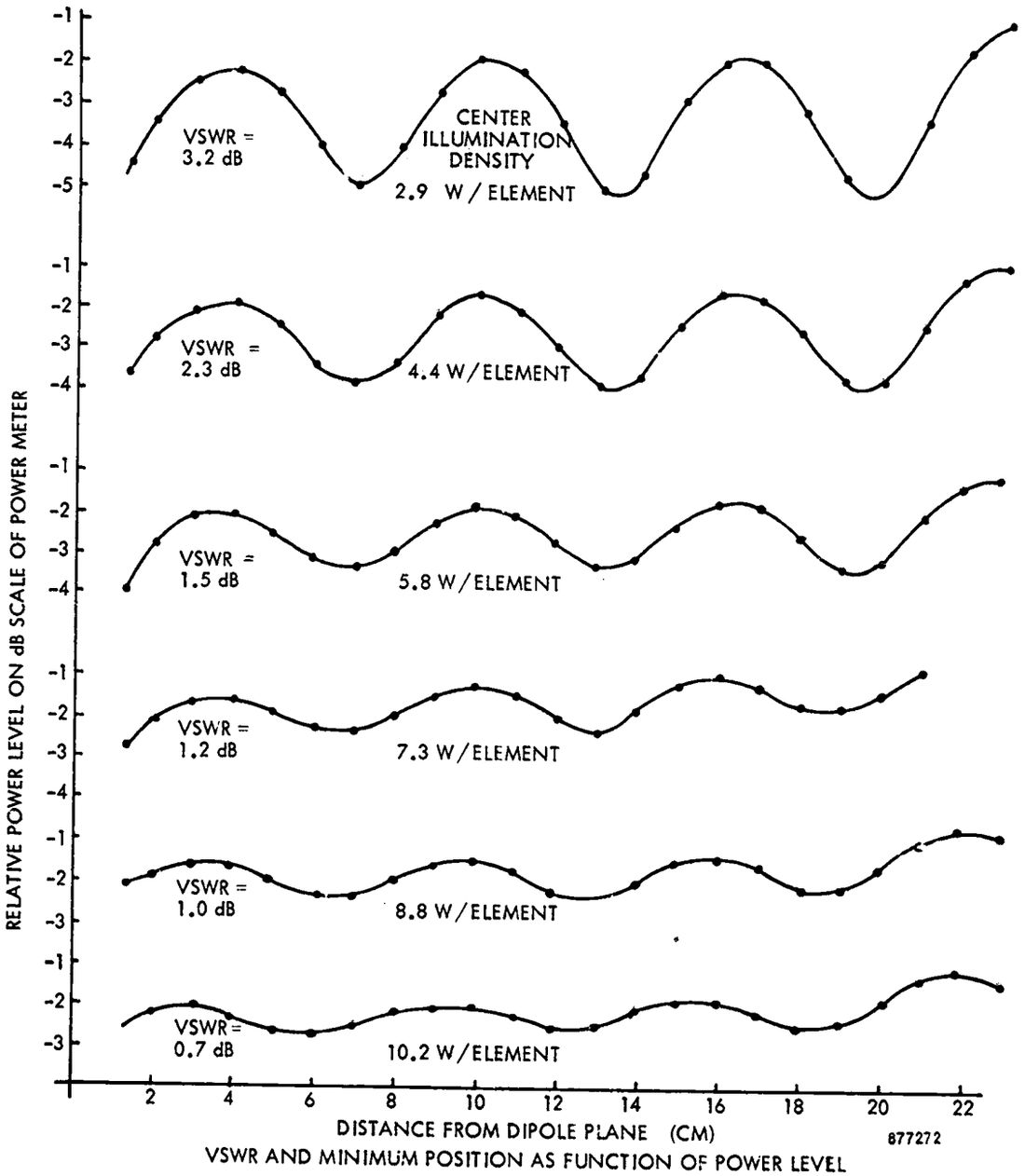

Figure 5-19. Rectenna Edge to Horn Mouth Spacing 67 Inches, Frequency 2382 MHz, Center Rectenna Element Matched at 9.4 Watts in Expanded Waveguide Fixture

6.0 SUMMARY OF RESULTS

The technology development covered by this final report was concerned with improvements in the reception and rectification of microwave power at the receiving terminal of a free-space power transmission system. More specifically, it was concerned with an application to the solar power satellite concept in which solar energy is captured in a geosynchronous satellite and then, after an imtermediate energy conversion process, transmitted to earth by a microwave beam. The background of previous effort in developing a suitable technological approach to this portion of the transmission system,together with system studies which have developed a set of specific requirements, indicated that development be carried forward in certain key areas with the following objectives:

1. More efficient operation in general, but particularly at lower incident microwave power densities.

2. Better confidence and finer resolution in efficiency measurements.

3. Better knowledge of the efficiency loss mechanisms.

4. Better understanding of the operation of the device through computer simulation.

5. Development of improved diodes.

6. A decrease in the radiation of harmonic energy.

7. The development of a design that is environmentally sound.

8. The development of a design that allows low cost production.

9. An assessment of life of rectenna elements.

These objectives were addressed in the technology development contract and significant progress was made in all of the areas. The results are discussed in the following material in the same sequence. Items 7 and 8 because of their close overlap are reported upon as a single item.

1. Improvements in Efficiency

Improvements in efficiency were accomplished through the use of higher impedance microwave circuits, higher DC load resistances, and the use of improved diodes developed under this study. These were changes incorporated into the rectenna element which is the basic building block of the rectenna. The improvements in efficiency ranged from a fraction of a percent at six to eight watt level of microwave power input to the rectenna element to twenty percent at an input level of 50 milliwatts. More specifically, the changes resulted

in an efficiency of 90.5 ± 0.5% at the 8 watt input level and to 79.5 ± 0.5% at the 50 milliwatt level.

In addition to achieving improved efficiencies at the lowest power levels of expected interest in a full scale satellite solar power system, good efficiencies were obtained at still lower power levels. For example, an efficiency of 45% was obtained with an input level of one milliwatt.

Despite the substantial improvements in efficiency at low power levels the resulting efficiencies do not represent the best that can be obtained. The measurements made on the diodes specifically designed for efficient operation at the lowest power levels indicated deficiencies that could probably be overcome with additional development effort and thereby substantially improve the efficiency.

Althouth the emphasis on efficiency improvement was at the lower power levels some measurements in an exploring mode were made at power levels in excess of ten watts. DC output levels as high as 17 watts were obtained at efficiencies which were estimated to be as good as at levels below 10 watts. An estimate was necessary because the measurements were outside the capability of the standard measuring equipment.

2. Efficiency-Measurement Confidence and Resolution

A considerable improvement in the confidence of efficiency measurements on the rectenna element was established by equating the microwave power absorbed by the rectenna element to the sum of the DC power output, the losses measured in the diode, and the circuit losses as measured experimentally and by computer simulation. The microwave power absorbed by the rectenna element is equal to the carefully calibrated incident microwave power upon the rectenna element less the reflected power which is typically less than one percent of the incident power. Each of the quantities going into the equating operation has associated with it a probable error. It was determined that the total probable error was ± 0.75%. The resulting difference between the two sides of the equation was within this probable error.

Prior to the technique of balancing power input against power output and losses, confidence in efficiency measurements had to depend upon the use of the Bureau of Standards service in calibrating a secondary standard at Raytheon Company and the use of this secondary standard plus calibrated attenuators to establish the calibration of the rectenna element test set.

In order to utilize the power balancing technique, however, it was necessary to carefully measure or estimate the losses in the rectenna element. This was done by developing a procedure to measure

the losses in the rectenna element. This was done by developing a procedure to measure the losses in the diode, which was determined to be the principal loss mechanism, and developing a procedure based partly on experimental measurement of losses and partly upon computer simulation to determine the circuit losses in the rectenna element.

As a result of this procedure there is a much greater confidence in the probable error of efficiency measurements established on the basis of calibration procedures originating with the Bureau of Standards and transferred by suitable means but with an estimated error to a test arrangement for measuring rectenna element efficiency. The probable error in efficiency measurements is ±0.6% for measurements over 100 milliwatts, and ±0.4% for measurements at 100 milliwatts.

There was an improvement effected in resolution of efficiency measurements by using a digital meter on the microwave power input measurement and a digital voltmeter to measure the DC voltage across the carefully calibrated DC load resistance.

It was also determined that the reproducibility of efficiency measurements depended heavily upon the electrical and mechanical symmetry of the rectenna element itself. Higher order modes in the expanded wave guide test fixture can also be a minor source of measurement difficulty depending upon the coupling symmetry of the rectenna element and upon the frequency of testing. This is a characteristic of the test fixture itself and would not be experienced in the use of the rectenna element in the rectenna array.

3. Quantitative Evaluation of Losses in the Rectenna Element

Prior to this contractual effort only engineering estimates of the quantitative values of loss mechanisms in the rectenna element were available. Under this contract a highly accurate method for experimentally determining the total losses in the diode was developed. Experimental measurements were also made on the losses in the input low pass filter section of the rectenna element. Losses in the rectifier tank circuit were obtained from the computer simulation program.

The measured losses in the diode agreed with previous engineering estimates. The minimum total losses in the diode were found to range from as low as 7.4% of the input power for microwave input levels of several watts to very high values for very low power inputs. At very low power inputs there was a substantial error involved in the experimental method.

Circuit losses other than those taking place inside the diode were found to be in the region of 2 to 3%. The probable error in these

measurements is greater than for the diode. For one set of measurements the circuit loss was set at 2.37% ± 0.4%.

A novel method for accurately measuring diode losses was developed under this contract. The method made use of a ground-plane test fixture in which the balanced rectenna element is simulated by splitting the element into two halves and then locating one half of the element above a ground plane. This permits the use of a thermistor bridge to measure the temperature rise in the diode as the result of power dissipated inside the diode. The bridge is calibrated in terms of power dissipated in the diode by injecting and accurately measuring DC power into the diode. However, the measurement technique is insensitive to whether the heating source is DC power or microwave power since both are dissipated within the diode semiconductor chip. Hence when the diode is operating normally in the rectenna element as a microwave power rectifier the power dissipation is determined from the thermistor bridge and assumed to be the total loss in the diode as it is normally used.

4. Mathematical Modeling and Computer Simulation

The rectenna element, although it has the mechanical appearance of being a simple device, and in the half wave rectifier configuration is indeed the simplest electrical device, is nevertheless an electrically very complex device when it is examined in detail. This complexity is caused by the high non-linearity of the device, which generates harmonic power which greatly complicates the waveforms of the voltage and current within the element. To analyze the behavior of the device in detail it is necessary to resort to computer simulation based upon a reasonable mathematical model of the element.

Under this contract, a successful effort in mathematical modelling the element and simulating its performance on a computer has been successfully carried out and has resulted in a technique that is certain to be of great importance in further refinement of the rectenna element.

The computer simulation program has generally given results that confirm the experimental results, but upon occasion has indicated differences which have led to investigations to resolve the differences. For example the diode losses were first computed on the basis of the theoretical design of the diode and found to be less than those measured. It was found that the forward voltage drop as measured by DC voltage measurements was greater than that predicted from theory leading to the conclusion that the ohmic contact is not purely ohmic but retains some Schottky barrier characteristics which contribute to the voltage drop.

The computer simulation program has also indicated that there is the possibility of a combination of effective diode capacitance, input microwave power level, and setting of the effective inductance in the rectifier tank circuit that can cause the generation of much power in the higher order harmonics and decrease the efficiency significantly. Thus the computer simulation program provides a useful means of providing a large variety of operating conditions that would be difficult to reproduce experimentally.

5. Development of Improved Diodes

A significant number of different diode designs were produced under this contract as an aid in investigating their impact upon improved rectenna element performance. The most significant development was the use of a GaAs-W barrier in place of the well-established GaAs-Pt Schottky barrier. As anticipated, this reduced the forward voltage drop by about 0.2 volts or about 25%. This reduction is of great significance in efficiency improvement when operating elements at a very low incident microwave power level.

The development of the GaAs-W barrier is a significant achievement because of the difficulty of the bonding properties of their physical interface. A solution to this problem was found under separate contractual support and enabled us to adapt the same fabrication techniques to the diodes that were developed under this contract.

The effort to develop diodes for improved performance of rectenna elements when they are subjected to low values of incident microwave power has established the importance of the resistance of the back contact as a limiting parameter. Improved diodes for low power operation are made with lower junction capacitance and therefore with reduced junction area. Because the distance between the junction area and the back contact is so small in the plated heat sink diode, the current does not have a chance to fan out before making contact with the back contact. Since the series resistance in the epitaxial layer is very small for these diodes which have a high doping density as well as a thin epitaxial layer the back contact resistance becomes a dominating element. Since the technique of applying the back contact for these diodes is the best available, there is no way of reducing the specific resistance (per unit area) of the back contact without active development effort. However, it is possible to increase the distance between the back contact and the epitaxial layer in order to let the current fan out. Diodes were made with this feature and it was found that the series resistance as measured by DC voltage was indeed reduced. However, it was found that these diodes did not provide improved performance and it was then found that the microwave resistance was higher than the DC resistance, indicating that there was a skin effect involved.

If further development is undertaken on diodes for low-power density applications it is recommended that the following items be examined:

a) The reduction of the specific resistance (ohms per unit area) of the back contact.

b) The increase of the back contact area.

c) A decrease in the skin resistance of the surface of the substrate over which the microwave current flows to the back contact.

d) An increase in the doping density of the substrate to decrease the spreading resistance and decrease the skin resistance.

6. Radiation of Harmonic Energy From the Rectenna Element

A two-section low pass filter is inserted between the half-wave dipole of the rectenna element and the rectification circuit to store energy between rectification periods and to reduce the radiation of harmonic energy from the dipole. It has been recognized that there is an opportunity to enhance this attenuation in the design of the two-plane rectenna construction, because the section of transmission line that connects one rectenna element with the next can be made a half-wavelength long at the second harmonic and provide an effective shorting out of second harmonic energy at the input terminals of the halfwave dipole. It is recognized that this would be a critical adjustment if full advantage were to be taken of it.

This approach was investigated with mixed and uncertain results. As the technique was studied on the ground plane fixture, it was determined that the absorption of second harmonic energy into a matched 50 ohm load, which represented the input to the dipole terminals, could be reduced by another 30 dB by adjusting the length of this section. There was even a slight improvement in efficiency noted. However, when the same technique was later applied to the section of the two-plane construction that was built and evaluated, it was found that there could be a two to three percent drop in efficiency at a point of adjustment of the electrical length of this line extremely close to the one found optimum for the reduction of harmonic energy. In any event the maximum reduction in harmonic content was nominal.

It was also found that an open circuited stub line resonant at the third harmonic could be added to the terminals of the dipole input and result in a reduction of third harmonic output energy from 40 dB to 55 dB.

7. The Development of a Design that is both Environmentally Sound and is Suited to Low Cost Speed Production

The development of basic technology for the rectenna for the full scale satellite solar power station is quite well advanced, but the adaptation

of this basic technology to a rectenna that is environmentally sound and that can be made at low cost in large volume production was recognized as an area of special study. The SSPS rectenna design problem is a complex one in that many different requirements must be met simultaneously. The active rectenna elements must be adequately shielded from the environment, it must be possible to interconnect the elements in such a manner as to produce an output DC voltage of 1000 volts with adequate electrical insulation, and the complete rectenna structure must be structurally sound and capable of withstanding sizeable wind and ice loads.

It has been recognized for some time that the approach to meeting these requirements should be based on the two-plane rectenna element construction. In this arrangement one plane is merely a reflecting plane which can be made from a coarse mesh with a surface which is highly resistive to deterioration under long life and harsh environmental conditions. The other plane then contains the elements of collecting the microwave power, converting it into DC power, and bussing it to some central point of DC power collection.

Two major accomplishments in achieving a practical two-plane construction were realized. The first of these was the adaptation of the RXCV rectenna element to the two plane construction and the electrical testing of the new configuration. The second was the development of a metallic shroud that is placed around the rectenna elements in the new configuration which functions as both an environmental shield and as a main structural element of the rectenna.

The whole assembly consisting of the rectenna elements in the new format and the metallic shroud surrounding it was thoroughly tested as a portion of the 199-element rectenna that has served as the laboratory test vehicle for many projects. The conclusions are that there is no substantial difference in the efficiency or other electrical behavior of the new two-plane format from that obtained from the normal elements in the array which they replaced. A high confidence level in the two plane construction has been provided.

However, the new two-plane design cannot be regarded as a completed development. The metallic shroud had holes cut into it for the protrusion of the half wave dipoles. The addition of some kind of grommet will be necessary to make a weather-proof seal between the leg of the dipole and the metallic shroud. The rectenna elements also need to be redesigned to eliminate the teflon machine screws and other features that are not indicative of a final production design.

8. An Assessment of Life of Rectenna Elements

Previous life tests were continued on a no-charge basis but with the use of test equipment available for this technology development program. The life test procedure involved 199 rectenna elements and diodes divided up into sets that were differentiated from each other by the value of the microwave power density falling upon them. A continuous run of 2763 hours was obtained with no element or diode failures corresponding to a 27.3 year MTBF with a 90% confidence factor. About 50% of the elements were run at power levels substantially above the maximum specified for the base line design of the SSPS.

7.0 CONCLUDING REMARKS AND RECOMMENDATIONS

The technology of microwave power transmission has been substantially advanced with the work covered by this report. Measurement and analytical tools are now available for additional, more refined, investigations into efficiency and other operational parameters of the rectenna element. A firm foundation for the first iteration of an electrical, mechanical, and environmentally protected design of a low-cost rectenna for the satellite solar power station application has been established with the effort on the design and test of the two-plane rectenna format covered in this report.

It is recommended that the next immediate technology development effort involve the detailed design and subsequent construction and testing of a section of rectenna that will:

1) Provide 1000 volts of DC potential at the terminals.

2) Use a revised mechanical design of the core-assembly of the foreplane structure aimed at reduced cost of manufacture and better compatibility with the use of an external metallic shield.

3) Use a fully environmentalized metal shield for the core assembly that will take all environmental conditions into account and which will serve as a structural element in the rectenna.

The activity in this proposed effort should be carried out with the construction of a larger rectenna, either as part of the effort itself or as part of a subsequent effort, in mind. The larger rectenna should be sufficiently large and with a sufficiently tapered illumination to permit its evaluation with the use of an efficient microwave generator of about five kilowatts of power output. A gaussian illumination should be provided so that accurate measurements can be made of the absorbing efficiency and overall efficiency of the rectenna. The kind of system recommended is shown in Figure 7-1.

The rectenna in the system should be fully environmentally protected and permit its evaluation under a wide variety of environmental conditions. The rectenna after initial evaluation for its efficiency and other parameters should be set up for life test and operated continuously.

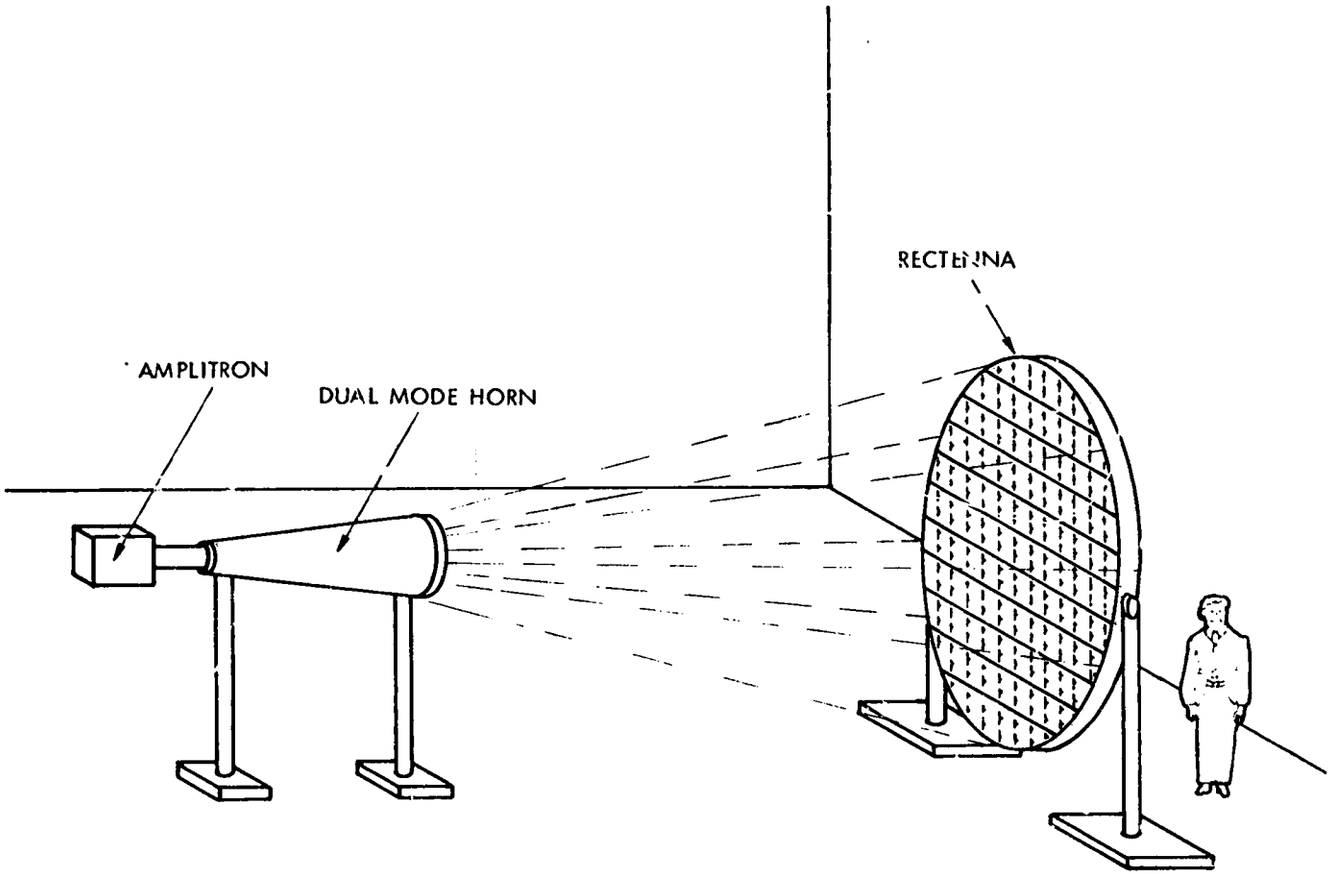

Figure 7-1. Sketch of Recommended System

APPENDIX A

DEVELOPMENT OF COMPUTER SIMULATION PROGRAM FOR THE RXCV RECTENNA ELEMENT

DEVELOPMENT OF COMPUTER SIMULATION PROGRAM FOR THE RXCV RECTENNA ELEMENT

The computer model is based around the element geometry used for the current rectenna element. The physical circuit shown as a photograph in Figure 1 models electrically for analysis purposes as Figure 2.

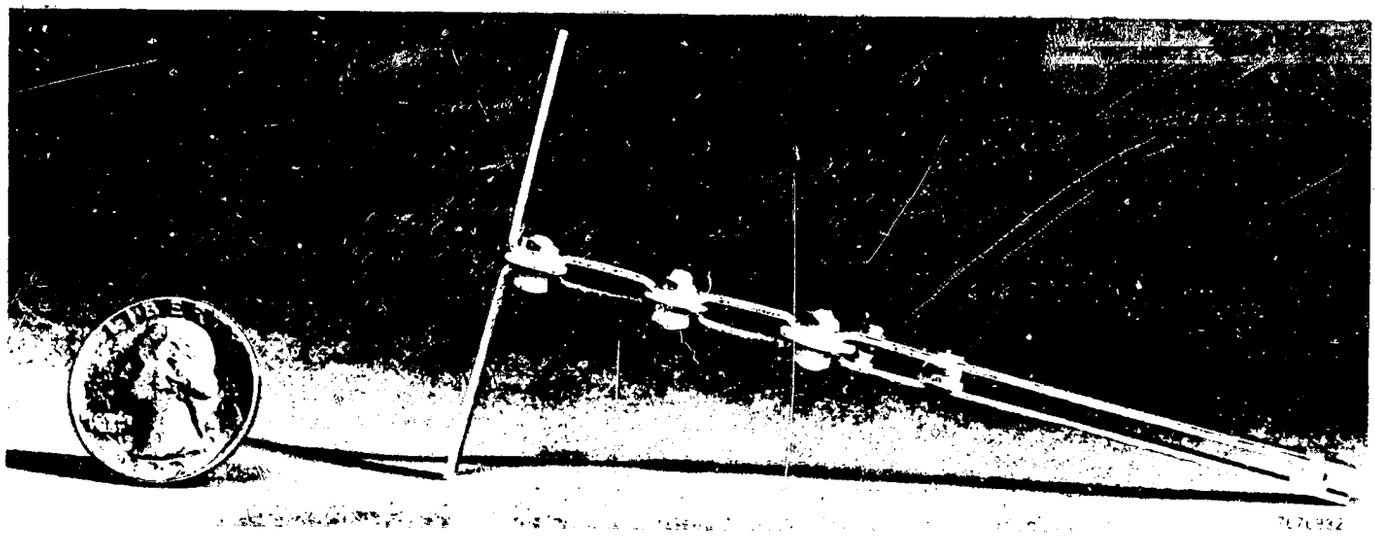

Figure 1. Rectenna Element

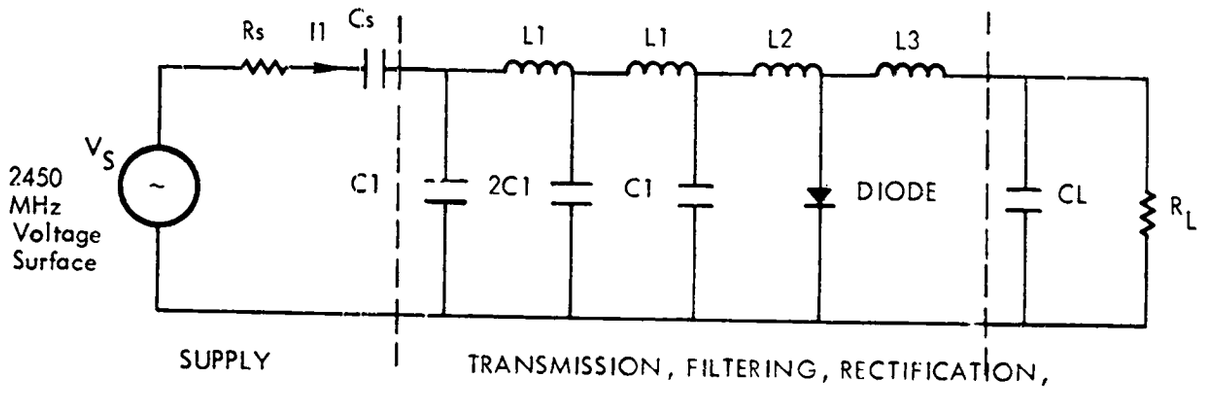

Figure 2. Electrical Model

The supply and load segments of the circuit are modeled mathematically using the components shown in Figure 2:

Vs (source) (t), Rs, Cs, Rl (load), Cl; while the other components of the rectenna element are broken into multiple subdivisions and modeled by transmission line elements with a conduction loss (Figure 3).

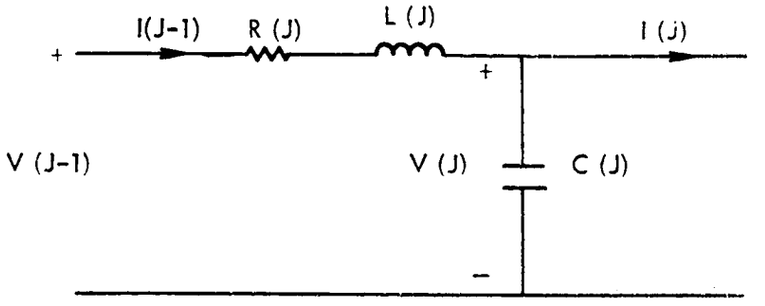

Figure 3. J^{th} Element of Transmission Filter and Rectification Section of Figure 2

The elements L(J), C(J), R(J) are the characteristic inductance, capacitance, and "skin" resistance of the line segments. Table 1 lists the number of segments, element values, and other parameters used in the direct analysis of the present element:

Major Element (See Figure 2)	# Segments	R (Ω)	L (nh)	C (pf)	Elect. Length (cm/)
C1	2	.034	.48	.20	.36
L1	3	.096	3.0	.07	.43
2C1	2	.034	.24	.40	.36
L2	1	.050	1.68	.044	.32
L3	2	.050	1.68	.044	.32

When the ground-plane fixture is used, all resistance and inductance values are halved and capacitances are doubled.

The diode is placed in the Kth node of the structure and that node is modeled as Figure 4.

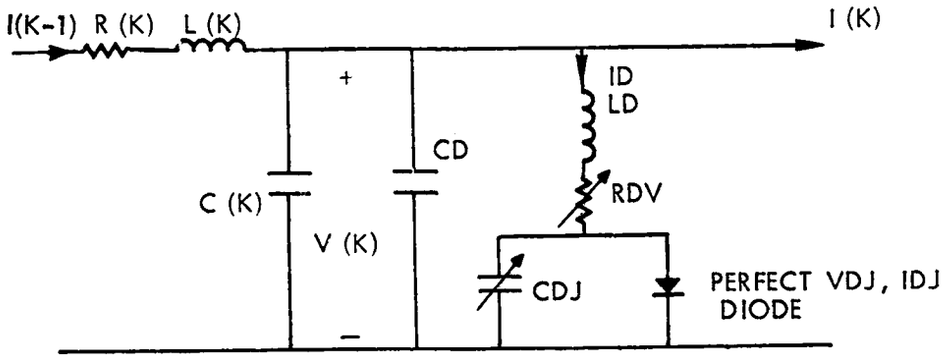

Figure 4. Model of Kth Node

In Figure 4:

R(K) = Loss resistance in element at diode location
L(K) = Characteristic line inductance in the element at diode location
C(K) = Characteristic line capacitance in the element at the line location
CD = Case capacitance of diode
LD = "Lead" inductance of diode
RDV = Voltage variable resistance of diode voltage
CDJ = Variable junction capacitance of diode
Perfect Diode: described as $I_{DJ} = Is\ (e^{\frac{qVDJ}{nkt}} - 1)$
ID = Total diode current
IDJ = Current through perfect diode
VDJ = Voltage across diode junction

The following equation set is used to describe the element at the input:

$$Vs(t) = VS \sin (2\pi f t)$$

gives VST = VS* sin (TWO P1F * TIME)

$$I(1) = -\frac{CsdV(1)}{dt}, \quad Vs(t) = V(2) - V(1) + I(1)\,Rs + L(2)\frac{dI(1)}{dt}$$

gives

$$\text{DEL } V(1) = - I(1) * C1NV(1)$$

$$\text{DEL } I(1) = \left(VST + V(1) - V(2) - I(1) * Rs\right) * L1NV(2)$$

In the transmission, filter, and rectification section at the Jth node

$$C(J) \frac{d\,V(J)}{dt} = I(J-1) - I(J)$$

$$L(J-1) \frac{dI(J)}{dt} = V(J) - V(J+1) - I(J) * R(J+1)$$

reducing to

$$\text{DELV}(J) = \left(I(J-1) - I(J)\right) * C1NV(J)$$

$$\text{DEL}I(J) = \left(V(J) - V(J+1) - I(J) * (R(J+1)\right) * L1NV(J+1)$$

In developing a model of the diode, the assumption was made that an n-type gallium-arsenide device operating at about room temperature would be used. The device characteristics to be specified are the case capacitance (CD), the load inductance (LD), the work function of the metal-semiconductor junction (Vmetal), the forward bias dc resistance (RD), the zero bias junction capacity (CDJO), and the reverse breakdown voltage (VDJR).

In addition, the thermal voltage (KT/Q) is included as an input and the resistance of the epitaxial layer (RHO) may be included in the data input or computed from other parameters.

The stages in the calculation of the other parameters follow. A relative doping density (DOPING) is derived from the reverse breakdown voltage

$$\text{DOPING} = (\text{VDJR}/75)^{1.45} \; (\times 10^{16}/\text{cm}^3)$$

The voltage difference (VDIFF) between the metal work function (VMETAL) and the Schottky barrier voltage (VDJO) is calculated from the doping density

$$VDIFF = KT/Q\,\ell n\,(47./DOPING)\ (VOLTS)$$

$$VDJO = VMETAL - VDIFF\ (VOLTS)$$

The junction capacity inverse (CDJ1) is calculated from VDJO and the present value of junction voltage (VDJ)

$$CDJI = 1/CDJO\left(\frac{VDJO - VDJ}{VDJO}\right)^{1/2}\ \frac{1}{\text{Farads}}$$

From other values above the thickness of the epitaxial layer at zero bias (THKEPO) and its ideal overall thickness (THKEPR) may also be calculated

$$THKEPO = 3.46 \times 10^{-5} \times (VDJO/DOPING)^{1/2}\ cm$$

$$THKEPR = THKEPO \times \left(\frac{VDJO - VDJR}{VDJO}\right)^{1/2}\ cm$$

Using the zero bias capacity (CDJO) the diode area (AREA) is

$$AREA = 3.59 \times 10^{7} \times CDJO \times (VDJO/DOPING)\ cm^2$$

In the diode the resistance (RDV) also varies with voltage and can be calculated from the forward resistance (TD) and the characteristics of the epitaxial layer.

$$RDV = RD - RDVO * CDJI$$

where

$$RDVO = 9.65 \times 10^{-13} \times RHO.$$

If the resistivity (RHO) of the epitaxial layer is not well known, it may be calculated as RHO = .15/DOPING.

The material properties of gallium arsenide assumed in the above calculations are relative dielectric constant (10.9) and density of conduction states ($4.7 \times 10^{17}/cm^3$).

The terminal characteristics are related by the equation set:

$$IDJ = Is\left(e^{\frac{qVDJ}{nKt}} - 1\right)$$

$$CDJ(VDJ)\frac{dVDJ}{dt} = ID - IDJ$$

$$Ld\ \frac{dID}{dt} = (V(K) - VDJ - RDV(VDJ) - ID$$

where voltage variable junction capacity and epitaxial resistance derived in the explanation of the diode model are used. These equations are written as

$$IDJ = IDJO * \left(EXP\ (QOKT * VDJ - 1)\right)$$

$$DELVDJ = CDJ1 * (ID - IDJ)$$

$$DELID = (V(K) - VDJ - RDV * ID) * LD1NV$$

At the output terminal (J = NUMNOD)

$$C(NUMNOD)\frac{dV(NUMNOD)}{dt} = I(NUMNOD) - I(NUMNOD - 1)$$

and I(NUMNOD) = V(NUMNOD)/RL

where RL is the load resistor.

All above equations describe the instantaneous characteristics of the system. A predictor-corrector routine is used to give the time integrals of the derived differentials so that

$$\int_{O}^{\tau} dI(J) = \sum_{\ell=O}^{M} \frac{dI(J,\ell)}{dt} \, dt = I(J,\tau)$$

and

$$\int_{O}^{\tau} dV(J) = \sum_{\ell=O}^{M} \frac{dV(J,\ell)}{dt} \, dt = V(J,\tau)$$

where M steps are used to go from the start of the program to time (τ).

In the numerical routine

$$I(J) = I(J) + DELI(J) * TO$$

$$V(J) = V(J) + DELV(J) * TO$$

where TO is the time interval (dt).

Power calculations use a similar integration technique where for example at a particular node

$$POWER\ (J) = POWER\ (J) + I(J) * I(J) * R(J+1)$$

or in the diode

$$POWERD = POWERD + V(K) * ID$$

Fourrier coefficients are calculated as for example

for a variable V(n), the cosine coefficient of the Kth harmonic is

$$A(n) = \sum_{\text{one cycle}} \cos(2\pi \cdot K \cdot f \cdot t) \cdot V(n,t) \cdot \Delta t$$

The output of the analysis has two parts: (1) an output calculated at the end of each cycle to give an idea of

a) the convergence of the solution
b) the absolute error in variable integration calculated in the predictor-corrector routine
c) the source of that absolute error.

(2) In the last cycle, the following information is given for a converged cycle:

a) at intervals through the cycle at 128 equally spaced points the values of eleven terminal parameters of voltage and current

   i) input voltage (VIN)
   ii) input current (I(1))
   iii) predictor-corrector error in diode junction voltage (ERVDJ)
   iv) predictor-corrector error in diode current (ERID)
   v) diode current (ID)
   vi) diode junction current (IDJ)
   vii) diode junction voltage (VDJ)
   viii) diode voltage (V(NODDIO))
   ix) load voltage (V(NUMNOD))
   x) current into diode node (I(NODDIO-1))
   xi) current from diode node (I(NODDIO))

b) the power integrated over the cycle in all "loss" mechanisms

   i) input power to the element (POWER(1))
   ii) power loss in each skin loss element (POWER(J) for J = 2 to J = NUMNOD-1)

iii) power in the source resistor Rs (PWRSRS)

iv) power in the load resistor Rl (POWERL)

v) power loss in the diode junction (POWRDJ)

vi) power loss in the diode series resistance (POWRRD)

vii) power loss in the total diode (POWERD)

(A good check on the convergence in the system is that POWERD should equal POWRDJ + POWRRD and

$$\text{POWER}(1) = \sum_{J=2}^{\text{NUMNOD}} \text{POWER}(J) + \text{POWERL} + \text{POWERD}$$

The element match to the input may be determined by comparing POWER(1) to PWRSRS. If there is a perfect match POWER(1) = PWRSRS.)

c) Sine, cosine, and dc Fourier coefficients are calculated for the first five harmonics of the input frequency. The variables so analyzed are

i) diode current (ID)

ii) diode voltage (VNODDIO)

iii) three current or voltage variables selected by the user (V(M1), I(M2), V(M3)).

d) An automatically scaled graphical display of four currents and four voltages at each of the 128 points tabulated is presented on two plots (one of voltage, one of current). The variables displayed are

i) I(1) as an asterisk

ii) ID as an X

iii) I(NODDIO-1) as a plus

iv) I(NODDIO) as a zero

v) VIN as an asterisk

vi) VDJ as an X

vii) V(NODDIO) as a plus

viii) V(NUMNOD) as a zero.

Input variables available to the user are presented in a NAMELIST format. All program inputs are backed up by default data in the program that will cause the program to run for an original set of inputs. The user may access and change the data variables with single cards in an unformatted input. The input variables are automatically listed under a heading of the associated NAMELIST.

Following is a list of input variables and their functional meanings.

LIST OF INPUT VARIABLES AND THEIR FUNCTIONAL MEANINGS

CNTROL (control elements)

VSTART	Initial bias placed on the structure - if this number is negative all voltages are assigned the bias value - if positive the program will read data inputs under NAMELIST INIT
MAXCYC	Number of rf cycles run before print out of last cycle.
STDERR CLOSER	Optional convergence criteria which may be used to initiate the end of the run on print out last cycle.
NUMNOD	Number of nodes in the elememt. If the maximum number of nodes (19) is chosen, the program assumes a ground plane fixture is being used and adjusts element parameters accordingly.
NPRINT	Number of data points printed in the final cycle

CIRELS (circuit elements outside the diode)

R(J)	Skin losses	Default values match the rectenna element used in RXCV
C(J)	Characteristic capacitances	
L(J)	Characteristic inductances	Will be adjusted to ground plane values if NUMNOD = 19
RS	Source res	
RL	Load resistor	

DIODELS (diode parameters)

NODDIO	Diode location in the rectenna element
CD	Package capacity
LD	Package lead inductance
VMETAL	Schottky metal work function (volts)
VDJR	Breakdown voltage (a negative number) (volts)
CDJO	Zero bias junction capacity (farads)
KTOQ	Exponent multiplier (thermal voltage of diode junction)
RHO	Epitaxial resistivity of diode (ohm cm) - if this is made negative the program calculates RHO = $.15 \times 10^{+16}$/DOPING LEVEL

TIMELS (timing elements for a cycle)

FREQ	Microwave frequency in Hz
VS	Drive source amplitude (volts)
NUMSTP	Number of subdivision of one microwave cycle
M1, M2, M3	Node number of V(M1), I(M2), V(M3) for which Fourrier coefficients will be calculated

INIT (initial conditions)

V(J), I(J), VDJ, ID	Initial values of node currents and voltages if VSTART < 0, this list will not be read and all V's will receive a default value equal to VSTART all I's will be set to zero.

ERRORS (error criteria for use in predictor corrector)

These values are present for future program expansion and are not currently in use.

Data may be changed from its default values by the following procedure (an example). Place at the end of program execution cards the following

```
- - $ CNTROL - VSTART = - 8 - $
- - $ CIRELS  - $
- - $ DIODELS - $
- - $ TIMELS  - VS = 16. - $
```

In this case only the operating level of the "default" element-diode combination has been changed to a low power case. Note that almost all NAMELIST names had to be read whether or not they were used to change "default" data. INIT was not read since VSTART was negative.

```
      PROGRAM RECTIN(INPUT,OUTPUT,TAPE5=INPUT,TAPE6=OUTPUT)
      COMPUTER PROGRAM MODEL OF A RECTIFYING ANTENNA
C
C     DIMENSIONING AND PRELIMINARY STATEMENTS
      REAL I,L,ID,IERROR,IERREL,IDEROR,IDERRL,LD,KTOO
      REAL IDJO,IDSAT,LINV,LDINV,IDJ,LINE
      INTEGER ABSIS
      DIMENSION V(19,3),I(19,3),DELI(19,3),DELV(19,3),DELVDJ(3)
      DIMENSION DELIC(3),ID(3),VDJ(3),IDJ(3),RDV(3),CDJI(3)
      DIMENSION R(19),L(19),C(19),PREDI(19),PREDV(19)
      DIMENSION POWER(19),FOURCC(5),FRCOS(5,5),FRSIN(5,5)
      DIMENSION REDOUT(12,130),LINV(19),CINV(19),FUNC(5),LINE(126)
      DIMENSION ND(4)
      NAMELIST/CONTROL/VSTART,MAXCYC,STDERR,CLOSER,NUMNOD,NPRINT
      NAMELIST/CIRELS/RS,L,C,RS,RL
      NAMELIST/DIODEL/NODDIO,CD,RD,LD,VMETAL,VDJR,CDJO,KTOO,RHO
      NAMELIST/TIMELS/FREQ,VS,NUMSTP,M1,M2,M3
      NAMELIST/INIT/V,I,VDJ,ID
      NAMELIST/ERRORS/IERROR,VERROR,IERREL,VERREL,IDEROR,IDERRL
     +,VDJERR,VDJERL
C
C     SET DEFAULT VALUES
      C(1)=5.E-12
      DATA VSTART,MAXCYC,STDERR,CLOSER,NUMNOD/-25.,15,0.,0.0,19/
      NPRINT=120
      DATA(R(J),J=2,19)/2*.017,3*.048,2*.017,3*.048,2*.017,
     +6*.025/
      DATA(L(J),J=2,19)/2*.24E-9,3*1.5E-9,2*.12E-9,3*1.5E-9,
     +2*.24E-9,6*.96E-9/
      DATA(C(J),J=2,19)/2*.40E-12,3*.14E-12,2*.810E-12,
     +3*.14E-12,2*.40E-12,5*.10E-12,4.0E-11/
      DATA RS,RL,NODDIO,CD,RD,LD/50.,.80,.14,.25E-12,.5,.4E-9/
      DATA VMETAL,VDJR,CDJO,KTOO,RHO/1.14,-.68,.3.7E-12,.032,.15/
      DATA FREQ,VS,NUMSTP/2.45E9,40,.8192/
      DATA IERROR,VERROR,IERREL,VERREL/1.E-6,1.E-5,1.E-5,1.E-4/
      DATA IDERROR,IDERRL,VDJERR,VDJERL/1.E-5,1.E-5,1.E-4,1.E-5/
      DATA M1,M2/14,1/
      NOTICE=0
      ERCRIT=1.0
C
C     READ REPLACEMENT VALUES AND INITIALIZE DEPENDENT VARIABLES
      READ(5,CONTROL)
      READ(5,TIMELS)
      READ(5,CIRELS)
      READ(5,DIODEL)
      READ(5,INIT)
      READ(5,ERRORS)
      M3=NUMNOD
C     CONVERT TO BALANCED FIXTURE
      IF(NUMNOD.GE.19) GO TO 6
      DO 5 J=1,NUMNOD
      C(J)=.5*C(J)
      L(J)=2.*L(J)
      R(J)=2.*R(J)
    5 CONTINUE
      C(NUMNOD)=2.E-11
      RS=120.
```

```
971
                  RL=180.
                6 CONTINUE
     60           DO 15 NS=1,3
                  DO 10 J=1,NUMNOD
                  V(J,NS)=VSTART
                  T(J,NS)=0.0
                  PHOTOR(J)=0.0
     65        10 CONTINUE
                  VDJ(NS)=VSTART
                  ID(NS)=0.0
                  VLAST=VSTART/2.
                15 CONTINUE
     70           DO 30 K=1,5
                  FOURDC(K)=0.0
                  DO 20 K=1,5
                  FRCOS(N,K)=0.0
                  FRSIN(N,K)=0.0
     75        20 CONTINUE
               30 CONTINUE
            C
            C     PRINT PARAMETER VALUES AND INITIAL CONDITIONS
               35 WRITE(6,CNTROL)
     80           WRITE(6,CIRCLS)
                  WRITE(6,DIODEL)
                  WRITE(6,TIMELS)
                  WRITE(6,INIT)
                  WRITE(6,ERRORS)
     85        C
            C     PRELIMINARY CALCULATIONS INCLUDING DIODE PARAMETERS
                  DOPING=(-75./VDJR)**1.45
                  QOKT=1./KTOQ
                  VDIFF=KTOQ*ALOG(47./DOPING)
     90           VDJO=VMETAL-VDIFF
                  CDJOV=1./(CDJO*SQRT(VDJO))
                  THKEPO=3.96E-5*SQRT(VDJO/DOPING)
                  AREA=CDJO*THKEPO*1.04E12
                  IF(RHO.LT.0.0)  RHO=.15/DOPING
     95           ROVO=RHO*9.65E-13
                  IDJO=1.37E7*AREA*EXP(-QOKT*VMETAL)
                  IDSAT=2.76E5*AREA*DOPING
                  THKEPR=THKEPO*SQRT((-VDJR+VDJO)/VDJO)
                  REPI=ROVO*CDJOV*SQRT(VDJO-VDJR)
    100           DOPE=DOPING*1.E16
                  C(NODCIO)=CO+C(NODCIO)
                  TWOPIF=4.2831853071*FREQ
                  TRIN=1./FREQ
                  TO=TRIN/FLOAT(NL*STP)
    105           NPOINTS=NUMSTP/APRINT
                  NCYCLE=0
                  NUMNO1=NUMNOD-1
                  DO 40 J=2,NUMNOD
                  CINV(J)=1./C(J)
    110           LINV(J)=1./L(J)
               40 CONTINUE
                  CINV(1)=1./C(1)
                  RS2=RS+R(2)
                  LOINV=1./L0
```

```
      RLINV=1./RL
C
C     PRINT IMPORTANT CALCULATED VALUES
      IF(RD.LT.REPI)  WRITE(6,50)
   50 FORMAT(//,34H TOO LITTLE ACTIVE EPITAXIAL LAYER)
      WRITE(6,60) DOPE,VDJO,THKEPR,AREA,REPI,IDJO,IDSAT
   60 FORMAT(////,34H CALCULATED DICOF PARAMETER VALUES//
     +1H ,28HDOPING DENSITY =             ,1PE10.2/1H ,
     +28HBUILT-IN JUNCTION VOLTAGE = ,1PE10.2,6H VOLTS/1H ,
     +28HEPITAXIAL LAYER THICKNESS = ,1PE10.2,3H CM/1H ,
     +28HEPITAXIAL LAYER AREA =      ,1PE10.2,6H SQ CM/1H ,
     +28HEPITAXIAL LAYER RESISTANCE =,1PE10.2,5H OHMS/1H ,
     +28HREVERSE SATURATION CURRENT =,1PE10.2,5H AMPS/1H ,
     +28HFORWARD SATURATION CURRENT =,1PE10.2,5H AMPS)
C
C     START OF NEW CYCLE ANALYSIS
  500 TIME=0.0
      NCOUNT=0
      VST=0.0
      ERIMAX=0.0
      ERVMAX=0.0
      NSAVE=NPOINTS
      NSTEP1=1
C     DETERMINE IF THIS IS FINAL CYCLE ANALYSIS
      IF(NCYCLE.GE.MAXCYC.OR.ERCRIT.LT.CLOSER) NOTICE=1
  400 NCOUNT=NCOUNT+1
      TIME=NCOUNT*TO
C
C     CALCULATION OF PARAMETER DERIVATIVES
      ME=2
  410 DELI(1,ME)=(VST+V(1,ME)-V(2,ME)-I(1,ME)*(RS+R(2)))*LINV(2)
      VST=VS*SIN(TWOPIF*TIME)
      DELV(1,ME)=-I(1,ME)*CINV(1)
      DO 420 J=2,NUMNC1
      DELI(J,ME)=(V(J,ME)-V(J+1,ME)-I(J,ME)*R(J+1))*LINV(J+1)
      DELV(J,ME)=(I(J-1,ME)-I(J,ME))*CINV(J)
  420 CONTINUE
      DELV(NUMNOD,ME)=(I(NUMNO1,ME)-I(NUMNOD,ME))*CINV(NUMNOD)
      DELV(NODDIO,ME)=DELV(NODDIO,ME)-ID(ME)*CINV(NODDIO)
      CDJI(ME)=CDJOV*SQRT(VDJO-VDJ(ME))
      IDJ(ME)=-IDJO
      IF(VDJ(ME).GT.-3.) IDJ(ME)=IDJO*(EXP(QOKT*VDJ(ME))-1.)
      RDV(ME)=RD-RDVO*CDJI(ME)
      DELVDJ(ME)=(ID(ME)-IDJ(ME))*CDJI(ME)
      DELID(ME)=(V(NODDIO,ME)-VDJ(ME)-RDV(ME)*ID(ME))*LDINV
C
C     PREDICTOR INTEGRATION
      IF(ME.NE.2) GO TO 520
      DO 510 J=1,NUMNC1
      I(J,3)=I(J,1)+2.*TO*DELI(J,2)
      V(J,3)=V(J,1)+2.*TO*DELV(J,2)
  510 CONTINUE
      V(NUMNOD,3)=V(NUMNOD,1)+2.*TO*DELV(NUMNOD,2)
      I(NUMNOD,3)=V(NUMNOD,3)*RLINV
      VDJ(3)=VDJ(1)+2.*TO*DELVDJ(2)
      IF(VDJ(3).GT.VDJO) VDJ(3)=VDJO
      ID(3)=ID(1)+2.*TO*DELID(2)
```

```
                      DO 515 J=1,NUMNOD
                      PREDI(J)=I(J,3)
                      PREDV(J)=V(J,3)
  175               515 CONTINUE
                      PROVOJ=VOJ(3)
                      PREDID=ID(3)
                      ME=3
                      GO TO 410
  180           C
                C     CORRECTOR INTEGRATION
                  520 DO 530 J=1,NUMNO1
                      I(J,3)=I(J,2)+.5*TO*(DELI(J,2)+DELI(J,3))
                      V(J,3)=V(J,2)+.5*TO*(DELV(J,2)+DELV(J,3))
  185               530 CONTINUE
                      V(NUMNOD,3)=V(NUMNOD,2)+.5*TO*(DELV(NUMNOD,2)+DELV(NUMNOD,3))
                      I(NUMNOD,3)=V(NUMNOD,3)*RLINV
                      VOJ(3)=VOJ(2)+.5*TO*(DELVOJ(2)+DELVOJ(3))
                      IF(VOJ(3).GT.VOJO) VOJ(3)=VOJO
  190                 ID(3)=ID(2)+.5*TO*(DELID(2)+DELID(3))
                C
                C     PARAMETER VALUE STORAGE SHIFT
                      DO 536 NS=1,2
                      DO 535 J=1,NUMNOD
  195                 I(J,NS)=I(J,NS+1)
                      V(J,NS)=V(J,NS+1)
                  535 CONTINUE
                      VOJ(NS)=VOJ(NS+1)
                      ID(NS)=ID(NS+1)
  200               536 CONTINUE
                C
                C     DETERMINE MAXIMUM ERRORS BETWEEN INTEGRATIONS
                      DO 537 J=1,NUMNOD
                      ERI=ABS(I(J,3)-PREDI(J))
                      ERV=ABS(V(J,3)-PREDV(J))
  205                 IF(ERI.GT.ERIMAX) NMAX=NCOUNT
                      IF(ERI.GT.ERIMAX) ERIMAX=ERI
                      IF(ERV.GT.ERVMAX) ERVMAX=ERV
                  537 CONTINUE
  210                 ERVOJ=ABS(VOJ(3)-PROVOJ)
                      ERID=ABS(ID(3)-PREDID)
                      IF(ERVOJ.GT.ERVMAX) ERVMAX=ERVOJ
                      IF(ERID.GT.ERIMAX) NMAX=NCOUNT
                      IF(ERID.GT.ERIMAX) ERIMAX=ERID
  215                 GO TO 546
                C
                C     DETERMINATION OF STEP SIZE FOR NEXT STEP
                C     HALVING
                      IF(ERIMAX.LT.IERROR.AND.ERVMAX.LT.VERROR) GO TO 542
  220                 NUMSTP=NUMSTP*2
                      NCOUNT=NCOUNT*2
                      NSAVE=NSAVE*2
                      NPRINT=NUMSTP/NPRINT
                      TO=TEND/FLOAT(NUMSTP)
  225                 DO 540 J=1,NUMNO1
                      I(J,1)=(I(J,1)+I(J,2))/2.
                      V(J,1)=(V(J,1)+V(J,2))/2.
                  540 CONTINUE
```

```
                V(NUMNOD,1)=(V(NUMNOD,1)+V(NUMNOD,2))/2.
230             VDJ(1)=(VDJ(1)+VDJ(2))/2.
                ID(1)=(ID(1)+ID(2))/2.
                GO TO 546
C       DOUBLING
  542 IF(ERIMAX.GT.(.01*IERROR).AND.ERVMAX.GT.(.01*VERROR))
235    +GO TO 546
                CHECK=FLOAT(NCOUNT)/2.
                NCHECK=NCOUNT/2
                IF(CHECK.NE.FLOAT(NCHECK)) GO TO 546
                NUMSTP=NUMSTP/2
240             NCOUNT=NCOUNT/2
                NSAVE=NSAVE/2
                NPOINTS=NUMSTP/NPRINT
                TO=TFIN/FLOAT(NUMSTP)
                DO 544 J=1,NUMNO1
245             I(J,1)=I(J,1)-(I(J,2)-I(J,1))
                V(J,1)=V(J,1)-(V(J,2)-V(J,1))
  544 CONTINUE
                V(NUMNOD,1)=V(NUMNOD,1)-(V(NUMNOD,2)-V(NUMNOD,1))
                VDJ(1)=VDJ(1)-(VDJ(2)-VDJ(1))
250             ID(1)=ID(1)-(ID(2)-ID(1))
  546 CONTINUE
C
C       CHECK IF LAST CYCLE
                IF(NOTICE.EQ.0) GO TO 600
255     C
C       CALCULATE POWERS FOR LAST CYCLE
                DO 550 J=2,NUMNOD
                POWER(J)=POWER(J)+R(J+1)*I(J,3)*I(J,3)
  550 CONTINUE
260             VIN=VST-RS*I(1,3)+V(1,3)
                POWER(1)=POWER(1)+VIN*I(1,3)
                PWRSRS=PWRSRS+RS*I(1,3)*I(1,3)
                POWERL=POWERL+V(NUMNOD,3)*I(NUMNOD,3)
                POWRDJ=POWRDJ+VDJ(3)*IDJ(3)
265             POWRRC=POWRRC+RDV(3)*ID(3)*ID(3)
                POWERC=POWERC+V(NCODIO,3)*ID(3)
C
C       CALCULATE FOURIER COEFFICIENTS FOR LAST CYCLE
                FUNC(1)=V(M1,3)
270             FUNC(2)=I(M2,3)
                FUNC(3)=V(M3,3)
                FUNC(4)=ID(3)
                FUNC(5)=VIN
                DO 570 K=1,5
275             FOURDC(K)=FOURDC(K)+FUNC(K)
                COSKPI=2.*COS(K*TWOPIF*TIME)
                SINKPI=2.*SIN(K*TWOPIF*TIME)
                DO 560 N=1,5
                FRCOS(N,K)=FRCOS(N,K)+COSKPI*FUNC(N)
280             FRSIN(N,K)=FRSIN(N,K)+SINKPI*FUNC(N)
  560 CONTINUE
  570 CONTINUE
C
C       CHOOSE CYCLE TIMES FOR DATA STORAGE
285             IF(NCOUNT.NE.NSAVE) GO TO 600
```

```
130
      C
      C     STORE DATA AT SELECTED TIMES
            REDOUT(1,NSTEP1)=FLOAT(NSTEP1)
            REDOUT(2,NSTEP1)=VIN
      290   REDOUT(3,NSTEP1)=I(1,3)
            REDOUT(4,NSTEP1)=ERVDJ
            REDOUT(5,NSTEP1)=ERID
            REDOUT(6,NSTEP1)=ID(3)
            REDOUT(7,NSTEP1)=IDJ(3)
      295   REDOUT(8,NSTEP1)=VDJ(3)
            REDOUT(9,NSTEP1)=V(NODDIC,3)
            REDOUT(10,NSTEP1)=V(NUMNOD,3)
            REDOUT(11,NSTEP1)=I(NODDIO-1,3)
            REDOUT(12,NSTEP1)=I(NODDIO,3)
      300   NSAVE=NSAVE+NPOINTS
            NSTEP1=NSTEP1+1
      C
      C     CHECK FOR END OF CYCLE
        600 IF(NCOUNT.LT.NUMSTP) GO TO 400
      305 C
      C     END OF CYCLE CALCULATIONS AND PRINTOUT
            NCYCLE=NCYCLE+1
            ERCRIT=ABS((V(NUMNOD,3)-VLAST)/V(NUMNOD,3))
            VLAST=V(NUMNOD,3)
      310   WRITE(6,650) NCYCLE,V(NUMNOD,3),ERCRIT,ERIMAX,ERVMAX,NAX
        650 FORMAT(1H ,3HAT ,I4,25H CYCLES, OUTPUT VOLTAGE =,
           +F10.4,10H  ERCRIT =,F7.4,12H   ERIMAX =,1PE10.2,12H   ERVMAX =,
           +1PE10.2,I10)
      C
      315 C     CHECK IF END OF LAST CYCLE
            IF(NOTICE.EQ.0) GO TO 500
      C
      C     FINAL CYCLE PRINTOUT PREPARATION
            DO 720 J=1,NUMNOD
      320   POWER(J)=POWER(J)/NUMSTP
        720 CONTINUE
            PORIN=PORIN/NUMSTP
            PWRSRS=PWRSRS/NUMSTP
            PORL=PORL/NUMSTP
      325   PORDJ=PORDJ/NUMSTP
            PORD=PORD/NUMSTP
            PORC=PORC/NUMSTP
            DO 740 K=1,5
            FOURDC(K)=FOURDC(K)/NUMSTP
      330   DO 730 N=1,5
            FRCOS(N,K)=FRCOS(N,K)/NUMSTP
            FRSIN(N,K)=FRSIN(N,K)/NUMSTP
        730 CONTINUE
        740 CONTINUE
      335 C
      C     FINAL CYCLE PRINTOUT
            WRITE(6,800)
        800 FORMAT(////,121H      STEP  VOLTS IN   AMPS IN   ERRVDJ    ERRIDIO
           +   DIODE I   JUNCT I   JUNCT V   DIODE V    LOAD V     AC I       D
      340  +C I  //)
            NSTEP1=NSTEP1-1
            WRITE(6,810) ((REDOUT(N,K),N=1,12),K=1,NSTEP1)
```

```
      810 FORMAT(1H ,0PF10.0,1P11E10.2)
C
          WRITE(6,820)
      820 FORMAT(////,36H POWER CALCULATION RESULTS, IN WATTS//)
          WRITE(6,830) (POWER(J),J=1,NUMNOD)
      830 FORMAT(1H ,1P10E12.3)
          WRITE(6,840) POWRIN,PWRSRS,POWERL,POWRDJ,POWERD,POWRRC
      840 FORMAT(1H ,1P6E12.3)
C
          WRITE(6,860)
      860 FORMAT(////,21H FOURIER COFFFICIENTS//1H ,58H      VDIODE        AMP
     *IN        VOUT        IDIODE        VIN)
          WRITE(6,870) (FOURDC(J),J=1,5)
          WRITE(6,870) ((FNCOS(N,K),N=1,5),K=1,5)
          WRITE(6,870) ((FNSIN(N,K),N=1,5),K=1,5)
      870 FORMAT(1H ,1P5E12.3)
C
C
C     PLOTTING ROUTINE
          DATA ND(1),ND(2),ND(3),ND(4),ABSIS/3,6,11,12,63/
          DATA BLANK,DOT,AST,X,PLUS,ZERO/1H ,1H.,1H*,1HX,1H+,1H0/
          DO 990 NPLOT=1,2
          IF(NPLOT.EQ.1) GO TO 910
          ND(1)=2
          ND(2)=8
          ND(3)=9
          ND(4)=10
          ABSIS=100
C     DETERMINE SCALING FACTOR
      910 VALMAX=ABS(REDOUT(ND(1),1))
          DO 930 NS1=1,4
          DO 920 NS2=1,NSTEP1
          IF(ABS(REDOUT(ND(NS1),NS2)).GT.VALMAX) VALMAX=ABS(REDOUT(ND(NS1)
     *,NS2))
      920 CONTINUE
      930 CONTINUE
          SCALE=(ABSIS-1)/VALMAX
C     PRINT ORDINATE
          DO 940 J=1,126
      940 LINE(J)=DOT
          WRITE(6,950) LINE
      950 FORMAT(1H1,126A1)
C     BLANK THE LINE
          DO 960 J=1,126
      960 LINE(J)=BLANK
C     PUT DOT IN LINE TO PRODUCE ABSCISSA
          LINE(ABSIS)=DOT
C     DATA LOOP
          DO 980 K=1,NSTEP1
          J1=REDOUT(ND(1),K)*SCALE+ABSIS+.5
          J2=REDOUT(ND(2),K)*SCALE+ABSIS+.5
          J3=REDOUT(ND(3),K)*SCALE+ABSIS+.5
          J4=REDOUT(ND(4),K)*SCALE+ABSIS+.5
C     PUT SYMBOLS IN SELECTED LINES AND PRINT
          LINE(J1)=AST
          LINE(J2)=X
          LINE(J3)=PLUS
```

```
132
      800               LINE(J4)=ZERO
                        WRITE(6,970) LINE
                  970 FORMAT(1H ,124A1)
                C     RE-BLANK DATA POSITIONS
                        LINE(J1)=BLANK
      805               LINE(J2)=BLANK
                        LINE(J3)=BLANK
                        LINE(J4)=BLANK
                        LINE(ABSIS)=DOT
                  980 CONTINUE
      810         990 CONTINUE
                        END
```

CARD NR. SEVERITY DETAILS DIAGNOSIS OF PROBLEM

219 I THERE IS NO PATH TO THIS STATEMENT.

SYMBOLIC REFERENCE MAP (R=1)

ENTRY POINTS
2115 RECTIN

VARIABLES SN TYPE RELOCATION

4043	ABSIS	INTEGER		4135	AREA	REAL	
4046	AST	REAL		4044	BLANK	REAL	
5075	C	REAL	ARRAY	3500	CD	REAL	
5047	CDJT	REAL	ARRAY	3505	CDJD	REAL	
4133	CDJDV	REAL		4171	CHECK	REAL	
10330	CINV	REAL	ARRAY	3473	CLOSER	REAL	
4201	COSKPI	REAL		4651	DELI	REAL	ARRAY
5036	DELID	REAL	ARRAY	4742	DELV	REAL	ARRAY
5033	DELVDJ	REAL	ARRAY	4141	DOPE	REAL	
4127	DOPING	REAL		4045	DOT	REAL	
4121	ERCSIT	REAL		4164	ERI	REAL	
4170	ERID	REAL		4155	ERIMAX	REAL	
4165	ERV	REAL		4167	ERVDJ	REAL	
4156	ERVMAX	REAL		5211	FOUROC	REAL	ARRAY
5216	FROOS	REAL	ARRAY	3510	FREQ	REAL	
4247	FRSTS	REAL	ARRAY	10353	FUNC	REAL	ARRAY
4215	I	REAL	ARRAY	4331	ID	REAL	ARRAY
3517	IDERDR	REAL		3520	IDERRL	REAL	
4357	IDJ	REAL	ARRAY	4113	IDJD	REAL	
4114	IDSAT	REAL		3515	IERREL	REAL	
3513	IFRROR	REAL		4122	J	INTEGER	
4211	J1	INTEGER		4212	J2	INTEGER	
4213	J3	INTEGER		4214	J4	INTEGER	
4126	K	INTEGER		3504	KTOR	REAL	
4306	L	REAL	ARRAY	3502	LC	REAL	
4115	LDINV	REAL		4362	LINE	REAL	ARRAY
4334	LINV	REAL	ARRAY	3471	MAXCYC	INTEGER	

VARIABLES	SN	TYPE	RELOCATION
4161	ME	INTEGER	
3524	M2	INTEGER	
4125	N	INTEGER	
4172	NCHECK	INTEGER	
4146	NCYCLE	INTEGER	
3477	NGOOIO	INTEGER	
4204	NPLOT	INTEGER	
4116	NPRINT	INTEGER	
4157	NSAVE	INTEGER	
4206	NS1	INTEGER	
3474	NUMNOD	INTEGER	
3512	NUMSTP	INTEGER	
5166	POWER	REAL	ARRAY
4175	POWERI	REAL	
4203	POWRIV	REAL	
4162	PRDVDJ	REAL	
4163	PREDID	REAL	
4174	PWRSRS	REAL	
5052	R	REAL	ARRAY
5044	RDV	REAL	ARRAY
5300	REDOUT	REAL	ARRAY
3507	RHO	REAL	
4151	RLINV	REAL	
4150	RS2	REAL	
4202	SINKPI	REAL	
4143	TFIN	REAL	
4137	THKEPS	REAL	
4144	TO	REAL	
4560	V	REAL	ARRAY
4131	VDIFF	REAL	
3522	VDJERL	REAL	
4132	VDJO	REAL	
3516	VERREI	REAL	
4173	VIN	REAL	
3503	VMETAL	REAL	
4154	VST	REAL	
4047	X	REAL	
3523	M1	INTEGER	
4117	M3	INTEGER	
4166	MAX	INTEGER	
4153	NCOUNT	INTEGER	
10360	NC	INTEGER	ARRAY
4120	NOTICE	INTEGER	
4145	NPOINTS	INTEGER	
4123	NS	INTEGER	
4160	NSTEP1	INTEGER	
4207	NS2	INTEGER	
4147	NUMNO1	INTEGER	
4050	PLUS	REAL	
4200	POWERO	REAL	
4176	POWRDJ	REAL	
4177	POWRRC	REAL	
5120	PREDI	REAL	ARRAY
5143	PREDV	REAL	ARRAY
4130	QOKT	REAL	
3501	RD	REAL	
4136	RDVO	REAL	
4140	REPI	REAL	
3476	RL	REAL	
3475	RS	REAL	
4210	SCALE	REAL	
3472	STDERR	REAL	
4134	THKEPO	REAL	
4152	TIME	REAL	
4142	THOPIF	REAL	
4205	VALMAX	REAL	
5041	VDJ	REAL	ARRAY
3521	VDJERR	REAL	
3504	VDJR	REAL	
3514	VERROR	REAL	
4124	VLAST	REAL	
3511	VS	REAL	
3470	VSTART	REAL	
4051	ZERO	REAL	

FILE NAMES MODE

0 INPUT 1043 OUTPUT 0 TAPE5 NAME 1043 TAPE6 MIXED

EXTERNALS	TYPE	ARGS			
ALOG	REAL	1 LIBRARY	COS	REAL	1 LIBRARY
EXP	REAL	1 LIBRARY	SIN	REAL	1 LIBRARY
SQRT	REAL	1 LIBRARY			

INLINE FUNCTIONS	TYPE	ARGS			
ABS	REAL	1 INTRIN	FLOAT	REAL	1 INTRIN

NAMELISTS

CIRCLS CNTROL CYCDEL ERRORS INIT TIMELS

STATEMENT LABELS

0	5		2157	6	0	10	
0	15		0	20	0	30	
0	35	INACTIVE	0	40	3602	50	FMT
3622	60	FMT	2343	300	2355	400	

133

134

STATEMENT LABELS

2382	410			0	420			0	510		
0	515			2526	520			0	530		
0	535			0	536			0	537		
0	540			2706	542			0	544		
2751	546			0	550			0	560		
0	570			3075	600			3703	650	FMT	
0	720			0	730			0	740		
3723	800	FMT		3746	810	FMT		3755	820	FMT	
3767	830	FMT		4003	840	FMT		4011	860	FMT	
4040	870	FMT		3216	910			0	920		
0	930			0	940			4056	950	FMT	
0	960			4068	970	FMT		0	980		
0	990										

LOOPS	LABEL		INDEX	FROM-TO	LENGTH	PROPERTIES
2145	5		J	51 55	4R	INSTACK
2160	15	*	NS	62 69	20R	NOT INNER
2165	10		J	61 65	4R	INSTACK
2201	30	*	K	70 76	15R	NOT INNER
2207	20		K	72 75	3R	INSTACK
2321	40		J	108 111	5R	INSTACK
2410	420		J	148 151	10R	OPT
2466	510		J	163 166	7R	INSTACK
2515	515		J	172 175	4R	INSTACK
2533	530		J	182 185	11R	OPT
2567	536	*	NS	193 200	17B	NOT INNER
2575	535		J	194 197	3R	INSTACK
2611	537		J	203 209	17R	OPT
2670	540		J	225 228	5R	INSTACK
2733	548		J	244 247	5R	INSTACK
2755	550		J	257 259	4R	INSTACK
3014	570	*	K	274 282	31B	EXT REFS NOT INNER
3038	580		K	278 281	5R	INSTACK
3117	720		J	319 321	3R	INSTACK
3138	740	*	K	328 334	21R	NOT INNER
3146	730		K	330 333	3R	INSTACK
3207	990	*	APLOT	366 410	125R	EXT REFS NOT INNER
3222	930	*	NS1	373 378	20B	NOT INNER
3227	920		NS2	374 377	7R	INSTACK
3247	940		J	381 382	3R	INSTACK
3257	960		J	386 387	3R	INSTACK
3266	980	*	K	391 409	44R	EXT REFS

STATISTICS

PROGRAM LENGTH	6255B	3245
BUFFER LENGTH	2107B	1095

NAMELIST DATA TERMINATED BY FOR NOT $
ERROR NUMBER 49 DETECTED BY NAMIN AT ADDRESS 000437
CALLED FROM RECTIN AT LINE 40

END-OF-FILE ENCOUNTERED ON FILENAME = INPUT
ERROR NUMBER 65 DETECTED BY NAMIN AT ADDRESS 000456
CALLED FROM RECTIN AT LINE 65

```
$CNTRCL
VSTART  = -.18E+02,
MAXCYC  = 15,
STOERR  = 0.0,
CLOSER  = 0.0,
NUMNOD  = 19,
NPRINT  = 128,
$END
```

```
 $CIRFLS
 W       = 0.0, .17E-01, .17E-01, .48E-01, .48E-01, .48E-01, .17E-01, .17E-01,
           .17E-01, .25E-01, .25E-01, .25E-01, .25E-01, .25E-01, .25E-01,
           .48E-01, .48E-01, .48E-01, .17E-01,
 L       = 0.0, .24E-09, .24E-09, .15E-08, .15E-08, .15E-08, .12E-09, .12E-09,
           .24E-09, .96E-09, .11SE-08, .11SE-08, .11SE-08, .11SE-08, .11SE-08,
           .15E-08, .15E-08, .15E-08, .24E-09,
 C       = .5E-11, .4E-12, .4E-12, .14E-12, .14E-12, .14E-12, .81E-12, .81E-12,
           .4E-12, .1E-12, .12E-12, .12E-12, .12E-12, .12E-12, .4E-10,
           .14E-12, .14E-12, .14E-12, .4E-12,
 RS      = .5E+02,
 RL      = .8E+02,
 $END
```

```
$DIODEL
NODDIO  = 14.
CO      = .25E-12.
RO      = .5E+00.
LO      = .4E-09.
VMETAL  = .11E+01.
VOJN    = -.6E+02.
COJO    = .37E-11.
XTOG    = .52E-01.
RHO     = .15E+00.
$END
```

```
$TIMELS
FREQ    = .245E+10,
VS      = .3E+02,
NUMSTP  = 8192,
M1      = 14,
M2      = 1,
M3      = 19,
$END
```

```
$INIT
V        = -.18E+02, -.18E+02, -.18E+02, -.18E+02, -.18E+02, -.18E+02, -.18E+02, -.18E+02, -.18E+02, -.18E+02, -.18E+02,
           -.18E+02, -.18E+02, -.18E+02, -.18E+02, -.18E+02, -.18E+02, -.18E+02, -.18E+02, -.18E+02, -.18E+02, -.18E+02,
           -.18E+02, -.18E+02, -.18E+02, -.18E+02, -.18E+02, -.18E+02, -.18E+02, -.18E+02, -.18E+02, -.18E+02, -.18E+02,
           -.18E+02, -.18E+02, -.18E+02, -.18E+02, -.18E+02, -.18E+02, -.18E+02, -.18E+02, -.18E+02, -.18E+02, -.18E+02,
           -.18E+02, -.18E+02, -.18E+02, -.18E+02, -.18E+02, -.18E+02, -.18E+02, -.18E+02, -.18E+02, -.18E+02, -.18E+02,
           -.18E+02, -.18E+02,
I        = 0.0, 0.0, 0.0, 0.0, 0.0, 0.0, 0.0, 0.0, 0.0, 0.0, 0.0, 0.0, 0.0, 0.0, 0.0, 0.0, 0.0, 0.0, 0.0, 0.0, 0.0,
           0.0, 0.0, 0.0, 0.0, 0.0, 0.0, 0.0, 0.0, 0.0, 0.0, 0.0, 0.0, 0.0, 0.0, 0.0, 0.0, 0.0, 0.0, 0.0, 0.0, 0.0,
           0.0, 0.0, 0.0, 0.0, 0.0, 0.0, 0.0, 0.0, 0.0, 0.0, 0.0, 0.0, 0.0, 0.0, 0.0, 0.0, 0.0, 0.0, 0.0, 0.0, 0.0,
VOJ      = -.18E+02, -.18E+02, -.18E+02,
IC       = 0.0, 0.0, 0.0,
$END
```

```
$ERROR$

IERROR  = .1E-05,

VERROR  = .1E-04,

IERRFL  = .1E-04,

VERRFL  = .1E-03,

IDERROR = .1E-04,

IDERRL  = .1E-04,

VDJERR  = .1E-03,

VDJERL  = .1E-04,

$END
```

CALCULATED DIODE PARAMETER VALUES

```
DOPING DENSITY =                1.15E+16
BUILT-IN JUNCTION VOLTAGE =     1.02E+00 VOLTS
EPITAXIAL LAYER THICKNESS =     2.48E-04 CM
EPITAXIAL LAYER AREA =          1.25E-04 SQ CM
EPITAXIAL LAYER RESISTANCE =    3.22E-01 OHMS
REVERSE SATURATION CURRENT =    5.79E-13 AMPS
FORWARD SATURATION CURRENT =    3.99E+01 AMPS
AT     1 CYCLES, OUTPUT VOLTAGE =  -15.3543; ERCRIT =   .4138;   ERIMAX =  3.18E-06;   ERVMAX =  1.40E-04          1
AT     2 CYCLES, OUTPUT VOLTAGE =  -15.4697; ERCRIT =   .0075;   ERIMAX =  6.46E-09;   ERVMAX =  3.26E-06       5984
AT     3 CYCLES, OUTPUT VOLTAGE =  -15.2635; ERCRIT =   .0448;   ERIMAX =  9.51E-09;   ERVMAX =  5.63E-06       6171
AT     4 CYCLES, OUTPUT VOLTAGE =  -15.5200; ERCRIT =   .0155;   ERIMAX =  1.02E-08;   ERVMAX =  7.50E-06       6118
AT     5 CYCLES, OUTPUT VOLTAGE =  -15.8179; ERCRIT =   .0440;   ERIMAX =  9.90E-09;   ERVMAX =  6.80E-06       6023
AT     6 CYCLES, OUTPUT VOLTAGE =  -15.5389; ERCRIT =   .0180;   ERIMAX =  1.18E-08;   ERVMAX =  7.62E-06       6202
AT     7 CYCLES, OUTPUT VOLTAGE =  -15.7061; ERCRIT =   .0106;   ERIMAX =  1.40E-08;   ERVMAX =  1.06E-05       6021
AT     8 CYCLES, OUTPUT VOLTAGE =  -15.9193; ERCRIT =   .0134;   ERIMAX =  1.17E-08;   ERVMAX =  7.03E-06       6100
AT     9 CYCLES, OUTPUT VOLTAGE =  -15.7419; ERCRIT =   .0113;   ERIMAX =  1.26E-08;   ERVMAX =  7.43E-06       6052
AT    10 CYCLES, OUTPUT VOLTAGE =  -15.7061; ERCRIT =   .0023;   ERIMAX =  1.30E-08;   ERVMAX =  6.99E-06       6143
AT    11 CYCLES, OUTPUT VOLTAGE =  -15.6579; ERCRIT =   .0031;   ERIMAX =  1.40E-08;   ERVMAX =  9.27E-06       6020
AT    12 CYCLES, OUTPUT VOLTAGE =  -15.6590; ERCRIT =   .0001;   ERIMAX =  8.49E-09;   ERVMAX =  5.41E-06       6124
AT    13 CYCLES, OUTPUT VOLTAGE =  -15.6512; ERCRIT =   .0005;   ERIMAX =  1.03E-08;   ERVMAX =  7.79E-06       6083
AT    14 CYCLES, OUTPUT VOLTAGE =  -15.7317; ERCRIT =   .0051;   ERIMAX =  1.12E-08;   ERVMAX =  7.39E-06       6101
AT    15 CYCLES, OUTPUT VOLTAGE =  -15.6388; ERCRIT =   .0059;   ERIMAX =  9.90E-09;   ERVMAX =  8.11E-06       6052
AT    16 CYCLES, OUTPUT VOLTAGE =  -15.6194; ERCRIT =   .0012;   ERIMAX =  1.21E-08;   ERVMAX =  6.83E-06       6128
```

STEP	VOLTS IN	AMPS IN	ERRVDJ	ERRIDIO	DIODE I	JUNCT I	JUNCT V	DIODE V	LOAD V	AC I	DC I
1.	-8.40E+01	4.24E-02	2.10E-08	2.04E-09	-2.05E-01	5.19E-04	6.60E-01	-7.39E+00	-1.56E+01	-6.26E-02	1.38E-02
2.	-7.72E+01	5.48E-02	1.63E-06	5.71E-10	-2.65E-01	8.77E-06	5.29E-01	-6.19E+00	-1.56E+01	-1.06E-01	2.41E-02
3.	-7.03E+01	9.12E-02	1.22E-08	9.84E-10	-3.10E-01	2.50E-08	3.42E-01	-5.01E+00	-1.56E+01	-1.50E-01	3.15E-02
4.	-6.33E+01	1.14E-01	6.44E-09	2.92E-09	-3.46E-01	9.42E-12	9.11E-02	-3.96E+00	-1.56E+01	-2.05E-01	3.59E-02
5.	-5.76E+01	1.33E-01	1.50E-09	3.59E-09	-3.72E-01	-5.79E-13	-2.29E-01	-3.12E+00	-1.56E+01	-2.59E-01	3.74E-02
6.	-5.19E+01	1.49E-01	1.55E-09	4.34E-09	-3.90E-01	-5.79E-13	-6.19E-01	-2.59E+00	-1.56E+01	-3.15E-01	3.58E-02
7.	-4.65E+01	1.63E-01	1.73E-09	4.57E-09	-4.02E-01	-5.79E-13	-1.08E+00	-2.41E+00	-1.56E+01	-3.71E-01	3.10E-02
8.	-4.16E+01	2.13E-01	1.10E-09	4.26E-09	-4.09E-01	-5.79E-13	-1.61E+00	-2.60E+00	-1.56E+01	-4.27E-01	2.27E-02

9.	-3.72E+00	2.37E-01	6.13E-09	4.02E-09	-4.15E-01	-5.79E-13	-2.21E+00	-3.13E+00	-1.56E+01	-4.80E-01	1.11E-02
10.	-3.33E+00	2.41E-01	1.21E-08	2.18E-09	-4.22E-01	-5.79E-13	-2.89E+00	-3.96E+00	-1.56E+01	-5.29E-01	-3.55E-03
11.	-2.99E+00	2.45E-01	1.75E-08	6.93E-10	-4.30E-01	-5.79E-13	-3.64E+00	-5.00E+00	-1.56E+01	-5.74E-01	-2.07E-02
12.	-2.70E+00	3.09E-01	2.08E-08	8.40E-10	-4.41E-01	-5.79E-13	-4.47E+00	-6.17E+00	-1.56E+01	-6.12E-01	-3.94E-02
13.	-2.46E+00	3.32E-01	2.07E-08	2.18E-09	-4.54E-01	-5.79E-13	-5.41E+00	-7.38E+00	-1.55E+01	-6.44E-01	-5.85E-02
14.	-2.26E+00	3.55E-01	1.64E-08	3.17E-09	-4.69E-01	-5.79E-13	-6.44E+00	-8.55E+00	-1.55E+01	-6.69E-01	-7.62E-02
15.	-2.11E+00	3.77E-01	7.78E-09	3.68E-09	-4.84E-01	-5.79E-13	-7.59E+00	-9.63E+00	-1.55E+01	-6.88E-01	-9.16E-02
16.	-1.99E+00	3.93E-01	4.80E-09	3.65E-09	-4.98E-01	-5.79E-13	-8.87E+00	-1.06F+01	-1.55E+01	-7.00E-01	-1.03E-01
17.	-1.90E+00	4.18E-01	2.01E-08	3.11E-09	-5.08E-01	-5.79E-13	-1.03E+01	-1.14E+01	-1.55E+01	-7.06E-01	-1.11E-01
18.	-1.84E+00	4.37E-01	3.63E-08	2.15E-09	-5.13E-01	-5.79E-13	-1.12E+01	-1.22E+01	-1.55E+01	-7.06E-01	-1.14E-01
19.	-1.82E+00	4.50E-01	5.12E-08	9.37E-10	-5.11E-01	-5.79E-13	-1.34E+01	-1.29E+01	-1.54E+01	-7.03E-01	-1.13E-01
20.	-1.78E+00	4.71E-01	6.27E-08	3.38E-10	-5.02E-01	-5.79E-13	-1.51E+01	-1.34E+01	-1.54E+01	-6.94E-01	-1.09E-01
21.	-1.77E+00	4.85E-01	6.89E-08	1.49E-09	-4.85E-01	-5.79E-13	-1.68E+01	-1.44E+01	-1.54E+01	-6.83E-01	-1.04E-01
22.	-1.77E+00	4.99E-01	6.93E-08	2.36E-09	-4.62E-01	-5.79E-13	-1.86E+01	-1.53E+01	-1.54E+01	-6.67E-01	-9.87E-02
23.	-1.80E+00	5.10E-01	6.40E-08	2.86E-09	-4.32E-01	-5.79E-13	-2.03E+01	-1.64E+01	-1.53E+01	-6.49E-01	-9.53E-02
24.	-1.84E+00	5.21E-01	5.43E-08	2.96E-09	-3.98E-01	-5.79E-13	-2.19E+01	-1.74E+01	-1.53E+01	-6.28E-01	-9.51E-02
25.	-1.91E+00	5.29E-01	4.20E-08	2.72E-09	-3.61E-01	-5.79E-13	-2.35E+01	-1.88E+01	-1.53E+01	-6.03E-01	-9.67E-02
26.	-2.01E+00	5.37E-01	2.91E-08	2.25E-09	-3.22E-01	-5.79E-13	-2.50E+01	-2.02E+01	-1.53E+01	-5.76E-01	-1.00E-01
27.	-2.15E+00	5.43E-01	1.70E-08	1.68E-09	-2.83E-01	-5.79E-13	-2.63E+01	-2.15E+01	-1.52E+01	-5.46E-01	-1.17E-01
28.	-2.33E+00	5.48E-01	6.75E-09	1.17E-09	-2.44E-01	-5.79E-13	-2.75E+01	-2.28E+01	-1.52E+01	-5.14E-01	-1.29E-01
29.	-2.55E+00	5.53E-01	1.65E-09	8.10E-10	-2.07E-01	-5.79E-13	-2.85E+01	-2.41E+01	-1.52E+01	-4.80E-01	-1.42E-01
30.	-2.83E+00	5.56E-01	8.71E-09	6.41E-10	-1.72E-01	-5.79E-13	-2.94E+01	-2.52E+01	-1.52E+01	-4.44E-01	-1.52E-01
31.	-3.15E+00	5.58E-01	1.52E-08	7.11E-10	-1.39E-01	-5.79E-13	-3.02E+01	-2.62E+01	-1.51E+01	-4.07E-01	-1.59E-01
32.	-3.53E+00	5.60E-01	2.19E-08	8.88E-10	-1.09E-01	-5.79E-13	-3.07E+01	-2.72E+01	-1.51E+01	-3.69E-01	-1.61E-01
33.	-3.96E+00	5.60E-01	2.91E-08	1.08E-09	-8.19E-02	-5.79E-13	-3.12E+01	-2.81E+01	-1.51E+01	-3.31E-01	-1.56E-01
34.	-4.43E+00	5.59E-01	3.65E-08	1.17E-09	-5.86E-02	-5.79E-13	-3.15E+01	-2.89E+01	-1.51E+01	-2.93E-01	-1.46E-01
35.	-4.96E+00	5.58E-01	4.34E-08	1.04E-09	-3.95E-02	-5.79E-13	-3.18E+01	-2.97E+01	-1.51E+01	-2.57E-01	-1.30E-01
36.	-5.52E+00	5.55E-01	4.85E-08	6.36E-10	-2.52E-02	-5.79E-13	-3.19E+01	-3.05E+01	-1.51E+01	-2.21E-01	-1.10E-01
37.	-6.11E+00	5.52E-01	5.05E-08	4.81E-11	-1.62E-02	-5.79E-13	-3.20E+01	-3.12E+01	-1.51E+01	-1.88E-01	-8.83E-02
38.	-6.73E+00	5.47E-01	4.80E-08	9.48E-10	-1.25E-02	-5.79E-13	-3.21E+01	-3.20E+01	-1.51E+01	-1.56E-01	-6.62E-02
39.	-7.38E+00	5.40E-01	4.15E-08	1.94E-09	-1.40E-02	-5.79E-13	-3.22E+01	-3.26E+01	-1.51E+01	-1.28E-01	-4.60E-02
40.	-8.05E+00	5.33E-01	2.98E-08	2.87E-09	-1.98E-02	-5.79E-13	-3.22E+01	-3.32E+01	-1.51E+01	-1.03E-01	-2.95E-02
41.	-8.74E+00	5.24E-01	1.41E-08	3.58E-09	-2.86E-02	-5.79E-13	-3.24E+01	-3.36E+01	-1.51E+01	-8.16E-02	-1.82E-02
42.	-9.44E+00	5.14E-01	4.26E-09	3.90E-09	-3.88E-02	-5.79E-13	-3.25E+01	-3.38E+01	-1.51E+01	-6.47E-02	-1.28E-02
43.	-1.01E+01	5.02E-01	2.34E-08	3.76E-09	-4.84E-02	-5.79E-13	-3.28E+01	-3.38E+01	-1.51E+01	-5.24E-02	-1.36E-02
44.	-1.09E+01	4.89E-01	4.11E-08	3.11E-09	-5.54E-02	-5.79E-13	-3.30E+01	-3.37E+01	-1.51E+01	-4.51E-02	-2.04E-02
45.	-1.16E+01	4.75E-01	5.08E-08	2.00E-09	-5.80E-02	-5.79E-13	-3.33E+01	-3.33E+01	-1.50E+01	-4.29E-02	-3.27E-02
46.	-1.23E+01	4.59E-01	6.22E-08	5.54E-10	-5.49E-02	-5.79E-13	-3.36E+01	-3.28E+01	-1.51E+01	-4.58E-02	-4.95E-02
47.	-1.31E+01	4.42E-01	6.17E-08	1.05E-09	-4.54E-02	-5.79E-13	-3.38E+01	-3.23E+01	-1.51E+01	-5.35E-02	-7.00E-02
48.	-1.39E+01	4.24E-01	5.26E-08	2.60E-09	-2.97E-02	-5.79E-13	-3.40E+01	-3.17E+01	-1.51E+01	-6.57E-02	-9.31E-02
49.	-1.45E+01	4.04E-01	3.54E-08	3.88E-09	-8.71E-03	-5.79E-13	-3.41E+01	-3.12E+01	-1.51E+01	-8.18E-02	-1.14E-01
50.	-1.52E+01	3.85E-01	1.22E-08	4.72E-09	1.58E-02	-5.79E-13	-3.41E+01	-3.09E+01	-1.51E+01	-1.01E-01	-1.44E-01
51.	-1.58E+01	3.61E-01	1.39E-08	4.98E-09	4.15E-02	-5.79E-13	-3.40E+01	-3.08E+01	-1.51E+01	-1.23E-01	-1.70E-01
52.	-1.64E+01	3.37E-01	3.93E-08	4.64E-09	6.59E-02	-5.79E-13	-3.37E+01	-3.08E+01	-1.51E+01	-1.47E-01	-1.97E-01
53.	-1.70E+01	3.11E-01	6.03E-08	3.73E-09	8.65E-02	-5.79E-13	-3.33E+01	-3.10E+01	-1.51E+01	-1.71E-01	-2.22E-01
54.	-1.76E+01	2.84E-01	7.84E-08	2.37E-09	1.01E-01	-5.79E-13	-3.28E+01	-3.14E+01	-1.51E+01	-1.96E-01	-2.47E-01
55.	-1.81E+01	2.56E-01	7.99E-08	7.32E-10	1.08E-01	-5.79E-13	-3.23E+01	-3.19E+01	-1.51E+01	-2.20E-01	-2.70E-01
56.	-1.86E+01	2.27E-01	7.47E-08	9.98E-10	1.07E-01	-5.79E-13	-3.18E+01	-3.25E+01	-1.51E+01	-2.42E-01	-2.91E-01
57.	-1.91E+01	1.97E-01	6.57E-08	2.62E-09	9.72E-02	-5.79E-13	-3.13E+01	-3.30E+01	-1.51E+01	-2.63E-01	-3.10E-01
58.	-1.95E+01	1.66E-01	4.86E-08	3.98E-09	8.03E-02	-5.79E-13	-3.09E+01	-3.33E+01	-1.51E+01	-2.81E-01	-3.26E-01
59.	-1.99E+01	1.35E-01	2.71E-08	4.94E-09	5.78E-02	-5.79E-13	-3.05E+01	-3.36E+01	-1.51E+01	-2.97E-01	-3.40E-01
60.	-2.03E+01	1.04E-01	3.25E-09	5.43E-09	3.22E-02	-5.79E-13	-3.03E+01	-3.36E+01	-1.51E+01	-3.09E-01	-3.51E-01
61.	-2.06E+01	7.24E-02	2.14E-08	5.42E-09	6.14E-03	-5.79E-13	-3.02E+01	-3.34E+01	-1.51E+01	-3.17E-01	-3.59E-01
62.	-2.12E+01	4.06E-02	4.51E-08	4.91E-09	-1.75E-02	-5.79E-13	-3.02E+01	-3.30E+01	-1.51E+01	-3.22E-01	-3.65E-01
63.	-2.16E+01	9.09E-03	6.62E-08	3.97E-09	-3.61E-02	-5.79E-13	-3.04E+01	-3.23E+01	-1.51E+01	-3.24E-01	-3.71E-01
64.	-2.20E+01	-2.11E-02	8.29E-08	2.68E-09	-4.73E-02	-5.79E-13	-3.06E+01	-3.15E+01	-1.51E+01	-3.21E-01	-3.75E-01
65.	-2.25E+01	-5.12E-02	9.35E-08	1.15E-09	-4.94E-02	-5.79E-13	-3.08E+01	-3.05E+01	-1.51E+01	-3.15E-01	-3.80E-01
66.	-2.29E+01	-8.07E-02	9.62E-08	-4.94E-10	-4.14E-02	-5.79E-13	-3.10E+01	-2.94E+01	-1.51E+01	-3.05E-01	-3.85E-01
67.	-2.33E+01	-1.10E-01	9.02E-08	-2.09E-09	-2.31E-02	-5.79E-13	-3.12E+01	-2.84E+01	-1.52E+01	-2.92E-01	-3.90E-01
68.	-2.37E+01	-1.38E-01	7.52E-08	-3.50E-09	4.74E-03	-5.79E-13	-3.12E+01	-2.72E+01	-1.52E+01	-2.75E-01	-3.95E-01
69.	-2.42E+01	-1.65E-01	5.23E-08	-4.54E-09	4.06E-02	-5.79E-13	-3.11E+01	-2.62E+01	-1.52E+01	-2.55E-01	-4.01E-01
70.	-2.46E+01	-1.91E-01	2.41E-08	-5.23E-09	8.24E-02	-5.79E-13	-3.08E+01	-2.53E+01	-1.52E+01	-2.31E-01	-4.05E-01
71.	-2.50E+01	-2.19E-01	6.29E-09	-5.35E-09	1.28E-01	-5.79E-13	-3.03E+01	-2.44E+01	-1.52E+01	-2.03E-01	-4.07E-01
72.	-2.54E+01	-2.45E-01	3.49E-08	-4.92E-09	1.73E-01	-5.79E-13	-2.96E+01	-2.39E+01	-1.52E+01	-1.71E-01	-4.05E-01
73.	-2.58E+01	-2.71E-01	5.81E-08	-3.94E-09	2.17E-01	-5.79E-13	-2.87E+01	-2.34E+01	-1.52E+01	-1.34E-01	-4.01E-01
74.	-2.61E+01	-2.96E-01	7.32E-08	-2.43E-09	2.56E-01	-5.79E-13	-2.76E+01	-2.34E+01	-1.52E+01	-9.17E-02	-3.91E-01

75.	-2.44E+01	-3.20E+01	7.87E+08	9.69E-10	2.89E-01	-5.70E-13	-2.66E+01	-2.26E+01	-1.53E+01	-8.47E-02	-3.78E-01
76.	-2.47E+01	-3.44E-01	7.05E+08	7.44E-10	3.15E-01	-5.70E-13	-2.51E+01	-2.22E+01	-1.53E+01	7.12E-03	-3.60E-01
77.	-2.49E+01	-3.47E+01	6.22E+08	2.05E-09	3.33E-01	-5.70E-13	-2.37E+01	-2.16E+01	-1.53E+01	6.35E-02	-3.39E-01
78.	-2.71E+01	-3.89E+01	8.39E+08	3.88E-09	3.48E-01	-5.79E-13	-2.22E+01	-2.09E+01	-1.53E+01	1.23E-01	-3.16E-01
79.	-2.73E+01	-4.10E+01	2.27E+08	4.89E-09	3.54E-01	-5.79E-13	-2.08E+01	-1.99E+01	-1.54E+01	1.85E-01	-2.92E-01
80.	-2.74E+01	-4.30E+01	1.52E+09	5.35E-09	3.59E-01	-5.79E-13	-1.94E+01	-1.86E+01	-1.54E+01	2.48E-01	-2.70E-01
81.	-2.76E+01	-4.49E+01	1.68E+08	5.21E-09	3.66E-01	-5.79E-13	-1.81E+01	-1.70E+01	-1.54E+01	3.11E-01	-2.49E-01
82.	-2.77E+01	-4.67E+01	2.99E+08	4.86E-09	3.75E-01	-5.79E-13	-1.67E+01	-1.51E+01	-1.55E+01	3.71E-01	-2.32E-01
83.	-2.77E+01	-4.83E+01	3.59E+08	3.17E-09	3.90E-01	-5.79E-13	-1.54E+01	-1.29E+01	-1.55E+01	4.27E-01	-2.19E-01
84.	-2.77E+01	-4.98E+01	3.34E+08	1.08E-09	4.13E-01	-5.79E-13	-1.40E+01	-1.05E+01	-1.55E+01	4.77E-01	-2.10E-01
85.	-2.78E+01	-5.12E+01	2.22E+08	4.08E-10	4.48E-01	-5.79E-13	-1.26E+01	-7.92E+00	-1.55E+01	5.21E-01	-2.06E-01
86.	-2.79E+01	-5.25E+01	1.18E+09	2.26E-09	4.85E-01	-5.79E-13	-1.12E+01	-5.36E+00	-1.56E+01	5.58E-01	-2.05E-01
87.	-2.78E+01	-5.36E+01	2.17E+08	3.45E-09	5.34E-01	-5.79E-13	-2.73E+00	-2.90E+00	-1.56E+01	5.87E-01	-2.08E-01
88.	-2.77E+01	-5.46E+01	4.92E+08	4.98E-09	5.90E-01	-5.79E-13	-8.22E+00	-6.41E-01	-1.56E+01	6.09E-01	-2.15E-01
89.	-2.77E+01	-5.55E+01	7.53E+08	5.40E-09	6.50E-01	-5.79E-13	-6.44E+00	1.32E+00	-1.56E+01	6.26E-01	-2.21E-01
90.	-2.76E+01	-5.64E+01	9.62E+08	5.29E-09	7.13E-01	-5.79E-13	-5.15E+00	2.92E+00	-1.56E+01	6.36E-01	-2.30E-01
91.	-2.74E+01	-5.68E+01	1.09E+07	4.43E-09	7.74E-01	-5.79E-13	-3.66E+00	4.12E+00	-1.57E+01	6.42E-01	-2.41E-01
92.	-2.73E+01	-5.73E+01	1.12E+07	3.17E-09	8.31E-01	-5.79E-13	-2.31E+00	4.92E+00	-1.57E+01	6.46E-01	-2.53E-01
93.	-2.71E+01	-5.76E+01	1.06E+07	1.54E-09	8.83E-01	-5.79E-13	-1.11E+00	5.36E+00	-1.57E+01	6.46E-01	-2.65E-01
94.	-2.69E+01	-5.77E+01	9.31E+08	1.89E-10	9.28E-01	-5.76E-13	-1.32E-01	5.47E+00	-1.57E+01	6.44E-01	-2.79E-01
95.	-2.67E+01	-5.76E+01	8.47E+08	1.81E+09	9.65E-01	5.72E-01	5.33E+00	5.37E+00	-1.57E+01	6.44E-01	-2.92E-01
96.	-2.65E+01	-5.73E+01	6.71E+08	2.87E+09	9.97E-01	8.96E-01	8.64E-01	4.58E+00	-1.58E+01	6.44E-01	-3.06E-01
97.	-2.63E+01	-5.70E+01	6.46E+10	1.79E+09	1.02E+00	1.02E+00	9.02E-01	4.49E+00	-1.58E+01	6.43E-01	-3.18E-01
98.	-2.61E+01	-5.66E+01	1.67E+11	1.22E+09	1.05E+00	1.04E+00	9.03E-01	3.87E+00	-1.58E+01	6.43E-01	-3.29E-01
99.	-2.59E+01	-5.62E+01	3.39E+12	6.24E+10	1.06E+00	1.06E+00	9.04E-01	3.17E+00	-1.58E+01	6.44E-01	-3.39E-01
100.	-2.57E+01	-5.47E+01	7.20E+12	3.43E+11	1.07E+00	1.07E+00	9.04E-01	2.43E+00	-1.58E+01	6.45E-01	-3.46E-01
101.	-2.54E+01	-5.37E+01	1.71E+11	5.65E+10	1.08E+00	1.08E+00	9.04E-01	1.69E+00	-1.58E+01	6.47E-01	-3.50E-01
102.	-2.51E+01	-5.25E+01	2.46E+11	6.59E+10	1.08E+00	1.08E+00	9.04E-01	9.72E-01	-1.58E+01	6.50E-01	-3.52E-01
103.	-2.48E+01	-5.12E+01	3.06E+11	1.30E+09	1.07E+00	1.07E+00	9.04E-01	3.18E-01	-1.58E+01	6.53E-01	-3.51E-01
104.	-2.44E+01	-4.99E+01	3.49E+11	1.51E+09	1.06E+00	1.06E+00	9.04E-01	-2.53E-01	-1.58E+01	6.56E-01	-3.47E-01
105.	-2.41E+01	-4.85E+01	3.69E+11	1.58E+09	1.04E+00	1.05E+00	9.03E-01	-7.27E-01	-1.58E+01	6.57E-01	-3.41E-01
106.	-2.38E+01	-4.70E+01	3.56E+11	1.50E+09	1.03E+00	1.03E+00	9.03E-01	-1.10E+00	-1.58E+01	6.57E-01	-3.33E-01
107.	-2.31E+01	-4.54E+01	3.10E+11	1.20E+09	1.01E+00	1.01E+00	9.02E-01	-1.38E+00	-1.57E+01	6.55E-01	-3.25E-01
108.	-2.26E+01	-4.39E+01	2.12E+11	8.87E+10	9.82E-01	9.85E-01	9.01E-01	-1.57E+00	-1.57E+01	6.49E-01	-3.15E-01
109.	-2.20E+01	-4.22E+01	7.50E+12	3.88E+10	9.58E-01	9.61E-01	9.00E-01	-1.71E+00	-1.57E+01	6.40E-01	-3.05E-01
110.	-2.14E+01	-4.05E+01	1.20E+11	1.99E+10	9.33E-01	9.36E-01	9.00E-01	-1.83E+00	-1.57E+01	6.26E-01	-2.95E-01
111.	-2.07E+01	-3.84E+01	3.42E+11	8.25E+10	9.07E-01	9.11E-01	8.99E-01	-1.96E+00	-1.57E+01	6.07E-01	-2.84E-01
112.	-2.02E+01	-3.73E+01	6.42E+11	1.43E+09	8.82E-01	8.84E-01	8.99E-01	-2.15E+00	-1.57E+01	5.84E-01	-2.71E-01
113.	-1.99E+01	-3.61E+01	9.47E+11	1.93E+09	8.62E-01	8.55E-01	8.97E-01	-2.43E+00	-1.57E+01	5.57E-01	-2.57E-01
114.	-1.98E+01	-3.51E+01	1.27E+10	2.27E+09	8.20E-01	8.25E-01	8.55E-01	-2.84E+00	-1.56E+01	5.27E-01	-2.40E-01
115.	-1.97E+01	-3.41E+01	1.61E+10	2.36E+09	7.85E-01	7.96E-01	8.94E-01	-3.41E+00	-1.56E+01	4.95E-01	-2.22E-01
116.	-1.97E+01	-2.93E+01	1.99E+10	2.16E+09	7.45E-01	7.51E-01	8.92E-01	-4.13E+00	-1.56F+01	4.61E-01	-1.97E-01
117.	-1.94E+01	-2.47E+01	2.45E+10	1.65E+09	6.99E-01	7.06E-01	8.91E-01	-4.99E+00	-1.56E+01	4.27E-01	-1.71E-01
118.	-1.91E+01	-2.05E+01	3.05E+10	8.32E+10	6.46E-01	6.55E-01	8.88E-01	-5.96E+00	-1.56E+01	3.94E-01	-1.42E-01
119.	-1.89E+01	-2.31E+01	3.99E+10	2.25E+10	5.95E-01	5.96E-01	8.85E-01	-6.98E+00	-1.56E+01	3.61E-01	-1.11E-01
120.	-1.88E+01	-1.96E+01	5.30E+10	1.43E+09	5.10E-01	5.29E-01	8.81E-01	-8.00E+00	-1.56E+01	3.29E-01	-7.59E-02
121.	-1.85E+01	-1.72E+01	7.62E+10	2.46E+09	4.40E+01	4.46E+01	8.77E-01	-8.92E+00	-1.56F+01	2.96E-01	-4.57E-02
122.	-1.84E+01	-1.44E+01	1.18E+09	3.78E+09	3.47E-01	3.78E+01	8.70E-01	-9.66E+00	-1.56E+01	2.67E-01	-2.06E-02
123.	-1.82E+01	-1.20E+01	1.98E+09	4.45E+09	2.70E-01	2.96E+01	8.63E-01	-1.02E+01	-1.56F+01	2.35E-01	4.49E-03
124.	-1.81E+01	-9.82E+02	3.44E+09	5.10E+09	1.80E-01	2.14E+01	8.52E-01	-1.06E+01	-1.56E+01	2.01E-01	2.53E-02
125.	-1.80E+01	-6.78E+02	7.23E+09	5.23E+09	9.03E-02	1.37E+01	8.38E-01	-1.02E+01	-1.56F+01	1.65E-01	4.12E-02
126.	-1.81E+01	-4.12E+02	1.45E+08	4.85E+09	3.62E-03	7.10E+02	8.17E-01	-9.76E+00	-1.56E+01	1.25E-01	5.21E-02
127.	-9.51E+00	-1.43E+02	2.45E+08	4.03E+09	-7.76E-02	2.50E-02	7.84E-01	-8.59E+00	-1.56F+01	8.06E-02	5.82E-02
128.	-8.88E+00	1.24E+02	2.55E+08	2.96E+09	-1.51E+01	4.31E+03	7.28E-01	-7.97E+00	-1.56E+01	3.16E-02	5.98E-02

142

FOURIER COEFFICIENTS

VDIODE	AMPIN	VOUT	IDIODE	VIN	
-1.523E+01	4.316E-04	-1.541E+01	1.892E-01	-1.554E+01	dc
1.227E+01	1.298E-02	-2.465E-01	-2.344E-02	6.750E+00	cos - 1
-3.552E+00	-4.485E-06	3.421E-02	-2.104E-01	-1.401E-01	sin 1
-1.005E-01	-1.122E-03	9.915E-03	-3.592E-02	7.000E-02	cos 3
1.396E-01	-5.512E-03	-3.745E-03	-1.811E-03	2.746E-01	cos 4
-7.422E-01	3.765E-03	-3.776E-03	1.303E-03	-1.884E-01	cos 5
-1.184E+01	5.695E-01	2.451E-01	-5.809E-01	1.137E+01	sin 1
3.151E+00	-2.169E-02	-3.458E-02	-2.743E-01	1.086E+00	sin 2
4.139E+00	3.206E-03	-6.892E-02	-3.289E-02	-1.517E-01	sin 3
-1.702E-01	-5.136E-04	3.382E-03	-1.210E-03	3.639E-02	sin 4
-1.258E-01	-7.284E-05	8.488E-04	2.041E-03	-3.898E-03	sin 5

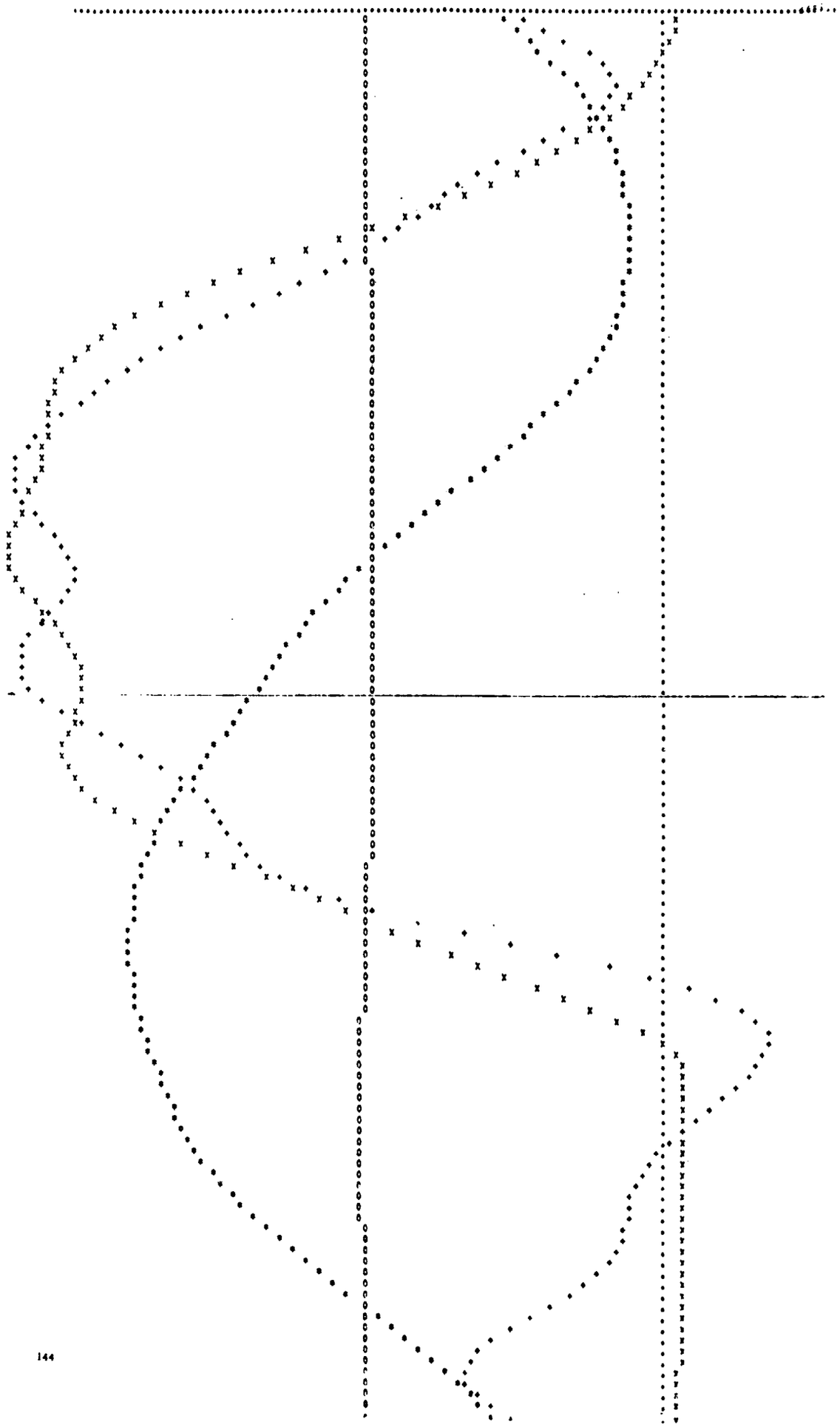

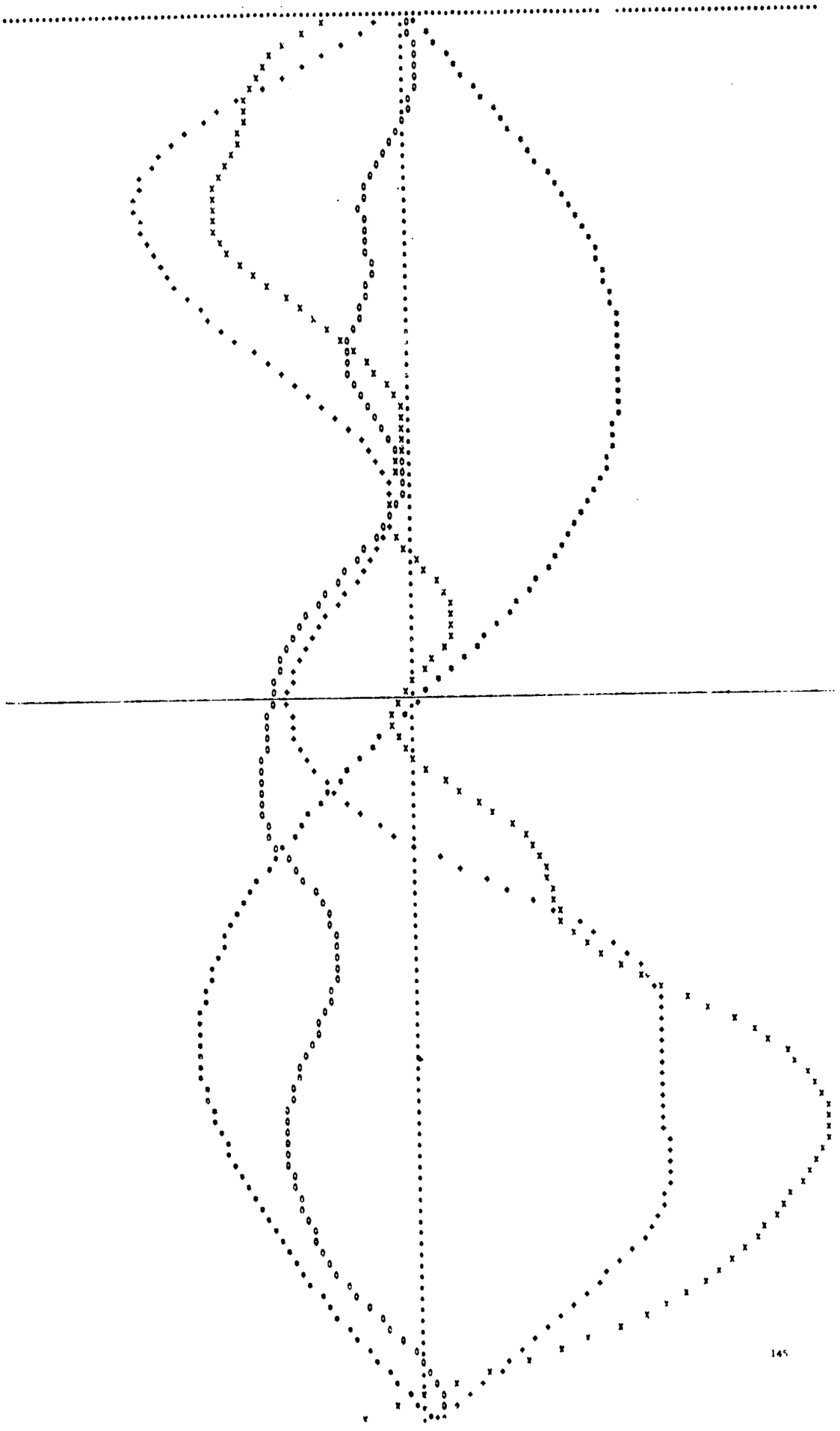

APPENDIX B

REFERENCES

1. W.C. Brown, "The Technology and Application of Free-Space Power Transmission by Microwave Beam", Proceedings of the IEEE, vol. 62, No. 1, Jan. 1974, pp. 11-25.

2. J.J. O'Neill, Prodigal Genius - The Life of Nikola Tesla. New York, Ives Washburn, 1944.

3. I. Hunt and W. Draper, Lightening in His Hand, the Life Story of Nikola Tesla. Denver, Colorado; Sage, 1964.

4. C. Susskind, "The experiments of Hertz", IEEE Spectrum, vol. 5, pp. 50-60, Dec. 1968.

5. J.F. Skowron, G.H. MacMaster, and W.C. Brown, "The super power CW amplitron," Microwave J., Oct. 1964.

6. W.C. Brown, "Experiments in the transportation of energy by microwave beam," in 1964 IEEE Int. Conv. Rec., vol. 12 pt. 2, pp 8-17.

7. W.C. Brown, "Experiments involving a microwave beam to power and position a helicopter," IEEE Trans. Aerospace Electron," Syst., vol. AES 5, pp. 692-702, Sept. 1969.

8. W.J. Robinson, "Wireless power transmission in a space environment", J. Microwave Power, vol. 5, Dec. 1970.

9. W.C. Brown, "Free-Space Microwave Power Transmission Study, Combined Phase III and Final Report", Raytheon Report No. PT-4601 Sept. 1975. NASA Contract No. NAS-8-25374.

10. R.M. Dickinson, W.C. Brown, "Radiated Microwave Power Transmission System Efficiency Measurements", Tech. memo 33-727 Jet Prop. Lab. Cal. Inst. Tech, March 15, 1975.

11. R.M. Dickinson, "Evaluation of a Microwave High-Power Reception-Conversion Array for Wireless Power Transmission", Tech. Memo. 33-741, Jet Propulsion Lab, Cal. Inst. Tech. Sept. 1, 1975.

12. "Reception - Conversion Subsystem (RXCV) for Microwave Power Transmission System", Raytheon Report No. ER75-4386, JPL Contract No. 953968, Sept. 1975.

13. W.C. Brown, "A Survey of the Elements of Power Transmission by Microwave Beam", 1961 IRE International Convention Record, Vol. 9, Part 3, pp. 93-105.

REFERENCES (Cont'd)

14. R.H. George and E.M. Sabbagh, "An efficient means of converting microwave energy to dc using semiconductor diodes", IEEE Intern. Conv. Record Electron Devices, Microwave Theory Tech., vol. II, Pt. 3, pp. 132-141, March 1963.

15. U.S. Patent No. 3,434,678, March 25, 1969, W.C. Brown, et al.

16. E.C. Okress, W.C. Brown, T. Moreno, G. Goubau, N.I. Heenan and R.H. George, "Microwave Power Engineering", IEEE Spectrum, October, 1964, pp. 76-96.

17. W.C. Brown, "Progress in the Design of Rectennas", Journal of Microwave Power, Vol. 4, No. 3, pp. 168-175, 1969.

18. R.H. George, Solid State Microwave Power Rectifiers, Rept. RADC-TR-65-224, Rome Air Develop. Center, Griffiss Air Force Base, New York, August 1965.

19. W.C. Brown, "The Receiving Antenna and Microwave Power Rectification" Journal of Microwave Power, Vol. 5, No. 4, pp. 279-292, 1970.

20. W.C. Brown, "Progress in the Efficiency of Free-Space Microwave Power Transmission", Journal of Microwave Power, Vol. 7, No. 3, pp. 223-230.

21. P.E. Glaser, "Power from the sun: its future", Science, vol. 162, pp. 857-861, Nov. 22, 1968.

22. J. Microwave Power, vol. 5 special issue on "Satellite solar power station and microwave transmission to earth," Dec. 1970.

23. J. Mockovciak, Jr., "A systems engineering overview of the satellite solar power station," Proc. 1972 Intersociety Energy Conversion Eng. Conf.

24. W.C. Brown, "Satellite Power Stations: A new source of energy?", IEEE Spectrum Vol. 10, No. 3, March 1973, pp. 38-47.

25. P.E. Glaser, O.E. Maynard, J. Mockovciak, Jr., E.L. Ralph, "Feasibility Study of a Satellite Solar Power Station", NASA Contractor Report, CR-2357, February 1974.

26. "Microwave Power Transmission System Studies" Raytheon Contractor Report ER75-4368 NASA CR-134886, December 1975.

27. "Space-Based Solar Power Conversion and Delivery Systems Study", Second Interim Report, Vol. III. Prepared by ECON, Inc., under NASA MSFC contract No. NAS8-31308, June 30, 1976.

28. J. Nahas, "Modeling and Computer Simulation of a Microwave-to-DC Energy Conversion Element", IEEE Trans. on Microwave Th. and Tech., Vol. MTT-23, pp. 1030-1035, Dec. 1975.

29. J. Nahas, "Final Report, Simulation and Experimental Studies of Microwave-to-DC Energy Conversion Systems", Prepared for NASA, Lewis Research Center, under Grant No. NSG-3070.

30. W.C. Brown, Chung K. Kim, "Recent progress in power reception efficiency in a Free-Space Microwave Power Transmission System", 1974 IEEE S-MTT Int. Micro. Symp. Digest. Lib. of Cong. No. 72-75863. pp. 332-222

31. K.J. Linden, "Advanced Mixer Technology", Technical Report, AFAL-TR-76-107, Jan. 1976.